

The Shu complex is a conserved regulator of Rad51 filament formation

by

Stephen Kenneth Godin

B.S. Biology, University of Massachusetts, 2011

B.S. Microbiology, University of Massachusetts, 2011

Submitted to the Graduate Faculty of
The School of Medicine in partial fulfillment
of the requirements for the degree of
PhD in Molecular Genetics and Developmental Biology

University of Pittsburgh

2015

UNIVERSITY OF PITTSBURGH

School Of Medicine

This dissertation was presented

by

Stephen Kenneth Godin

It was defended on

December 7, 2015

and approved by

Bennett Van Houten, PhD, Department of Pharmacology

Judith Yanowitz, PhD, Department of Molecular Genetics and Developmental Biology

Andrew VanDemark, PhD, Department of Biological Sciences

Patricia Opresko, PhD Department of Molecular Genetics and Developmental Biology

Dissertation Advisor: Kara Bernstein, PhD, Department of Molecular Genetics and

Developmental Biology

Copyright © by Stephen Kenneth Godin

2015

The Shu Complex is a conserved regulator of Rad51 filament formation

Stephen Kenneth Godin, PhD

University of Pittsburgh, 2015

The budding yeast Shu complex, a heterotetramer of Shu1, Shu2, Csm2, and Psy3, is important for homologous recombination (HR)-mediated chromosome damage repair and was first characterized a decade ago as promoting Rad51-dependent HR in response to replicative stress, but its mechanistic function and conservation in eukaryotes has remained unknown. Here we provide evidence that the Shu complex is evolutionarily conserved throughout eukaryotes, where it is comprised of a clear Shu2 orthologue physically associating with Rad51 paralogues. The Shu complex itself physically interacts with the rest of the HR machinery during DNA damage repair. Finally, we uncover that the mechanistic function of the Shu complex as a stimulatory co-factor of Rad51 filament formation *in vitro*, likely explaining the *in vivo* function of the eukaryotic Shu complex in suppressing error-prone repair. Moving forward, our findings provide a framework for studying the function of the human Shu complex, which will have broad importance in our understanding of DNA damage repair.

TABLE OF CONTENTS

PREFACE.....	XIV
1.0 INTRODUCTION.....	1
1.1 HOMOLOGOUS RECOMBINATION.....	2
1.1.1 Resection	5
1.1.2 Rad51 filament formation, structure, and components	6
1.1.3 Rad51-dependent strand invasion and resolution of HR	10
1.2 HOMOLOGOUS RECOMBINATION AT A REPLICATION FORK	13
1.3 THE SHU COMPLEX	16
1.4 RELEVANCE OF THE HUMAN SHU COMPLEX TO HUMAN HEALTH	19
1.5 USE OF THE BUDDING YEAST MODEL SYSTEM.....	20
1.6 MAJOR HYPOTHESES.....	23
1.6.1 The Shu complex is well conserved from budding yeast to humans	23
1.6.2 The Shu complex interacts with the HR machinery and promotes Rad51- dependent HR.....	25
1.6.3 The mechanistic function of the Shu complex is to stimulate Rad51 filament formation	26
2.0 EVOLUTIONARY AND FUNCTIONAL ANALYSIS OF THE INVARIANT SWIM DOMAIN IN SHU2/SWS1 PROTEIN FAMILY FROM SACCHAROMYCES CEREVISIAE TO HOMO SAPIENS.....	28
2.1 RESULTS	30

2.1.1	Characterization of <i>shu2</i> Δ recombination phenotype and its physical interactions with other Shu complex members	30
2.1.2	Shu2 orthologues are conserved across eukaryotes.....	33
2.1.3	Shu2 and its orthologs have evolutionary histories strongly correlated with recombination and meiosis-related proteins.....	36
2.1.4	Expansion of the SWIM domain to include an invariant alanine three amino acids down-stream of the canonical CXC...Xn...CXC motif.....	39
2.1.5	The SWIM domain is important for Shu2's functionality <i>in vivo</i>	40
2.2	DISCUSSION.....	45
2.3	MATERIALS AND METHODS	48
2.3.1	Yeast strains, plasmids, and media	48
2.3.2	Serial dilutions.....	49
2.3.3	Yeast-2-Hybrids	50
2.3.4	Homology searching and phylogenetics.....	50
2.3.5	Evolutionary rate covariation of Shu2 and fly SWS1 with meiotic and mitotic proteins.....	51
2.3.6	Spore viability assay	52
2.3.7	Mitotic recombination assays.....	52
2.4	ACKNOWLEDGEMENTS	53
3.0	THE SHU COMPLEX INTERACTS WITH THE RAD51 NUCLEOPROTEIN FILAMENT TO MEDIATE ERROR-FREE RECOMBINATION	54
3.1	INTRODUCTION	54
3.2	RESULTS.....	57

3.2.1	Csm2 and Psy2 preferentially bind forked and 3' overhang DNA substrates	57
3.2.2	Csm2 interacts with Rad51 and the Rad51 paralogues Rad55-Rad57 ..	60
3.2.3	The Shu complex and Rad55-Rad57 function in the same epistasis group	61
3.2.4	Csm2 is necessary for the recruitment of Rad55 to DNA damage sites.	64
3.2.5	Unlike <i>rad55</i> Δ , the cold sensitivity of <i>csm2</i> Δ cells exposed to MMS is not suppressed by over-expression of Rad55-Rad57 or Rad51	64
3.2.6	The Shu complex promotes Rad51-dependent recombination events ...	66
3.3	DISCUSSION.....	68
3.4	MATERIALS AND METHODS.....	73
3.4.1	Strains, plasmids and media	73
3.4.2	Purification of Csm2 and Psy3.....	73
3.4.3	Competition electrophoretic mobility shift assay (EMSA)	74
3.4.4	Fluorescence anisotropy assays for DNA binding	74
3.4.5	Yeast-2-Hybrids	75
3.4.6	Serial dilutions.....	76
3.4.7	Fluorescent microscopy	76
3.4.8	Mitotic recombination assays.....	76
3.5	ACKNOWLEDGEMENTS	77
4.0	PROMOTION OF RAD51 PRESYNAPTIC FILAMENT ASSEMBLY BY THE ENSEMBLE OF <i>S. CEREVISIAE</i> RAD51 PARALOGUES WITH RAD52	78
4.1	INTRODUCTION	78

4.2	RESULTS	79
4.2.1	The Shu complex interacts with the regulators of Rad51 filament formation and acts upstream of Rad51 filament formation	79
4.2.2	The Shu complex acts with Rad55-Rad57 and Rad52 to stimulate Rad51 filament formation	82
4.2.3	Csm2's interaction with Rad55-Rad57 is essential for its function <i>in vitro</i> and <i>in vivo</i>	85
4.3	DISCUSSION	89
4.4	MATERIALS AND METHODS	90
4.4.1	Strains, plasmids, and media	90
4.4.2	Yeast-2-Hybrid analysis	91
4.4.3	Serial dilutions.....	91
4.4.4	Mitotic recombination assay	91
4.4.5	Canavanine mutagenesis assay	92
4.4.6	Suppression of <i>rad54</i> Δ <i>srs2</i> Δ synthetic lethality	92
4.4.7	Protein expression and purification	92
4.4.8	Affinity pull-down assays	95
4.4.9	Rad51 loading onto ssDNA immobilized on magnetic beads.....	96
4.4.10	Homologous DNA pairing and strand exchange reaction.....	96
4.4.11	Electron microscopy	97
4.4.12	DNA binding assay.....	97
4.5	ACKNOWLEDGEMENTS	98
5.0	DISCUSSION	99

5.1	DOES THE SHU COMPLEX REMAIN ASSOCIATED WITH THE RAD51 FILAMENT?.....	102
5.2	WHAT UNDERLIES THE SPECIFIC ROLE OF THE SHU COMPLEX IN THE REPAIR OF MMS-INDUCED DNA DAMAGE?	105
5.2.1	Lesion specificity of the Shu complex.....	105
5.2.2	Regulation of the Shu complex activity by post-translational modifications.....	108
5.3	WHAT DIFFERENTIATES THE ROLE OF THE SHU COMPLEX AT AN HU-INDUCED STALLED FORK FROM AN MMS-INDUCED STALLED FORK.....	109
5.4	WHAT IS THE IMPORTANCE OF THE PHYSICAL ASSOCIATION BETWEEN SHU2 AND SRS2?.....	112
5.5	DOES THE SHU COMPLEX HAVE A ROLE DOWNSTREAM OF RAD51 FILAMENT FORMATION?	114
5.6	HOW DOES THE FUNCTION OF THE SHU COMPLEX IN MEIOSIS DIFFER FROM MITOSIS?	116
5.7	CONCLUDING REMARKS	118
	APPENDIX A	119
	APPENDIX B	128
	APPENDIX C	132
	BIBLIOGRAPHY	140

LIST OF TABLES

Table 1. The major homologs of the HR proteins discussed for five eukaryotic model systems..	6
Table 2. Chapter 2 Strains and Plasmids	121
Table 3. Chapter 2 Primers	126
Table 4. Chapter 3 Strains and Plasmids	129
Table 5. Chapter 3 Primers used	131
Table 6. Chapter 4 Strains and Plasmids	138

LIST OF FIGURES

Figure 1. Homologous recombination pathways and proteins.....	4
Figure 2. A schematic of two proposed models for post-replicative repair at a replication fork. 14	
Figure 3. <i>SHU2</i> mutants have phenotypes similar to the Rad51 paralogues.	32
Figure 4. The SWS1 protein family extends across eukaryotes.	35
Figure 5. Co-evolutionary signatures indicate Shu2/SWS1 has highly conserved functional relationships with Rad51 paralogues and meiosis proteins.	37
Figure 6. Analysis of the highly conserved SWIM domain residues in the human SWS1 protein.	40
Figure 7. The SWIM domain is important for Shu2's function.....	42
Figure 8. The Csm2 and Psy3 heterodimer preferentially bind forked and 3' overhang DNA substrates.....	58
Figure 9. Csm2 physically interacts with Rad51, Rad55, and Rad57 by yeast-2-hybrid.	61
Figure 10. Csm2 is in the same epistasis group as Rad55 and regulated Rad55 recruitment to DNA damage sites.	63
Figure 11. Over-expression of Rad55-Rad57 or Rad51 does not suppress the MMS sensitivity of <i>csm2Δ</i> cells at 23°C.....	65
Figure 12. Disruption of <i>CSM2</i> or <i>PSY3</i> leads to more Rad51-independent recombination events.	67
Figure 13. Schematic of the role of the Shu complex during error-free HR.	69
Figure 14. Interactions of Rad55-Rad57 with the Shu complex and Rad52.	81

Figure 15. Enhancement of Rad51 loading onto RPA-coated ssDNA by the Shu complex and Rad55-Rad57.	84
Figure 16. Impairment of physical interaction and functional synergy of the Shu complex with Rad55-Rad57 by the <i>csm2-F46A</i> mutation.....	86
Figure 17. Impairment of homologous recombination by the <i>csm2-F46A</i> mutation.....	88
Figure 18. Model for Shu complex function in presynaptic filament assembly.	99
Figure 19. Models of how the Shu complex and Rad55-Rad57 may interact with the Rad51 filament.	103
Figure 20. Distributions of ERC with Shu complex members PSY3.....	119
Figure 21. A deep evolutionary alignment of Shu2/SWS1 orthologues clearly reveals conserved residues of the SWIM domain.	120
Figure 22. The SWIM domain is important for Shu2's function.....	121
Figure 23. Competition electrophoretic mobility shift assay (EMSA).	128
Figure 24. Purity analysis of Shu complex and Rad55-Rad57.	132
Figure 25. Interactions of Rad55-Rad57 with the Shu complex and Rad51.	133
Figure 26. Genetic analyses of <i>csm2Δ</i> for functions independent of <i>RAD54</i> and <i>SRS2</i>	133
Figure 27. Electron microscopy visualization of the nucleoprotein complexes formed via Shu complex and Rad55-Rad57 facilitated loading of Rad51.	134
Figure 28. Analysis of the effect of Rad55-Rad57 and Shu complex on Rad51 loading at 23°C and 30°C.....	135
Figure 29. Analysis of Shu complex and Csm2-Psy3 complex in Rad51-mediated DNA strand exchange.	136

Figure 30. Analysis of the Csm2-Psy3 structure to identify potential protein-protein interaction surfaces. 137

Figure 31. Comparison of human and yeast Rad51 paralogue complexes. 137

PREFACE

To all who provided help, support, and guidance:

To Kara Bernstein, my graduate thesis advisor, who guided my scientific development and without whom this project would never have been possible.

To all current and former members of the Bernstein lab. In particular, a special thanks to Faiz Kabbinavar, Dominique Bratton-Palmer, Jared Baird, Meghan Sullivan, and Alison Lee who all contributed data to this dissertation, and to Michael Mihalevic for saving more experiments from disaster than he can possibly imagine.

To all of my collaborators, particularly Nathan Clark, William Gaines, and Adam Wier, who contributed critical data throughout this dissertation.

To the members of my thesis committee, for their invaluable advice on this project and for my career.

To my friends and family, who supported my time here in Pittsburgh, especially to Michael Starke, Lindsay Alberts, and Michael Mihalevic.

And finally, to my fiancé Johanna Geoghegan, for her continued support and understanding throughout this dissertation.

Thank you.

1.0 INTRODUCTION

Cells are constantly bombarded with a complex mixture of endogenous and exogenous sources of stress that can lead to DNA damage. Exogenously, the cells face multiple sources of DNA damage, such as ultraviolet (UV) light exposure, which can cause cyclobutane pyrimidine dimers (CPD), exposure to natural sources of psoralen from foods which can cause interstrand crosslinks in DNA, and exposure to radioactive radon in the home, which can cause DNA double-strand breaks (DSBs). Cells also face numerous endogenous forms of DNA damage as well. During normal metabolism, multiple forms of reactive oxygen species, e.g. superoxide, are created which can give rise to different modifications of the DNA bases that could potentially lead to DSBs. As a cell tries to replicate through damaged DNA during S-phase, replication forks often stall and/or collapse, giving rise to further, spontaneous DNA damage such as DSBs.

In order to protect the stability of the genome from these numerous sources of damage, eukaryotic cells utilize a wide variety of DNA damage recognition and repair pathways and mechanisms to remove the different lesions that arise in the DNA, which are briefly summarized here and in greater detail in (1). To deal with the modified bases that arise from H_2O_2 , free radicals, and from certain forms of methylation damage, cells employ the base excision repair (BER) pathway to remove damaged bases and a limited patch of DNA around the lesion. The kinds of damage generated by UV light exposure, such as covalently linked bases, e.g. CPD, are recognized and removed by the nucleotide excision repair pathway (NER), that functions to recognize the

structural distortion in the DNA helix generated by these lesions, and then excises a patch of nucleotides around the linked dimer to allow repair. To cope with the DSBs generated by radiation exposure, eukaryotic cells can utilize non-homologous end joining (NHEJ), which functions to recognize a DSB, minimally process the ends to remove damaged bases, then ligate both ends of the break back together. This is potentially an error-prone pathway, as there is little proofreading that takes place and this process can result in insertions or deletions at the break site. Alternatively, the cell can utilize homologous recombination (HR), which is usually considered an error-free or high-fidelity alternative to NHEJ, and as the primary focus of this dissertation, is discussed in detail below.

1.1 HOMOLOGOUS RECOMBINATION

Homologous recombination is a DNA double-strand break repair pathway important for genomic stability (2). Mutations in many HR genes underlie numerous human diseases, including cancer, Fanconi anemia, ataxia telangiectasia, Bloom, Werner, Rothmund-Thomson, and Nijmegen breakage syndromes (3-10). When HR is impaired, mutant cells are often hypersensitive to DNA damaging agents, accumulate gross chromosomal rearrangements, and exhibit a mutator phenotype (2,11,12).

The HR pathway is utilized at many types of lesions including a direct DSB or a damaged replication fork (12). HR-initiating lesions at replication forks are incredibly varied and include missing nucleotides at abasic sites and altered DNA bases that block DNA polymerase activity and stall replication forks. Similarly, inter-strand crosslinks that prevent the opening of the DNA helicase also block replication fork progression, and are repaired and bypassed, in part, by the HR

pathway during inter-strand crosslink repair (12). Additionally, HR is utilized when replication forks encounter a single-stranded DNA (ssDNA) break that causes the fork to collapse into a one-ended DSB. Due to the wealth of knowledge about HR at direct DSBs, such as those induced by IR or endonuclease-induced breaks, HR is first discussed in the context of these direct breaks for the rest of this section and in Figure 1. Section 1.2 will cover models of HR at replication forks (Figure 2), and is the primary focus of this dissertation. In all cases, yeast protein names are used when describing each step of HR, although human names are frequently included for clarity. Table 1 lists the human, budding yeast, fission yeast, *C. elegans*, and fruit fly homologues for the major HR proteins that are discussed in this dissertation and in Figures 1 and 2.

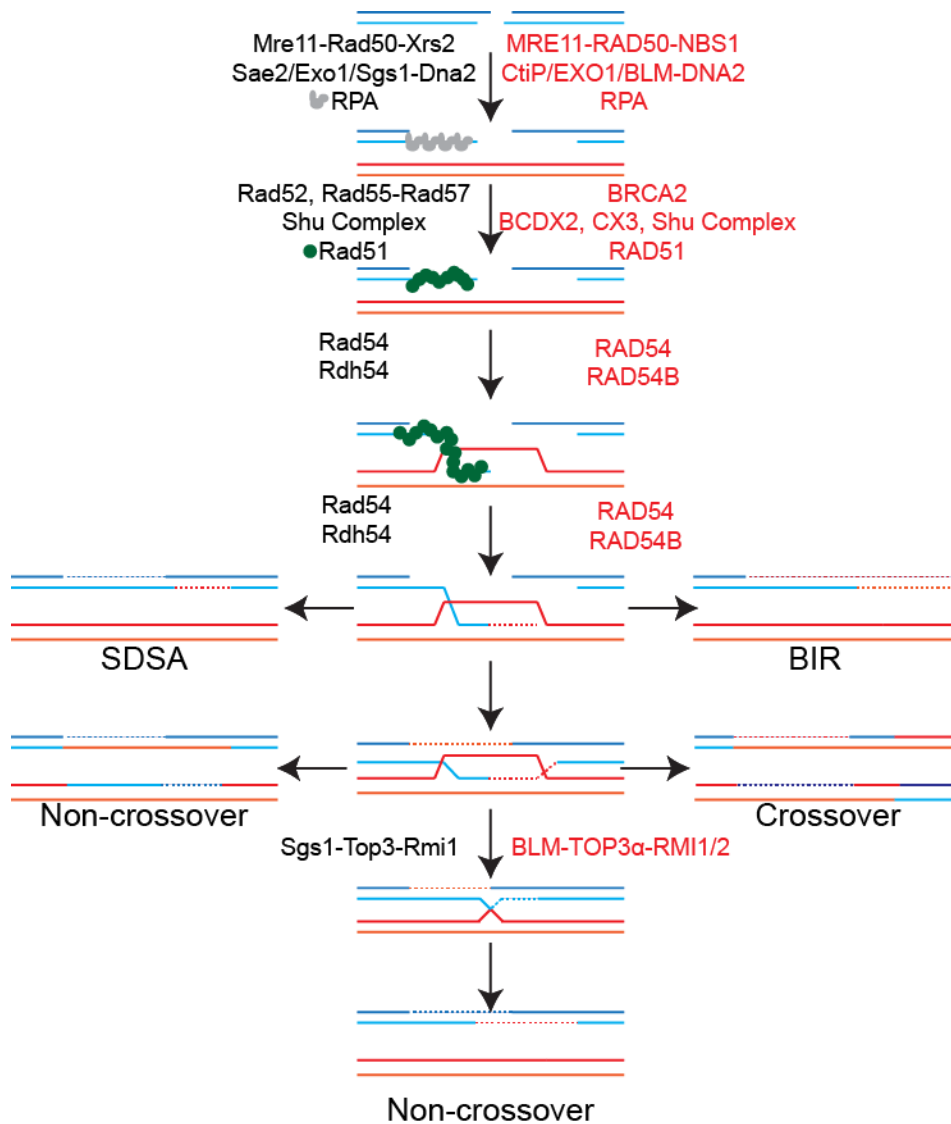


Figure 1. Homologous recombination pathways and proteins.





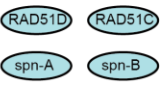
A schematic indicating how HR can be channeled into synthesis-dependent strand annealing (SDSA), break-induced replication (BIR), or through a double-Holliday junction into different kinds of crossover and non-crossover repair outcomes. Yeast proteins are shown on the left in black, while human proteins are shown on the right in red.

1.1.1 Resection

During HR, the DSB is first recognized and then resected by a specific set of nucleases to give rise to 3' single-stranded DNA overhangs (ssDNA). DNA end resection is first initiated by the Mre11-Rad50-Xrs2 (MRX) complex in budding yeast or the MRE11-RAD50-NBS1 (MRN) complex in human cells (13). After the MRX complex binds to the DSB ends, the endonuclease Sae2/CtIP interacts with the complex and stimulates resection in the 5' to 3' direction to generate 3' ssDNA overhangs (14-16). The short-range resection by Sae2/CtIP and the MRX/MRN complex is expanded by the redundant activities of the 5'-3' exonuclease Exo1/EXO1 and a complex of the Sgs1/BLM helicase with the endonuclease Dna2/DNA2 (17-20). The ssDNA that is generated is immediately coated by the ssDNA binding protein replication protein A (RPA). RPA coated DNA protects the DSB ends from further degradation and signals to the cell the presence of unrepaired DNA damage (21,22).

Table 1. The major homologs of the HR proteins discussed for five eukaryotic model systems.

Graphical summaries of the Rad51 paralogue complexes are included.

Protein Group and Function	<i>Saccharomyces cerevisiae</i>	<i>Schizosaccharomyces pombe</i>	<i>Homo sapiens</i>	<i>Caenorhabditis elegans</i>	<i>Drosophila melanogaster</i>
ssDNA Binding and Protection RPA	Rfa1, Rfa2, Rfa3	Rpa1, Rpa2, Rpa3	RPA1, RPA2, RPA3	RPA-1, RPA-2, RPA-3	RpA-70, RpA-30, RpA-8
Rad51 Filament Formation Rad52 and Brca2	Rad52	Rhp22	BRCA2, RAD52	BRC-2	Brca2
Rad51 Filament Formation Rad51 Paralogues					
Shu Complex	Shu2/SWS1	Shu2	SWS1	SWS-1	SWS-1
Rad51 Inhibitors	Srs2	Srs2, Fbh1	RTEL, PARI, REQL5, FBH1	RTEL-1	Unknown
Rad51 Dependent Strand Exchange SWI/SNF Translocases	Rad54, Rdh54	Rhp54, Rdh54	RAD54, RAD54B	RAD-54	RAD-54 (Okra)
Resolution of Double Holliday Junctions RecQ Helicases	Sgs1	Rqh1	BLM, WRN, RECQL4	HIM-6, WRN-1, RECQL4	Blm, WRNexo, RecQ5

1.1.2 Rad51 filament formation, structure, and components

The next step of HR is the formation of a Rad51 filament on the ssDNA (2), which is essential for the strand exchange and homology search steps that allow HR to occur. Rad51 filament formation is tightly regulated to prevent excessive recombination and genomic instability. The first barrier to Rad51 filament formation is the presence of RPA, which blocks Rad51 binding to ssDNA (2). The inhibition of RPA is overcome by the activity of Rad51's regulators. In budding yeast, these include Rad52 and two Rad51 paralogues, Rad55 and Rad57, which form an obligate heterodimer *in vitro* (Table 1, (21,23-26)). These proteins function by forming nucleation sites for Rad51 to bind to RPA-coated ssDNA and by promoting the elongation of Rad51 filaments by directing incoming Rad51 monomers to bind to DNA-bound Rad51 monomers. Recent models have

indicated that Rad52 and Rad55-Rad57 do not function to destabilize RPA, as RPA remains bound to the sites of DNA damage *in vivo*, and *in vitro*, RPA is interspersed inside Rad51 filaments (23,27).

To prevent unnecessary HR, the activity of Rad52 and Rad55-Rad57 are controlled by post-translational modifications, such as SUMOylation and phosphorylation respectively, which are regulated by DNA damage checkpoint signaling (28-31). For instance, Rad55-Rad57 have been shown to be phosphorylated by Rad53 in response to alkylation damage such as by methyl methanesulfonate (MMS) treatment. This phosphorylation has been shown to be important for promoting full resistance to MMS (29). Similarly, Rad52 is a known target of the SUMO pathway, and SUMOylation regulates Rad52's localization and activity during stress (32). These regulatory systems ensure that functional Rad51 filaments form only at sites of damage and only after proper DNA damage checkpoint signaling appropriately modifies the regulators of Rad51 filament formation.

Rad51 filaments are additionally regulated by other proteins, such as the anti-recombinase Srs2, whose major function is to prevent excessive HR by removing Rad51 from ssDNA (33,34). Srs2 is a helicase that translocates along ssDNA and, when it physically encounters a Rad51 molecule causes it to release the ssDNA (33,34). Rad51's ability to bind ATP is required for its association with ssDNA, and Srs2 is able to stimulate Rad51 to hydrolyze its ATP and release ssDNA (33,34). This activity of Srs2 is strictly ATP-dependent, as mutations in Srs2's ATPase domain prevents its helicase activity and Rad51-disassembly functions (33,34). Srs2's anti-recombinase activity is also strongly inhibited by the Rad51 paralogues, Rad55-Rad57, which are able to block the destabilization of Rad51 by Srs2 *in vitro* (35), although the mechanism by which they inhibit Srs2 has not fully been characterized. Additionally, other proteins involved in HR are

known to interact with Srs2, such as the Shu complex, which is discussed in greater detail below, although the functional significance of this interaction remains unknown.

Despite the central importance of the Rad51-ssDNA nucleoprotein filament in HR, many questions remain unanswered about the structure and components of the Rad51 filament *in vitro* and *in vivo*. As of the start of this dissertation work, the prevailing knowledge in the field was that as Rad51 binds to RPA-coated DNA, RPA was displaced to make room for Rad51. However, recent work has strongly contradicted this model. Work from Eric Greene's lab, using cutting-edge, single-molecule DNA curtain assays, has found that as Rad51 binds to RPA-coated ssDNA, RPA is not displaced. Instead, the DNA elongates as Rad51 binds, and RPA remains interspersed inside the larger Rad51 filament, perhaps functioning to break up several monomers of Rad51, thus maintaining the flexibility of the nucleoprotein filament (27). Further work from the same group has suggested that this may function to improve the efficiency of the Rad51-dependent homology search steps that define homologous recombination.

Recent work has strongly indicated that Rad51 filaments are not homogenous as many electron or atomic force microscopy (EM and AFM respectively) images would suggest (as an example, see chapter 4), and likely contain numerous other proteins involved in HR. For instance, Claire Wyman's group have recently visualized human RAD51 filaments using a new technique called combined total internal reflection fluorescence and scanning force microscopy (TIRF-SFM), which allows a RAD51 filament to be visualized in conjunction with fluorescently labeled proteins such as RAD54. Using this technique, they were able to discover that RAD54 binds to both ends of the RAD51 nucleoprotein filament and is present inside the RAD51 filament. The

observation that RAD54 can integrate into the middle of a RAD51 filament has important implications in RAD51 strand invasion and turnover as discussed below (36). Additionally, Eric Greene's group has also visualized Rad51 filaments using their DNA curtains technique, and has identified several exciting phenomena. In addition to the small clusters of RPA interspersed throughout the Rad51 filament, mentioned above, they also found that Rad52 is also interspersed throughout the filament, preferentially in a complex with RPA. They find that Rad52, far from causing RPA turnover as had previously been predicted, actually stabilizes RPA within the Rad51 filament, suggesting the presence of RPA in the filament may be critical for HR., They also found that Rad52-RPA complexes will coat the external surface of the Rad51 filament, which has broad implications for how the second end of a DSB is captured and stabilized at the break site in addition to raising the exciting possibility that other proteins may coat the Rad51 filament as well.

The idea that Rad51 filaments may contain multiple classes of proteins has raised several important questions in the field. For example, Rdh54, which is structurally very similar to Rad54, may also integrate into the filament and would help explain its role in destabilizing Rad51 filaments on double-stranded DNA (37,38). Additionally, if Rad51 filaments can contain other proteins, would they also contain the Rad51 paralogues, such as Rad55-Rad57? The similar structure of Rad55 and Rad57 to Rad51 might serve to allow them to integrate seamlessly into a larger filament of Rad51. The capability to integrate into the filament would likely contribute significantly to their ability to regulate and stimulate Rad51 filament formation. Similarly, if Rad55-Rad57 are present inside the filament it would suggest a clear mechanism by which Rad55-Rad57 can inhibit Srs2, as was reported in Wolf Dietrich-Heyer's laboratory (35). In this work, Rad55-Rad57 was found to block the ability of Srs2 to unwind Rad51-coated DNA. If Rad55-Rad57 were integrated into the Rad51 filament formation, a logical model for how this activity

would function would be to serve as a physical barrier or block that prevents the Srs2 helicase from freely translocating along DNA, disassembling Rad51 filaments. In order to determine the function of the different regulators of HR it will be essential to determine how these proteins interact with the Rad51 filament.

1.1.3 Rad51-dependent strand invasion and resolution of HR

Once a Rad51 filament forms, it is stimulated to invade duplex DNA by the Swi/Snf translocase Rad54 and search for a homologous stretch of DNA (39,40). Several recent advances have changed our views of how Rad51-dependent strand invasion occurs. Using DNA curtains to directly visualize Rad51 filaments, Eric Greene's group have reported that Rad51 filaments are broken into multiple segments by clusters of Rad52 and RPA (27). They predict that this segmentation is critical to allow each patch of Rad51 in the larger filament to perform its own homology search, dramatically improving the predicted efficiency of the homology search (27,41). Critically, this data is supported by their recent observation that the minimal number of nucleotides needed for Rad51 to interrogate DNA for homology is eight, and that just fifteen nucleotides is sufficient to allow stable association of the Rad51 nucleoprotein filaments with a homologous stretch of DNA (41). These findings support a model where the larger filament of Rad51 is intentionally split into many smaller filaments by complexes of Rad52-RPA to allow several smaller segments of Rad51 to independently carry out the homology search. Previous studies have suggested variable tract lengths for Rad51 filaments during HR, ranging from 100 to 4000 nucleotides. Given how Rad51 filaments tend to extend DNA and reduce flexibility, these clusters of Rad52-RPA may additionally act by breaking up the relatively rigid Rad51 filament, to introduce flexibility into the Rad51 filament during homology search (27).

After Rad51 filaments identify the homologous template, they are induced to form a stable strand invasion product by the activity of Rad54 and Rdh54 (Figure 1). Once the strand invasion product forms, Rad51 monomers at the end of the strand invasion product need to be disassembled by Rad54 to allow DNA polymerases to access the heteroduplex DNA, a process that requires the ability of both Rad51 to hydrolyze its ATP and release dsDNA (42-44). The recent observation that human RAD54 can be integrated into the RAD51 filament, where it occupies both the ends of the filament as well as internal sites suggests that RAD54 may be able to disassemble the RAD51 filament from the inside-out as well as from the ends (36). Interestingly, work in budding yeast has found that the invading ssDNA is extended by an average of 1700 base pairs (45,46), which is significantly greater than the minimal amount of homology required for the extended strand invasion product to find a homologous sequence on the other side of the DSB. For instance, work from Eric Greene's laboratory has suggested that with as little as 15 BP of homology past the DNA break site, the extended strand should be capable of reannealing to the other side of the break to allow repair (41), while commonly used gene knockout strategies in budding yeast have found that 50 base pairs of homology is sufficient to allow robust HR to occur (47). Why such long tracts of DNA are copied during strand invasion and extension remains an open question in the field.

After the strand invasion product is extended, the newly extended ssDNA end needs to be disassembled from the template DNA to allow reannealing and ligation to the other side of the break. Resolution of HR can take the form of several, multi-step processes outlined here and in Figure 1 which can result in either crossover or non-crossover outcomes. In the simplest form of repair, called synthesis dependent strand annealing, the second end of the DSB is not engaged, the heteroduplex is unwound to allow the extended ssDNA end to reanneal to the other side of the

DSB, and the remaining gaps are then filled in and ligated (Figure 1, SDSA). This repair process forms a fully intact DNA helix without a crossover (2).

Alternatively, the second end of a DSB can be “captured”, forming a double Holliday junction (dHJ). The mechanisms underlying second end capture of the DSB have remained mostly unresolved, although recent observations that complexes of Rad52-RPA will coat a filament of Rad51 have suggested that these proteins and their ssDNA binding activity may be essential for the capture of the second end of a DSB. Once formed, the double Holliday junction can be cleaved by various nucleases, most commonly Mms4-Mus81 and Yen1 in budding yeast. Cleavage by nucleases can result in both non-crossovers and crossovers depending on how the dHJ is cleaved (Figure 1, left and right sides respectively). Alternatively, the double Holliday junction can be unwound to a hemicatene structure and dissolved by Sgs1-Top3-Rmi1 ((Figure 1, center, (2,48-52)). Disruption of the normal resolution of double Holliday junctions, such as in an *sgs1*Δ cell, leads to an extreme sensitivity to DNA damaging agents, a hyper-recombinogenic phenotype, and slow growth caused by the accumulation of these unrepaired, or misrepaired, double Holliday junctions. Importantly, disruption of the HR machinery, which generates these double Holliday junctions, can dramatically suppress the phenotypes of mutations in Sgs1, Top3, or Rmi1 (Figure 1).

In an alternative form of HR called break induced replication (Figure 1, BIR), the second end of a DSB is never captured and the strand invasion product becomes a full-fledged replication fork (53). BIR appears to be primarily used to repair replication forks that collapse into a one-ended DSB, although BIR can also be observed in various assays at an inducible DSB when the second-end of the break is never captured (54). While BIR is technically HR, as it appears to require Rad52 in all instances studied, there appear to be both Rad51-dependent and independent

mechanisms of initiating BIR (55). Importantly, BIR has recently emerged as a critical repair pathway in different cancer cells experiencing replicative stress (53). Additionally, several kinds of gross chromosomal rearrangements observed in cancers seem to arise from BIR at replication forks, which makes understanding this form of HR critical for the treatment of cancer (53). While BIR plays an important role during replicative stress in cancer cells, other forms of HR, which are discussed in detail below, appear to be the primary form of HR used at a stalled replication forks in otherwise healthy cells.

1.2 HOMOLOGOUS RECOMBINATION AT A REPLICATION FORK

While use of direct DSB systems, such as inducible endonucleases, were invaluable for elucidating the critical steps of HR, the most physiologically relevant substrate for HR in normal cells is likely to be ssDNA gaps accumulating at a stalled replication forks (12,56,57). These ssDNA gaps can accumulate whenever a replication fork encounters a lesion that blocks polymerase extension, such as a methylated base, as generated by MMS treatment, abasic sites caused by aborted base excision repair, protein-DNA adducts such as those formed from crosslinking agents, or even the photoproducts generated in DNA by UV treatment. Additionally, replication forks that encounter a ssDNA break can collapse into a one ended DSB that can be repaired by a break induced replication-like method, as shown in Figure 1. This dissertation focuses almost exclusively on the kinds of HR thought to initiate from ssDNA gaps produced at stalled replication forks, which is discussed in greater detail below and in Figure 2.

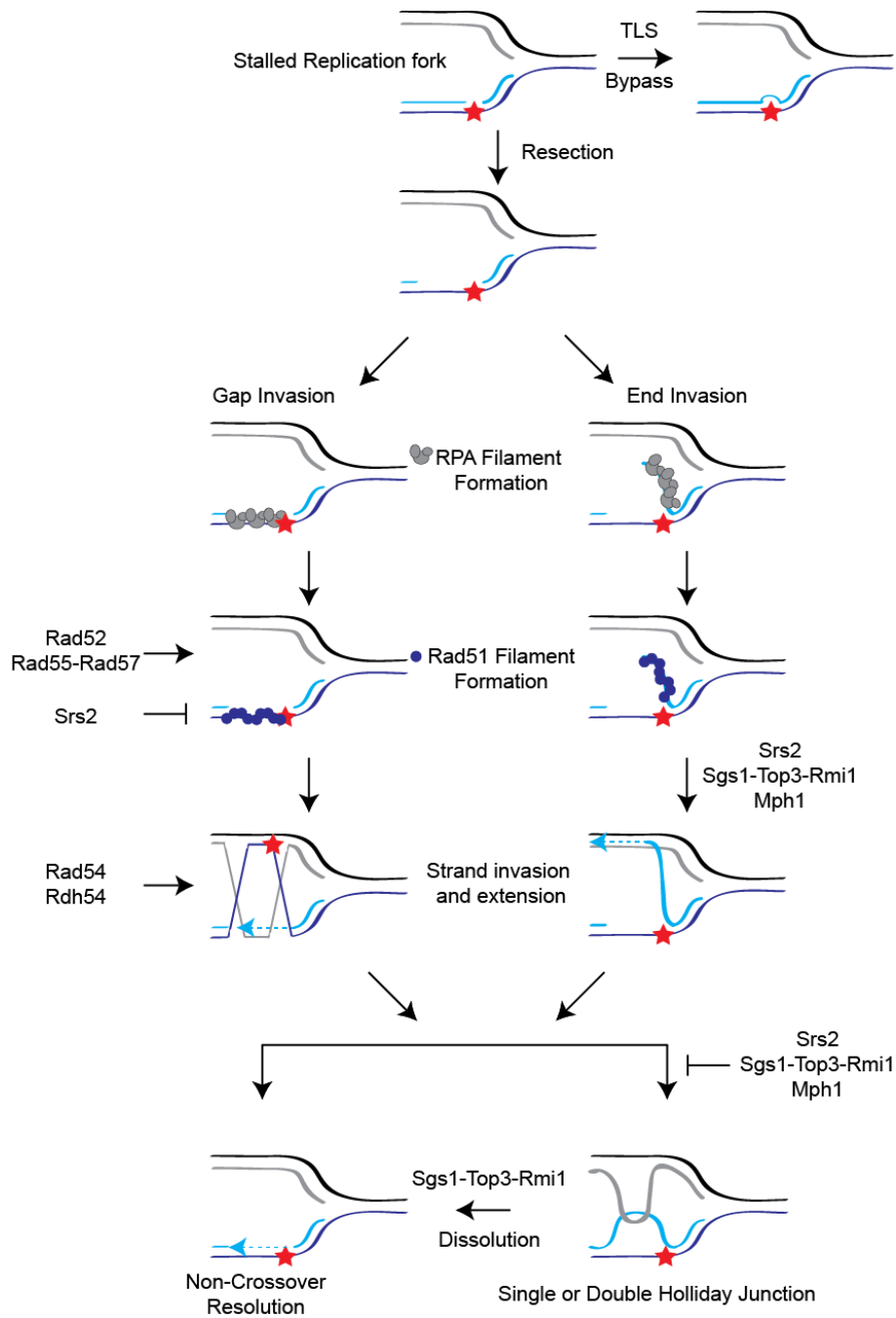


Figure 2. A schematic of two proposed models for post-replicative repair at a replication fork.

Error-prone post-replicative repair is shown in the top right as bypass by translesion synthesis polymerases, while two different models for error-free post-replicative repair by homologous recombination are shown on the bottom. Yeast proteins are included in black.

In a broad sense, the steps of HR at a replication fork are likely very similar to direct DSBs, comparing the different pathways in Figure 1 and Figure 2. After a replication fork stalls, there is resection mediated by the MRX complex that generates ssDNA gaps (56). As has been shown for Exo1(58), these gaps are further extended by the same set of nucleases as in a direct DSB. The ssDNA gaps (Figure 2, gap invasion) have been hypothesized to be the sites where HR initiates, and as such they are predicted to accumulate RPA before Rad51 filaments form (12).

Despite their central role in the models of HR at replication forks, direct evidence that HR initiates from ssDNA gaps at stalled replication forks has only very recently been produced. Dana Branzei's group purified the stalled replication forks produced in MMS treated cells and visualized them by EM (59). They found different HR structures in the MMS-treated strains, such as structures resembling Holliday junctions, double Holliday junctions, and the hemicatenanes predicted to form during Sgs1-mediated dissolution of dHJs (as shown in Figure 2). Critically, these substrates all appear to initiate from gaps of ssDNA present in the dsDNA rather than ssDNA ends like those found at DSBs (Figure 2, gap repair). These striking findings strongly support the prevailing models where ssDNA gaps at replication forks are substrates for Rad51-mediated HR, and that Rad51-mediated HR is in turn critical for fork progression in response to damaged DNA.

Although direct evidence for HR at replication forks has only recently emerged, a wealth of genetic evidence has been reported detailing the pathways that regulate bypass of different lesions at a replication fork, called post-replicative repair (PRR). The PRR pathway can be broken into two components, the potentially error-prone translesion synthesis (TLS) pathway, and the error-free PRR pathway, which is carried out through HR-mediated bypass of lesions at a stalled fork (Figure 2). Error-prone PRR relies upon the availability of the TLS polymerases, as encoded by *REV1*, *REV3*, and *REV7* (60,61). PRR is initiated by a complex of Rad6-Rad18, which

monoubiquitinates PCNA (Pol30), which then recruits the error-prone PRR machinery. Error-free PRR, however, is initiated by the polyubiquitination of PCNA which is largely dependent upon the Mms2-Ubc13 complex and Rad5 (60). Once PCNA is polyubiquitinated, HR mediated bypass of the lesions that caused the replication fork to stall is initiated. HR at the replication forks has been found to require all of the normal HR machinery such as Rad51 and Rad52, in addition to a novel regulator of HR that seems to work exclusively at replication forks, the Shu complex (60,61).

1.3 THE SHU COMPLEX

The budding yeast Shu complex (suppressor of Hydroxyurea sensitivity) was first characterized a decade ago in Dr. Rodney Rothstein's laboratory as genes whose deletion would suppress the slow growth, hydroxyurea (HU), and MMS sensitivity of *SGS1* or *TOP3* mutants (62,63). The initial characterization of the Shu complex found that it functions as an obligate heterotetramer comprised of Shu1, Shu2, Csm2, and Psy3, where deletion of any one gene would similarly suppress *sgs1Δ* and *top3Δ* cells' phenotypes. This original characterization of the Shu complex found that it acted in the Rad52 epistasis group during treatment with MMS, indicating that the Shu complex functioned during HR. Moreover, due to the suppression of the phenotypes of *sgs1Δ* and *top3Δ* cells, it was presumed that the Shu complex acted early in HR to help promote the formation of the double Holliday junctions that cause toxicity in *sgs1Δ* cells. Interestingly, loss of the Shu complex, despite their modest sensitivity to DNA damaging agents when compared to Rad52, creates a mutator phenotype identical to deletion of Rad52, suggesting that the mutator phenotype generated by loss of Rad52 may be caused by impaired function of the Shu complex. Finally, this work found that the Shu complex's mutator phenotype was entirely dependent upon the translesion

polymerase Rev3, which importantly placed the Shu complex as acting at the kinds of stalled and broken DNA replication forks where translesion polymerases could act. These findings were largely reconfirmed in a separate manuscript by the Xiao group, which additionally expanded upon the observation that the Shu complex's mutator phenotype was caused by Rev3, to place the Shu complex in the error-free branch of post-replicative repair (PRR) downstream of MMS2, UBC13, and RAD5 (60).

A year after the budding yeast Shu complex was characterized, Paul Russel's group identified potential Shu complexes in both fission yeast and humans, which suggested that the Shu complex may be conserved throughout eukaryotic lineages (64). This work found that the budding yeast Shu2, which contains a SWIM domain that regulates zinc binding, has a clear homologue in fission yeast. Importantly, this homologue of Shu2 was found to physically associate with Srs2, confirming a high-throughput yeast-2-hybrid screen that found budding yeast Shu2 also interacts with Srs2 (63). This homologue of Shu2 was named Sws1, SWIM domain-containing and Srs2-interacting protein 1 (64). The fission yeast Sws1 was found to physically associate with two divergent Rad51 paralogues, Rdl1 and Rlp1. Critically, disruption of Sws1, Rlp1, or Rdl1, produced a phenotype of weak sensitivity to MMS, and suppression of the slow growth and HU and MMS sensitivity of the fission yeast homologue of Sgs1, Rqh1. These phenotypes are very similar to those observed after disruption of the budding yeast Shu complex, supporting the hypothesis that these are functionally similar complexes. Importantly, this work also found that disruption of Sws1 would significantly decrease Rad51-dependent HR using a recombination assay that can measure Rad51-dependent and independent repair outcomes, producing the first piece of evidence that the Shu complex might act upstream of Rad51 filament formation. These findings were further supported by work from Ian Hickson's laboratory that found the budding

yeast Shu complex was likely acting at the same epistasis steps of Rad51 and Rad54 to promote the formation of Rad51-dependent repair intermediates, again placing the Shu complex at an early step of Rad51-dependent repair (65). By studying fission yeast Sws1, the authors also identified a Shu2/Sws1 homologue in humans, called SWS1 (64). They found that SWS1 also interacts with a Rad51 paralogue, RAD51D, and that loss of SWS1 would result in defects in RAD51 focus formation in IR-treated human cells. These findings were corroborated by a publication in 2011 that found that human SWS1 forms an obligate heterodimer with a novel Rad51 paralogue, SWSAP1 (SWS1-associated protein 1), and that disruption of either gene leads to an identical phenotype of MMS sensitivity (66). Interestingly, this work also discovered that SWS1-SWSAP1 is capable of interacting with most of the human Rad51 paralogues and that the human Shu complex has DNA binding capabilities. These two critical papers laid out many important foundations for our understanding of the Shu complex, such as the fact that the Shu complex is likely conserved throughout eukaryotes where it is comprised of a SWIM-domain containing protein interacting with Rad51 paralogues, and that its function is likely to promote Rad51-dependent repair in each organism studied.

The observation that the fission yeast and human forms of SWS1 form complexes with the Rad51 paralogues led to speculation that some members of the budding yeast Shu complex may also be Rad51 paralogues, but this was not confirmed until 2012 when two groups published the crystal structure of Csm2 and Psy3 (67,68). These papers both determined that Csm2 and Psy3, despite sharing little sequence similarity with one another or with Rad51, structurally look like one another and the core of Rad51, making them novel, divergent Rad51 paralogues. Additionally, these papers both found that Csm2 and Psy3 together contain a DNA binding activity, and that Shu1 and Shu2 were dispensable for this activity. The finding that the Shu complex was comprised,

in part, of Rad51 paralogues was an incredibly important finding for the field. Most other examples of Rad51 paralogues, such as Rad55-Rad57, the Shu complexes in fission yeast and humans, and the Rad51 paralogue complexes in human (BCDX2 and CX3 complexes) are all known to associate with Rad51 or to regulate its function (24,69). Combined with all the previous data discussed on the known functions of the Shu complex in promoting Rad51-dependent HR at an early step, the observation that the Shu complex contained Rad51 paralogues strongly supported a model where the Shu complex would likely also regulate Rad51's activity.

1.4 RELEVANCE OF THE HUMAN SHU COMPLEX TO HUMAN HEALTH

In addition to the basic science benefit of understanding the mechanistic function of this novel complex in promoting HR, there were several compelling reasons to study the Shu complex due to its importance in human health. Many of the putative members of the human Shu complex, especially the Rad51 paralogues, have repeatedly been found to play an important role in cancer development. Hundreds of epidemiological studies have found that individuals who inherit homozygous mutations in the Rad51 paralogues have an elevated risk of cancer (70-75). Originally these studies principally found these mutations predispose carriers to breast and ovarian cancers, but subsequent work has also found elevated risk of colorectal cancer for some mutations (70-75). Certain individual mutations, such as the XRCC3 threonine 241 to methionine mutation have turned up in hundreds of studies finding a potential role for this mutation in cancer development (75). Despite this central role of the Rad51 paralogues in cancer predisposition, studying the causative effects of these mutations on cancer are hampered by the difficulty in studying the human

proteins, discussed in detail in section 1.4, as well as the fact that, to-date, no well-supported mechanistic function for the Rad51 paralogues in humans has been demonstrated.

Beyond a role in cancer development, mutations in RAD51C were recently characterized as causing Fanconi Anemia, leading to RAD51C being categorized as FANCO (76). A major question raised by this study is how do different mutations in RAD51C result in cancer predisposition in some patients, but other mutations result in the development of Fanconi Anemia. Moreover, the finding that the Rad51 paralogues in humans had potential separation-of-function mutations that would distinguish their roles in HR from their role in interstrand crosslink repair, which underlies Fanconi Anemia, raised excitingly possibilities that these naturally occurring mutations would help elucidate the functions of these proteins in each repair pathways. However, the ability to use these separation-of-function mutations was stymied by the poor mechanistic understanding of the Rad51 paralogue complexes in humans, as well as the essential nature of these proteins in human DNA repair. In order to study these critically important regulators of human health, it became apparent that establishing the mechanistic function of these complexes in a more tractable model system might be the most productive approach to take.

1.5 USE OF THE BUDDING YEAST MODEL SYSTEM

Owing to the important role of the putative human Shu complex members in diseases such as cancer and Fanconi anemia, the focus of this dissertation project was on understanding the mechanistic function of the Shu complex. However, there were multiple obstacles present to studying the Shu complex in mammalian systems that made using the budding yeast system preferable. Several groups had tried to make mice models by disrupting the Rad51 paralogues and

have found that these genes are essential for viability, as the mice display early embryonic lethality (77-80). In human cell culture, disruption of these proteins has also proven problematic as they appear essential for growth in culture as well (Maria Jasin, correspondence), and similar, unpublished work from our lab has found that lentiviral knockdown of SWS1 in different human cell lines prevents sustained growth of the cells. Together, the essential nature of the putative Shu complex genes has made studying the mechanistic function of the Shu complex difficult in human cells or mouse models. Fortunately, the Shu complex and Rad51 paralogue genes are not essential in budding yeast and can readily be disrupted *in vivo* (62,81,82). This has enabled researchers to study the phenotype of the full deletion of the Shu complex, which has led to several important discoveries about the Shu complex that have helped place its roles at an early stage of HR. The fact that the Shu complex can readily be disrupted in budding yeast, allowing easy, high-throughput analysis of the phenotype of cells without the Shu complex was one important reason we chose to study the mechanistic function of the Shu complex using the budding yeast system.

The second critical limitation to studying the Shu complex in humans is that the human versions of the Shu genes, especially the Rad51 paralogues, have proven to be difficult to purify and work with due to their insolubility (83). The studies where these proteins have been purified have necessitated purifying many proteins simultaneously, e.g. RAD51B, RAD51C, RAD51D, and XRCC2 in the BCDX2 complex, which makes *in vitro* studies more difficult, costly, and time consuming to perform with the human Rad51 paralogues (83). Fortunately, these problems are lessened when using the budding yeast proteins. The Rad51 paralogues Rad55-Rad57 have been purified and studied *in vitro* for nearly twenty years (24), and the recent papers crystallizing Csm2-Psy3 have found that the Shu complex is readily purified as a pair of dimers (Csm2-Psy3 and Shu1-Shu2), as a trimer (containing Psy3-Shu1-Shu2), or as a tetramer (Csm2-Psy3-Shu1-Shu2).

Critically, at least Csm2-Psy3 have been shown to readily form crystals, enabling many potential studies which are discussed further in the discussion (chapter 5). Furthermore, many of the mechanistic studies involving HR have utilized budding yeast proteins such as Rad51, Rad52, Srs2, or Rad54, so any future *in vitro* work we would want to perform on the Shu complex would likely benefit from having available known protocols to purify and work with these other HR proteins (24,33,34). Given our ongoing collaborations with both crystallographers at the University of Pittsburgh and other experts in *in vitro* biochemical studies of HR proteins, we felt that the budding yeast Shu complex was an excellent candidate for rapid, effective studies on the mechanistic function of the Shu complex in eukaryotes.

Beyond the reasons directly related to the Shu complex, the budding yeast model system offered numerous benefits relative to human cell culture or other model systems. These included intangible benefits, such as a laboratory-wide expertise in yeast techniques that enabled new protocols in yeast to be rapidly implemented, as well as a close relationship with Rodney Rothstein's laboratory, which originally characterized the budding yeast Shu complex and was able to provide invaluable advice and material support in the form of related yeast strains. Additionally, our laboratory was equipped with several unique pieces of equipment that made specialized study of the budding yeast Shu complex possible. These included an automated pinning robot that is capable of performing high-throughput synthetic growth analysis studies in yeast. As an example, this machine is able to generate growth analysis for a deletion of a Shu complex gene combined with every single non-essential gene in the yeast genome in approximately two weeks. Furthermore, our lab contained a state-of-the-art fluorescent microscope specifically set up to visualize fluorescent yeast strains that was invaluable in generating data for this dissertation (see chapter 3). Finally, yeast have multiple intrinsic benefits compared to other model systems that

were important for this study. Yeast grows incredibly quickly and in inexpensive media, allowing rapid experimentation. Additionally, yeast is a genetic model system, allowing the combination of gene deletions and genetic assays (e.g. recombination or mutagenesis assays) into a single strain. This kind of genetic analysis is incredibly powerful when determining where genes function in a specific pathway and for analyzing the interplay between different DNA repair pathways.

1.6 MAJOR HYPOTHESES

At the start of this dissertation, there were several essential, unanswered questions remaining about the Shu complex that formed the basis of this body of work. The first asked how well the Shu complex was conserved from budding yeast to humans, and served to confirm the budding yeast Shu complex would serve as a useful model system for studying the more inaccessible human Shu complex. The second hypothesis dealt with which portions of the HR machinery the Shu complex was interacting with, and helped place the Shu complex in an early step of HR. Finally, the third hypothesis was about the mechanistic function of the Shu complex in HR. Each hypothesis is discussed in detail below with a summary of the pertinent background information that supported the hypothesis.

1.6.1 The Shu complex is well conserved from budding yeast to humans

The budding yeast system has been extensively studied because many genes in yeast have clear homologues and orthologues in humans. Many genes are so well conserved that a recent study looking at essential yeast genes found that half could be replaced with their human counterpart and

still produce viable cells (84). At the start of this work, several lines of evidence supported the first hypothesis discussed in this work, that the Shu complex is well conserved from budding yeast to humans. The first, crucial observation was that Shu2 has a potential homologue in fission yeast, and that this homologue seemed to perform an analogous function to promote HR (64). Additional work revealed that Shu2 likely also has a potential homologue in humans, Sws1 (64,66). However, two critical questions remained from these studies. Importantly, these studies had not determined if the SWS1 proteins in humans and fission yeast were truly orthologous to the budding yeast Shu2, or if these proteins had arisen separately in these organisms through parallel evolutionary pressures. Additionally, due to the study of HR across numerous other model organisms, it was necessary to determine if Shu2/SWS1 was conserved in other eukaryotic model systems, such as in *C. elegans* or *D. melanogaster*.

The second set of data supporting the hypothesis that the Shu complex is conserved throughout eukaryotes came from the two crystallization papers published in 2012 (67,68) that discovered that Csm2 and Psy3, two members of the Shu complex, were in fact structurally Rad51 paralogues. Combined with the findings in fission yeast that Sws1 interacts with the Rad51 paralogues Rlp1 and Rdl1, and the observation that human SWS1 is an obligate heterodimer with the divergent Rad51 paralogue SWSAP1, this supported the hypothesis that the Shu complex is conserved from yeast to humans, where it is comprised of a Shu2/SWS1 protein interacting with divergent Rad51 paralogues (64,66). However, in order to further support this hypothesis, potential Shu complexes in other species would need to be catalogued and screened for any evidence that they may also be comprised of Rad51 paralogues.

Chapter two of this dissertation provides evidence in support of the hypothesis that the Shu complex is well conserved throughout all eukaryotic lineages, where it is comprised of a Shu2/SWS1 orthologue physically associating with novel Rad51 paralogues.

1.6.2 The Shu complex interacts with the HR machinery and promotes Rad51-dependent HR

At the start of this dissertation, two manuscripts crystallizing the Shu complex proteins Csm2 and Psy3 had recently been published (67,68). Their findings that Csm2 and Psy3 are structurally Rad51 paralogues with a DNA binding activity was highly informative for the different hypotheses tested in this dissertation, and in particular chapter 3. In all cases we are aware of, proteins that look like Rad51 tend to associate with one another or with Rad51 itself, and to regulate homologous recombination (24). With this in mind, we hypothesized that the Shu complex would also associate with Rad51 or the Rad51 paralogues, Rad55-Rad57. Additionally, the finding in fission yeast that Sws1 acts to promote Rad51-dependent gene conversion strongly supported the additional hypothesis that the Shu complex would function to promote HR, which is the focus of the end of chapter 3 (64). Finally, several lines of evidence led us to hypothesize that the Shu complex would also preferentially interact with the kinds of structured DNA utilized during HR. First, the crystallization studies discovered that the Csm2-Psy3 dimer, even without Shu1-Shu2, contained a DNA binding activity. Second, some of the only published work on the purified human Rad51 paralogues found that the BCDX2 complex, which is comprised of Rad51 paralogues, preferentially binds to forked DNA like that at a replication fork or double Holliday junction (85). Finally, the Shu complex itself only seems to function in the repair of stalled or broken replication

forks, which would likely also contain structured DNA substrates such as forked DNA that would act as a substrate for the initiation of HR.

Together, these lines of evidence supported the hypothesis that the Shu complex would interact with the HR machinery, including both the protein regulators of HR and the DNA substrates used during HR, and promote Rad51-dependent HR, which is the focus of chapter 3.

1.6.3 The mechanistic function of the Shu complex is to stimulate Rad51 filament formation

The final hypothesis of this dissertation, that the Shu complex stimulates Rad51 filament formation, was conceived after most of the data in chapter 3 had been generated, which is briefly summarized here. In our study of the Shu complex, we found that Csm2, but not other members of the Shu complex, physically associates with the Rad51 paralogues, Rad55-Rad57, whose function is to stimulate Rad51 filament formation *in vitro* and *in vivo* (24). Importantly, we also found that the Shu complex's function *in vivo* depended upon the presence of Rad55, suggesting the Shu complex acted at the same step as, or downstream of, Rad55. Additionally, in agreement with fission yeast, we found that the Shu complex stimulates Rad51-dependent HR, and we also discovered that the Shu complex could bind to the kinds of DNA substrates where HR would initiate. Combined with other genetic data suggesting the Shu complex acts upstream of double Holliday junction formation (Suppressing *sgs1* Δ and *top3* Δ cells) and upstream of Rad54 in *rad54* Δ cells, this essentially placed the Shu complex at the Rad51 filament formation step with Rad55 (65).

With these data strongly suggesting the Shu complex acts at the Rad51 filament formation step, we hypothesized that the Shu complex, like its binding partner Rad55-Rad57, would also

stimulate Rad51 filament formation. The data supporting this hypothesis is presented in chapter 4, and strongly suggests that the mechanistic function of the Shu complex is to stimulate Rad51 filament formation *in vitro* and *in vivo*.

2.0 EVOLUTIONARY AND FUNCTIONAL ANALYSIS OF THE INVARIANT SWIM DOMAIN IN SHU2/SWS1 PROTEIN FAMILY FROM SACCHAROMYCES CEREVISIAE TO HOMO SAPIENS

There are many proteins that both promote Rad51-filament formation as well as disassemble inappropriate filaments. Interestingly, in many organisms the proteins that stabilize Rad51-filaments themselves share structural homology with Rad51 and evolved from the archaeal *RADB* homologue (86). In humans these RAD51 paralogues include *RAD51B*, *RAD51C*, *RAD51D*, *XRCC2*, *XRCC3* and *SWSAP1* while in the budding yeast they include *RAD55*, *RAD57*, *CSM2*, and *PSY3* (64,67,68,87-90). It has been proposed that *SHU1* is also a Rad51 paralogue (64). A great deal of work has been done to characterize these proteins *in vitro*, *in vivo*, as well as phylogenetically (2,86,91,92). Importantly, many human RAD51 paralogues are mutated in cancers and associated with cancer pre-disposition (92-98). Consistent with a critical role in genome maintenance, disruption of the yeast Rad51 paralogues results in a mutator phenotype and in some cases increased chromosomal rearrangements, which are often observed in tumor cells (62,99). In budding yeast, Shu1 and the Rad51 paralogues Csm2 and Psy3 form an obligate heterotetramer called the Shu complex (also referred to as the PCSS complex) with a fourth member, Shu2, whose major defining feature is a SWIM domain (62,64). The association of divergent Rad51 paralogues with a SWIM domain-containing protein is conserved in fission yeast *Schizosaccharomyces pombe*, where the Rad51 paralogues, Rlp1 and Rdl1, interact with a Shu2-homologue Sws1 (64). Similarly, the human homologue of Shu2, hSWS1, interacts with the RAD51 paralogues RAD51D and XRCC2 (64,66). Importantly, hSWS1 functions as an

obligate heterodimer with hSWSAP1, which itself resembles a previously unidentified, highly divergent hRAD51 paralogue (66).

The conserved association between Shu2-like proteins and the Rad51 paralogues promote Rad51-dependent HR through a largely undetermined mechanism (89). In all species where Shu2-like proteins have been described, their disruption results in a reduction in Rad51 filament formation and a corresponding decrease in HR (62,64,66,90). Strikingly, these defects are similar to disruption of the Rad51 paralogues (90). It remains to be determined what the functional significance of the SWIM domain is, or why Rad51 paralogues associate with SWIM domain containing proteins to promote HR throughout several eukaryotic lineages.

To further our understanding of the Shu2/SWS1 protein family we characterized its evolution across taxonomic groups with a special focus on the conservation of the defining SWIM domain. During this process we confirmed the orthologous relationship of Shu2 and hSWS1 and discovered previously unknown SWS1 orthologues in multiple species, including *Caenorhabditis elegans* and *Drosophila melanogaster*. Interestingly, evolutionary analysis implicates yeast Shu2 and its fly orthologue CG34314 in meiosis, as they show strong rate covariation with meiotic proteins – specifically with those that contribute to HR. Through analysis of eukaryotic Shu2/SWS1 orthologues, we find that the SWIM domain is invariant and can be expanded to include an invariant alanine residue after the canonical SWIM domain. Furthermore, we identified in the literature a cancer patient from the COSMIC database, who harbors a mutation in this invariant alanine (100). *In vivo* disruption of the invariant SWIM domain residues likely results in protein instability and loss of function. Together, our work indicates that the *SHU2* gene is found in all major eukaryotic lineages where it promotes HR in both mitosis and meiosis.

2.1 RESULTS

2.1.1 Characterization of *shu2* Δ recombination phenotype and its physical interactions with other Shu complex members

The Rad51 paralogues have a number of defining features, which are related to promoting Rad51 filament formation such as decreased rates of Rad51-mediated gene conversion upon disruption (24,89,101). Consistently, we previously found that deleting either *CSM2* or *PSY3* results in a decrease in gene conversion and a subsequent increase in Rad51-independent repair (89). To determine if Shu1 or Shu2 have similar roles in promoting Rad51-dependent repair, we performed a heteroallelic recombination assay in wild-type (WT), *shu1* Δ , or *shu2* Δ cells (Figure 3A). In this assay a recombination event between two *leu2* heteroalleles with an intervening *URA3+* gene can generate a *LEU2+* prototroph through repair by Rad51-dependent sister chromatid gene conversion (GC; *LEU2+* *URA3+*) or Rad51-independent intrachromosomal single-strand annealing (SSA; *LEU2+* *URA3-*). Similar to *csm2* Δ or *psy3* Δ cells (89), we find that *shu1* Δ or *shu2* Δ cells significantly decrease rates of Rad51-dependent GC ($p \leq 0.02$ and $p \leq 0.005$ respectively) with a corresponding increase in rates of error-prone SSA (Figure 3A). These results demonstrate that although Shu2 is not a Rad51 paralogue, it exhibits many of the same phenotypes as the other Shu complex members.

The human Shu2 homologue, hSWS1, interacts with multiple RAD51 paralogues either directly or indirectly through hSWSAP1 (64,66). We asked if other yeast Shu members similarly bridge the protein-protein interactions between Shu2 and Shu1 or Psy3 (60,62). To address this

question, we performed yeast-2-hybrid (Y2H) analysis of yeast expressing *SHU2* in the GAL4 DNA binding domain (pGBK-*SHU2*) and tested its interaction with either *SHU1* or *PSY3* expressed in the GAL4 DNA activating domain (pGAD-*SHU1*, pGAD-*PSY3*) in a genetic background where one of the four *SHU* genes is disrupted (Figure 3B and data not shown). We find that loss of *SHU1* disrupts the Shu2-Psy3 Y2H interaction (Figure 3B). Therefore, similar to hSWS1, which interacts with the other hRAD51 paralogues through hSWSAP1, Shu2's interaction with the Rad51 paralogue Psy3 is likely stabilized by Shu1.

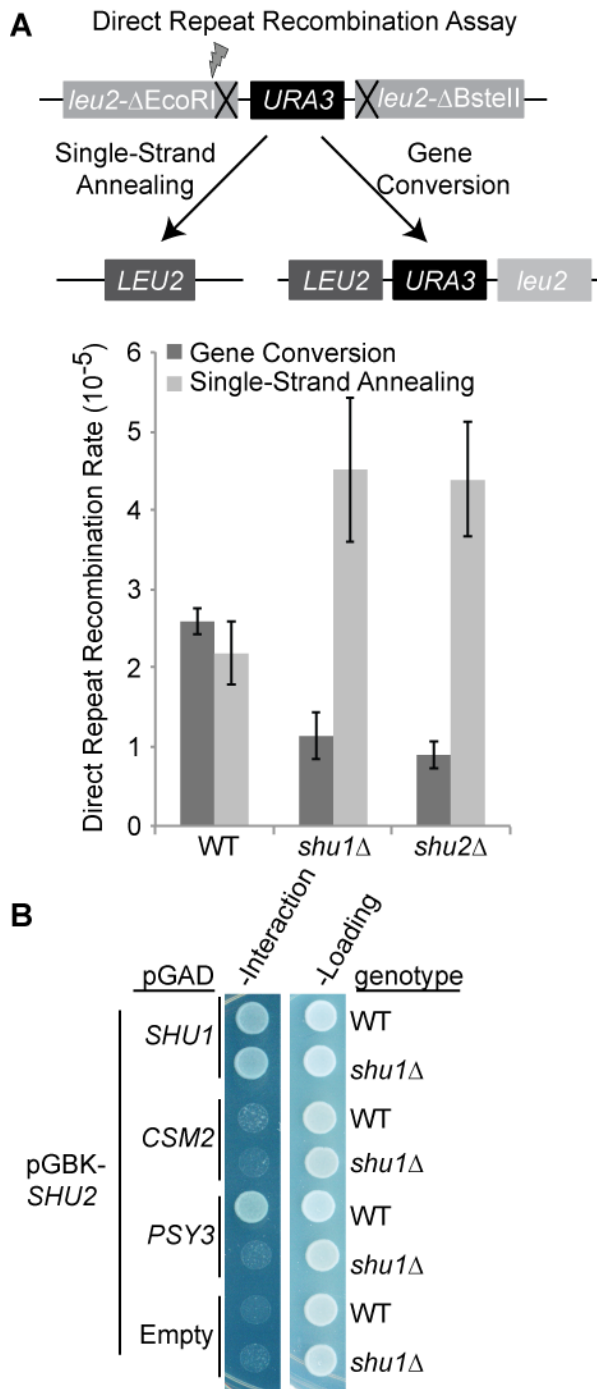


Figure 3. *SHU2* mutants have phenotypes similar to the Rad51 paralogues.

A. Disruption of *SHU1* or *SHU2* leads to decreased rates of Rad51-dependent repair. Diagram of direct repeat recombination assay (*leu2*-ΔEcoRI::*URA3*::*leu2*-ΔBstEII) used to measure rates of direct repeat recombination by Rad51-dependent GC (right side of diagram, Ura+Leu+ colonies) or Rad51-independent

SSA (left side of diagram, Ura-Leu⁺ colonies). The rates of GC and SSA events in *shu1Δ* or *shu2Δ* cells were compared to WT and standard deviations shown. B. Shu1 bridges the interaction between Shu2 and Psy3. Yeast-2-hybrid analysis of pGBK-*SHU2* (containing a GAL4-binding domain) with pGAD-*SHU1*, pGAD-*CSM2*, pGAD-*PSY3*, and pGAD-C1 empty plasmid (containing a GAL4-activating domain) in the presence or absence of the endogenous *SHU1* gene. Interaction is indicated by growth on medium lacking histidine. Growth on medium lacking leucine and tryptophan selects for the individual plasmids and serves as a loading control.

2.1.2 Shu2 orthologues are conserved across eukaryotes

While Shu2 homologues were identified in fission yeast and humans (62,64), their phylogenetic orthology with budding yeast Shu2 has not been demonstrated, nor have Shu2 orthologues been identified in other major eukaryotic lineages, including important model organisms. To produce a complete picture of the SWS1 family we searched for Shu2 homologues across eukaryotic and outgroup archaeal lineages. PSI-BLAST queried with yeast Shu2 yielded hits across fungal species and metazoans. PSI-BLAST queried with human SWS1 (ZSWIM7) led to hits across eukaryotes, including plants, and to archaeal proteins containing a SWIM domain. In addition, we identified putative SWS1 orthologues in several early-branching eukaryote lineages including Diplomonadida (*Giardia lamblia*), Euglenozoa (*Leishmania*, *Phytomonas*), green algae (*Coccomyxa*, *Bathycoccus*), Stramenopiles (*Aphanomyces*, *Albugo*, *Phaeodactylum*, *Ectocarpus*), Alveolata (*Paramecium*, *Plasmodium*, *Oxytricha*), and Ichthyosporea (*Capsaspora*). These sequences clustered with known SWS1 orthologues in phylogenetic trees, separated from archaea outgroup sequences. This deep diversity in addition to known fungal, metazoan, and plant orthologues suggests an ancient origin of the SWS1 protein family. PSI-BLAST recovered

a single protein sequence from each species, suggesting that there were few or no Shu2/SWS1 family duplications and that these orthologues are well conserved.

To define a comprehensive Shu2/SWS1 protein family, we constructed a phylogeny using Shu2 homologues from major eukaryotic and archaeal lineages (Figure 4A). In the resulting phylogeny, eukaryotic sequences were cleanly separated from the archaeal sequences with high branch support (aLRT = 0.98). Moving forward from the archaeal root, the well-supported branches between eukaryotic sequences were in agreement with accepted speciation events, thus supporting the orthology of these Shu2/SWS1 sequences. Although the short alignment (219 amino acids) of Shu2/SWS1 did not provide sufficient power to infer all branch nodes with strong support, these sequences appear to be true orthologues. Notably, this tree revealed Shu2 orthologues in *Drosophila melanogaster* and *Caenorhabditis elegans*, which we will refer to as dmSws1 and ceSws-1 hereafter, as well as an *Arabidopsis thaliana* orthologue AT4G33925. The archaeal SWIM domain-containing proteins served only to root the tree, and we are not able to comment on the orthology or specific function of those sequences.

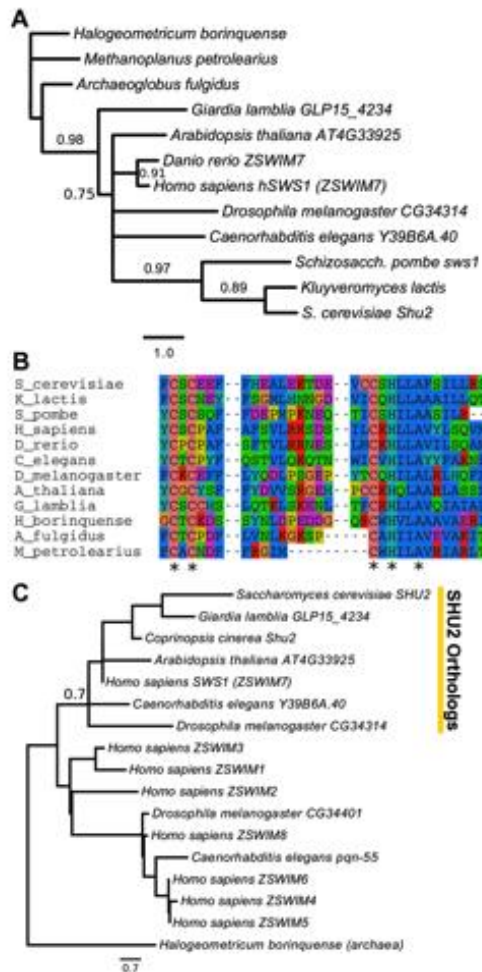


Figure 4. The SWS1 protein family extends across eukaryotes.

A. A phylogeny based on amino acid sequences shows the deep conservation of the SWS1 protein from *Giardia lamblia*, an early branching eukaryote lineage, to plants, fungi and metazoans. The short sequence length did not allow resolution of some interior branches; however, all well supported nodes support the orthology of these sequences. B. A partial multiple alignment shows the highly conserved SWIM domain. Absolutely conserved residues (*) include the defining CXC X_n CXH motif. Double gap columns (--) indicate trimmed regions of low sequence identity. C. The Shu2-SWS1 protein family is a monophyletic clade in this phylogeny of all proteins with SWIM domains from humans, *Drosophila melanogaster*, *C. elegans*, and yeast. The alignment for this phylogeny contained only the 30 most highly conserved residues in the SWIM domain. These relationships further support the newly discovered Shu2-SWS1 orthologues.

A defining feature of the Shu2/SWS1 protein is the SWIM domain, a zinc-binding feature (Figure 4B) (64). To further ensure orthology between yeast Shu2 and human SWS1 (also known as ZSWIM7) in exclusion of other SWIM-domain containing proteins in humans (ZSWIM1 – 6, and ZSWIM8), *C. elegans* (pqn-55) and *D. melanogaster* (CG34401), we constructed a phylogeny with all SWIM domain proteins from these species and all putative eukaryotic SWS1 orthologues (Figure 4C). Homology between these proteins is limited to the SWIM domain so their alignment is limited to a region of 30 highly conserved amino acids. As is expected for a small alignment, many branching nodes were not well resolved; however, the branching pattern cleanly separates the SWS1 orthologues from the other SWIM domain proteins with moderate support (aLRT = 0.70). This topology further supports the putative orthology of the sequences in Figure 4A (i.e. they descended from a single common ancestor).

2.1.3 Shu2 and its orthologs have evolutionary histories strongly correlated with recombination and meiosis-related proteins

To better define the biological function of the Shu complex we performed co-evolutionary analysis in both budding yeast and *Drosophila*. This analysis exploits the observation that functionally related proteins tend to have co-varying rates of evolution, because they experience shared evolutionary pressures. This property can be quantified as evolutionary rate covariation (ERC), reflecting the degree to which two proteins have rates of sequence evolution that covary between species (102-104). ERC for a protein pair is quantified as a correlation coefficient (ranging between -1 and 1) for which higher values reflect stronger rate covariation. ERC values are typically elevated between functionally related proteins genome-wide in yeasts, *Drosophila*, and

also between meiosis and DNA repair proteins in mammals (102,105,106). Hence, elevated ERC for a protein pair suggests co-functionality between them.

We first demonstrated that members of the yeast Shu complex have significantly co-varying rates with each other, as we might predict given their co-functionality (Figure 5A); their pairwise ERC values were highly elevated as a group (mean ERC = 0.52, permutation test $P < 0.00001$), while the expected mean ERC for a random gene set is zero. These ERC values were calculated across a phylogeny of 18 fungal species, including *S. cerevisiae*. We also found elevated ERC values between the Shu complex members and Srs2 (Figure 5A), consistent with a conserved physical and/or genetic interaction between Shu2 and Srs2 (a DNA helicase that disassembles Rad51 filaments) in both budding and fission yeast (63,64,107).

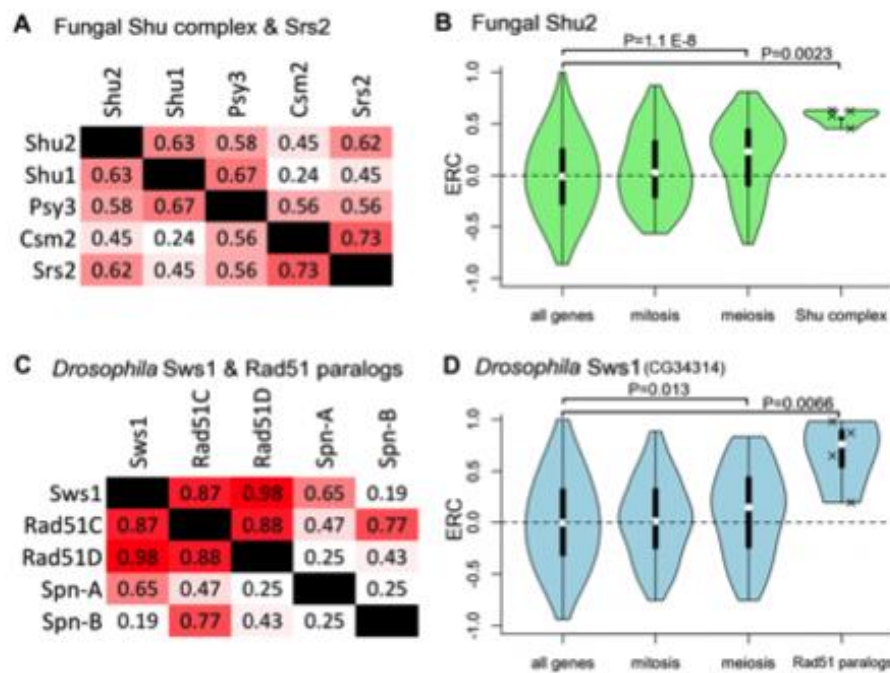


Figure 5. Co-evolutionary signatures indicate Shu2/SWS1 has highly conserved functional relationships with Rad51 paralogues and meiosis proteins.

A. Evolutionary Rate Covariation (ERC) values between members of the Shu complex are highly elevated ($P < 1 \times 10^{-5}$). The degree of red shading in a cell indicates higher ERC for that protein pair compared to the

null expectation of zero. B. Violin plots depict the distributions of ERC values between Shu2 and proteins from various functional classes. Violin width is proportional to density at that ERC value. The genome-wide distribution (all genes) of ERC with Shu2 is centered at zero, as is Shu2 with mitosis genes (N=107 genes). Meiosis (N=126) and Shu complex genes (N=4) show a strong enrichment of high ERC values with Shu2, consistent with co-functionality between them. P-values (horizontal bars) strongly reject similarity between those distributions and the genome-wide distribution. Each of the 4 values in the Shu complex are also plotted with an 'X'. C. *Drosophila* Sws1 (dmSws1), orthologue of fungal Shu2, similarly shows elevated ERC values with Rad51 paralogues. D. DmSws1 also has high ERC values with meiosis proteins (N=116) and Rad51 paralogues (N=4), but not with mitosis proteins (N=129).

To determine the co-evolutionary relationship of the Shu complex with broader functional groups within fungi, we studied Shu2's ERC values with mitotic and meiotic proteins. Shu2 did not show significant rate covariation with mitotic proteins; however, ERC values between Shu2 and meiotic proteins were significantly elevated, suggesting strong co-evolution between them ($P = 1.1 \times 10^{-8}$) (Figure 5B). Importantly, these results were unchanged when recombination-related genes and genes shared by the 2 sets were removed from analysis and so the association is not limited to HR proteins (mitosis $P = 0.27$; meiosis $P = 1.1 \times 10^{-6}$). Similar to Shu2, Psy3 also exhibits significantly increased ERC values with meiotic, but not mitotic, proteins (Figure 21A). In contrast to Shu2 and Psy3, both Shu1 and Csm2 show significant rate covariation with both mitotic and meiotic proteins (Figure 21B and 21C). In addition, the *D. melanogaster* Shu2 orthologue dmSws1 (CG34314) also showed rate covariation with meiotic proteins ($P = 0.013$) and with Rad51 paralogues ($P = 0.0066$), but not with mitotic proteins as a class (Figure 5D). The *Drosophila* dmSws1 results also remained unchanged after removing recombination-related and shared genes (mitosis $P = 0.62$; meiosis $P = 0.0238$). Most notably, Rad51C and Rad51D showed extremely high rate covariation while the other two Rad51 paralogues Spn-A and Spn-B showed modestly elevated levels (Figure 5C). Finally, we tested for co-evolutionary associations of meiotic and

mitotic genes with the mammalian Shu2 orthologue, SWS1 (ZSWIM7). Contrary to results in fungi and *Drosophila*, ERC values between mammalian SWS1 and meiotic and mitotic genes were not generally elevated. Overall, results from fungi and *D. melanogaster* suggest that the Shu complex has conserved meiotic and mitotic roles in eukaryotic species.

2.1.4 Expansion of the SWIM domain to include an invariant alanine three amino acids down-stream of the canonical CXC...Xn...CXC motif

The SWIM motif was originally defined as a zinc binding motif that contains the canonical CXC...Xn...CXH sequence (108-110). However, upon analysis of our evolutionarily deep alignment we identified an invariant alanine located three amino acids downstream from the CXH motif (Figure 6A, Figure 21). Interestingly in humans, this invariant alanine in hSWS1 is mutated to a threonine (A108T) in a cancer patient from the COSMIC database (100). To determine if alanine 108 may be functionally important, we constructed a Y2H vector containing hSWS1 mutagenized to include this mutation, SWS1-A108T, and as well as mutations in the canonical SWIM domain residues (C85S, C87S, C103S, and H105A)(Figure 6B). Suggesting that these residues are functionally important, disruption of the canonical SWIM domain or the invariant alanine (A108) results in a reduced Y2H interaction with hSWS1's obligate binding partner hSWSAP1 (Figure 6B). Interestingly, another highly conserved residue F90, does not result in reduced Y2H interaction when mutated to an alanine (Figure 6B, SWS1-F90A). These results suggest that the SWIM domain in hSWS1 including the invariant alanine are likely important for the hSWS1 function.

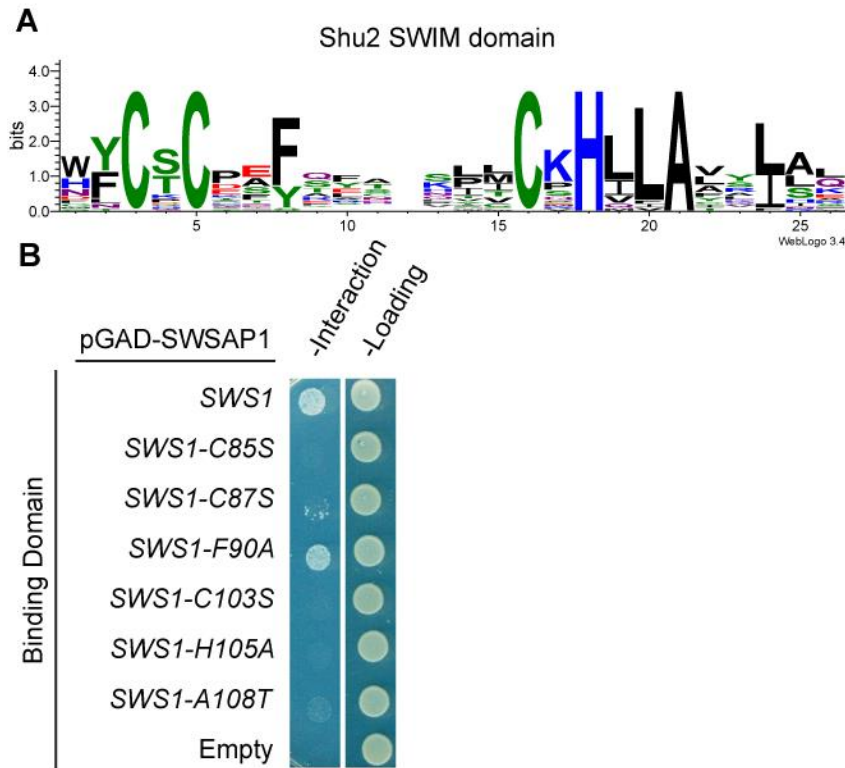


Figure 6. Analysis of the highly conserved SWIM domain residues in the human SWS1 protein.

A. Sequence logo of the SWIM domain reveals a highly conserved phenylalanine two residues after the CXC motif and an invariant alanine two residues after the CXH motif. B. Mutating the SWIM domain in human SWS1 impairs its interaction with hSWSAP1. Y2H analysis of pGAD-hSWS1 with mutations in the SWIM domain (C85, C87, C103, H105) as well as F90 and A108 were assayed for interaction with human SWSAP1 (pGBD-SWSAP1) as described in Figure 3B.

2.1.5 The SWIM domain is important for Shu2's functionality *in vivo*

To investigate the role of the SWIM domain and the invariant alanine, we created Y2H vectors harboring the analogous mutations in budding yeast *SHU2* SWIM domain (Figure 7A). By Y2H, we find that mutating the canonical SWIM domain residues (C114S, C116S, C176S, H178S) in *shu2* results in an undetectable Y2H interaction with Shu2's binding partners Shu1 and Psy3

(Figure 7A). Interestingly, mutating alanine 181 to a threonine leads to a reduced Y2H interaction with Psy3 but not Shu1. Furthermore, while the *hSWS1-F90A* mutant maintains its Y2H interaction with *hSWSAPI*, we find that the corresponding mutation in yeast *shu2*, F119A, results in a reduced Y2H interaction with Psy3 but not Shu1 (Figure 7A). These results suggest that the canonical SWIM domain in yeast Shu2 is likely important for function and that the conserved alanine and phenylalanine may also be components of this domain.

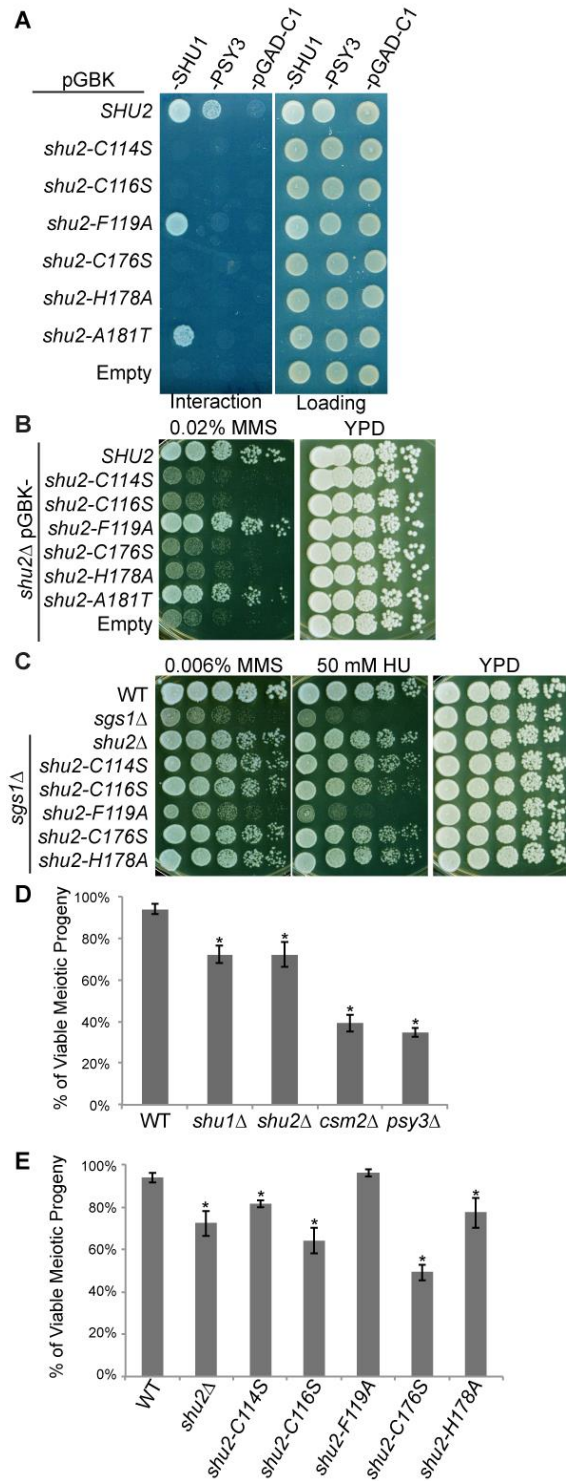


Figure 7. The SWIM domain is important for Shu2's function.

A. Mutating the SWIM domain in *SHU2* impairs its interaction with *SHU1* and/or *PSY3*. Y2H analysis of pGBK-*SHU2* or pGBK-*shu2* mutant interactions with pGAD-*SHU1* or pGAD-*PSY3* as described in Figure

3B. B. Canonical SWIM domain mutants are non-functional. *shu2Δ* cells harboring the indicated pGBK plasmids were 5-fold serially diluted onto YPD medium or YPD medium containing 0.02% MMS and incubated at 30°C for 2 days. C. Disruption of the canonical SWIM domain suppresses *sgs1Δ* DNA damage sensitivity. WT, *sgs1Δ*, *sgs1Δ shu2Δ*, *sgs1Δ shu2-C114S*, *sgs1Δ shu2-C116S*, *sgs1Δ shu2-F119A*, *sgs1Δ shu2-C176S*, *sgs1Δ shu2-H178A* cells were 5-fold serially diluted onto YPD medium or YPD medium containing 50mM HU or 0.006% MMS and incubated at 30°C for 2 days. D. Loss of the Shu complex results in reduced spore viability. Diploid yeast with the indicated mutations were sporulated and individual spores were tetrad dissected onto rich medium. Viable spore colonies from twenty-two individual tetrads were quantitated and the average number of viable meiotic progeny was calculated. Standard deviations are shown from three experiments and significance determined by t-test ($p < 0.05$). E. Same as D except that *shu2* SWIM domain containing mutants were analyzed.

To determine if the impaired Y2H interactions of the SWIM domain mutants result in diminished DNA damage tolerance in yeast, we complemented *shu2Δ* cells with a wild-type *SHU2* or a mutant *shu2* expressing plasmid. We find that the wild-type *SHU2* plasmid complements the MMS sensitivity of *shu2Δ* cells while mutations in the canonical SWIM domain (C114S, C116S, C176S, and H178A) do not (Figure 7B). Interestingly, despite the altered protein-protein interactions observed in both *shu2-F119A* and *shu2-A181T*, both these mutant plasmids complement the MMS sensitivity of a *shu2Δ* cell (Figure 7B). These results indicate that the interaction between Shu2 and Psy3 may be dispensable for Shu2's mitotic function. These findings were confirmed when we stably integrated the canonical SWIM domain mutants (C114S, C116S, C176S, and H178A) as well as F119A at the endogenous *SHU2* locus (Figure 21). Unfortunately, we were unable to integrate A181T into our yeast strains. Since the Shu genes were originally characterized for their ability to suppress a *top3Δ* or *sgs1Δ* strain's sensitivity to MMS or HU treatment, we also examined if the integrated SWIM domain alleles

would also rescue *sgs1Δ* DNA damage sensitivity like disruption of *SHU2*, and find that the canonical SWIM domain mutants do (Figure 7C). Similar findings are also observed with a SWIM-domain mutation in the fission yeast gene *sws1-C152S* (64). Thus, our analysis of the four canonical SWIM domain mutants demonstrate that the conserved SWIM domain is important for this protein family's function in the repair of MMS-induced DNA lesions.

Given the conserved nature of the Shu complex in meiotically dividing yeast, we asked how disruption of the SWIM domain would affect meiotic outcome in *S. cerevisiae*. To test this, we sporulated diploids homozygous for deletion of a single Shu complex member and screened for viability of the resulting offspring. In agreement with two recent reports (90,111), we find that loss of any member of the Shu complex causes a marked decrease in spore viability, with Csm2 and Psy3 resulting in a more severe defect (Figure 7D, $p \leq 0.02$ for all). Next we tested if mutations of the SWIM domain would similarly lead to decreased meiotic progeny. We find that the SWIM domain mutants C114S, C116S, C176S, and H178A, are also defective for spore viability compared to WT (Figure 7E; $p \leq 0.05$ for all). In contrast, the *shu2-F119A* allele spore viability was similar to WT (Figure 7E). These results demonstrate that the canonical SWIM domain is necessary for Shu2's role during meiosis.

2.2 DISCUSSION

Here we describe how the SWS1 protein family has evolved throughout major eukaryotic lineages to interact with the Rad51 paralogues to promote HR. One defining feature of the SWS1 protein family is its invariable SWIM domain (consisting of CXC...X_n...CXH motif where X is any amino acid and n is a variable number of amino acids) and we show that this domain is important for protein functionality. Furthermore, our analysis indicates that the SWIM domain contains an invariant alanine two residues after the CXH motif, which would expand the domain to CXC...X_n...CXHXXA. Specifically, in budding yeast, mutation of the canonical SWIM domain residues reduces Rad51-dependent repair, meiotic viability, and protein-protein Y2H interactions. Additionally, we show further evidence that the Shu complex has an important meiotic function and that this function is evolutionarily conserved. We demonstrate that the SWS1 family is found across eukaryotes and are the first to identify orthologues of SWS1 in important model organisms such as *D. melanogaster* and *C. elegans* as well as in additional fungal and ancient eukaryotic lineages.

Regulation of meiotic recombination is critical for maintenance of chromosome copy number and genetic diversity. Consistent with a central role for the yeast Shu complex during meiosis, loss of Shu2 or its binding partners reduces the viability of meiotic offspring, implicating this complex as a critical meiotic regulator (Figures 7D and 7E). It was recently demonstrated that the Shu complex has an important function in the recruitment of Rad51 to meiotic DSB sites and that Shu1 promotes homologue bias (90,111). In agreement with these findings, patterns of co-evolution also highlight the importance of the Shu complex in meiosis as we find that all the Shu complex members, including Shu2, are co-evolving with other meiotic

proteins as shown by elevated ERC values (Figure 5, Figure 20). Importantly, we do not observe elevated ERC values between Shu2 or Csm2 with mitotic proteins unlike the other Shu complex members, Shu1 or Psy3 (Figure 5, Figure 20).

Upon further analysis we identified the *D. melanogaster* SWS1 orthologue, which is also likely to function during meiosis. dmSws1 is primarily expressed in the ovaries which are the site of meiotic crossing over in flies (112,113). In contrast, dmSws1 is not significantly expressed in other adult tissues including the testes, which do not produce recombinant gametes in *Drosophila*. Consistent with dmSws1's ovarian expression, we find that dmSws1 also exhibits strong co-evolutionary signatures (ERC) with meiotic proteins, just as observed for its budding yeast orthologue Shu2 (Figure 5B and 5D). Also similar to Shu2, which physically interacts with the Rad51 paralogues, we find dmSws1 strongly co-evolves with the Rad51 paralogues dmRad51D and dmRad51C (Figure 5A and 5C), which are also primarily expressed in the ovaries. Despite this conserved evolutionary pattern, we were unable to detect a physical Y2H interaction between dmSws1 and dmRad51D, or between ceSws-1 and Rfs-1. However, this may be due to the lack of a third unidentified binding partner as is required for Y2H interaction between the human SWS1 and its hRAD51 paralogues. For example, we only detect a Y2H interaction between hSWS1 with its obligate binding partner hSWSAP1 despite hSWS1's physical interaction with other RAD51 paralogues (64,66). Alternatively, the strong ERC values between dmSws1 and the Rad51 paralogues may be explained by a conserved genetic, but not physical interaction. Together, our work implicates that the SWS1 protein family are likely conserved pro-recombinogenic factors for meiotic HR in multiple eukaryotic lineages. In the

future, direct experimental evidence to examine dmSws1 role in meiotic and mitotic Rad51 filament formation will be necessary to confirm this hypothesis.

While our work indicates that the SWS1 family of proteins functions in meiosis, it is clearly evident that these proteins also promote mitotic HR (60-62,65,89,107). Multiple groups including our own have demonstrated that loss of *SHU2* confers sensitivity to replication fork-damaging MMS in various budding yeast strains, and, consistent with these findings, previous reports have indicated that loss of SWS1 results in a sensitivity to replication fork-blocking agents in both fission yeast and human HeLa cells (64,66). Furthermore, we show here that the SWIM domain in Shu2 is important for the Shu complex resistance to MMS-induced DNA damage. The role and importance of Shu2 and the Shu complex in promoting mitotic HR is not completely understood, although it appears to act in part by regulating the activity of Srs2.

Srs2 is a DNA helicase that destabilizes Rad51 filaments *in vitro* which in turn regulates HR *in vivo* (33,34,114,115). Previous reports have shown that Shu2 physically interacts with Srs2 (63,64) and that loss of Shu1 results in increased Srs2 occupancy at DSB sites (107). Together these findings support a model where the Shu complex may promote Rad51 filament formation by inhibiting Srs2 in mitosis. However, a new report indicates Srs2 has an additional important function in regulating Rad51-dependent repair during meiosis (90,111). In contrast to its role in mitosis, Srs2's function in meiosis is pro-recombinogenic. Furthermore, disruption of *SRS2* does not rescue or alter the meiotic defect observed in a Shu complex mutant suggesting that the genetic interaction between the Shu complex and Srs2 is different during mitosis and meiosis (90). Despite the differing mitotic and meiotic roles of Srs2, the conserved physical interaction between Shu2 and Srs2 and the strong evolutionary covariation clearly indicate that

these proteins have a functionally important relationship (Figure 5A). In the future, the strong ERC observed between Shu complex members could be exploited to identify additional protein modifiers of its HR function, as demonstrated in a recent ERC study (106). Moreover, it remains uninvestigated if hSWS1 or its binding partner hSWSAP1 retains this physical interaction with the putative Srs2 homologues such as PARI or RTEL or if they promote meiotic HR. In conclusion, the SWS1 protein family is an important factor in both mitotic and meiotic HR where future work will shed light on its unique regulatory mechanisms for RAD51.

2.3 MATERIALS AND METHODS

2.3.1 Yeast strains, plasmids, and media

The strains used in this study are listed in Table 2 and are isogenic to *RAD5+ W303*, except for the PJ69-4A and PJ69-4 α yeast-2-hybrid strains (116-118). The primers used are listed in Table

3. Standard protocols were used for yeast culturing, transformation (LiOAc method), sporulation, and tetrad dissection. The media was prepared as previously described with twice the amount of leucine (119). The Y2H plasmid for *hSWS1* was created by PCR amplification using pJ636 (pcDNA3-3HA-*hSWS1*) from Paul Russell as a template with oligonucleotides hSWS1.F and h.SWS1.R and sub-cloned into the EcoRI and SalI restriction sites of pGBD-C1 (64). hSWSAP1 was PCR amplified from the MYC-SWSAP1 vector from Jun Huang with oligonucleotides SWSAP1.F and SWSAP1.R and sub-cloned into the EcoRI and SalI restriction sites of pGAD-C1(66). Creation of pGBK-*shu2-C114S* (Shu2.C114S.F and Shu2.C114S.R),

pGBK-*shu2-C116S* (Shu2.C116S.F and Shu2.C116S.R), pGBK-*shu2-F119A* (Shu2.F119A.F and Shu2.F119A.R), pGBK-*shu2-C176S* (Shu2.C176S.F and Shu2.C176S.R), pGBK-*shu2-H178A* (Shu2.H178A.F and Shu2.H178A.R), pGBK-*shu2-A181T* (Shu2.A181T.F and Shu2.A181T.R), pGBD-*SWS1-C85S* (hSWS1.C85S.F and hSWS1.C85S.R), pGBD-*SWS1-C87S* (hSWS1.C87S.F and hSWS1.C87S.R), pGBD-*SWS1-F90A* (hSWS1.F90A.F and hSWS1.F90A.R), pGBD-*SWS1-C103S* (hSWS1.C103S.F and hSWS1.C103S.R), pGBD-*SWS1-H105A* (hSWS1.H105A.F and hSWS1.H105A.R), and pGBD-*SWS1-A108T* (hSWS1.A108T.F and hSWS1.A108T.R) were created using site-directed mutagenesis of the pGBK-*SHU2* or pGBD-*SWS1* plasmids.

Integration of C114S mutation at the endogenous *SHU2* locus was done by creating an integration vector by subcloning with EcoRI and PstI from pGBK-*shu2-C114S* in the yiPLAC211 integration vector. WT yiPLAC-*SHU2* was made by reversing the C114S mutation by site directed mutagenesis using Shu2.S114C.F and Shu2.S114C.R. yiPLAC211 was subsequently mutagenized to C116S, F119A, C176S, H178A, and A181T with the primers listed in Table 3. The WT and mutant versions of yiPLAC211-*shu2* was linearized with BamHI and transformed into W9100-2D. Pop-outs were screened on 5-Fluorooritic acid and PCR verified. All inserts were verified by DNA sequence analysis.

2.3.2 Serial dilutions

The indicated strains were grown to an OD₆₀₀ of 0.5 and then 5-fold serially diluted onto rich medium (YPD) or YPD with either 0.006, 0.012, 0.02% methyl methanesulfonate (MMS) or 50 mM hydroxyurea (HU). For strains harboring pGBK-*shu2* vectors, serial dilutions were performed as above with the exception that cells were grown up in SC-TRP medium prior to

plating onto YPD medium or YPD with 0.02% MMS. Plates were incubated for 2 days at 30°C prior to imaging.

2.3.3 Yeast-2-Hybrids

The GAL4 DNA activating domain (pGAD) expressing plasmids were transformed into PJ69-4A and the GAL4 DNA binding domain (pGBK or pGBD) expressing plasmids were transformed into PJ69-4 α . The *SHU1* gene was disrupted with NatNT2 using pFA6A-NatNT2 as described in (47) in both the PJ-694A or PJ69-4 α strain backgrounds where indicated. The plasmid containing PJ69-4A and PJ69-4 α haploid yeast cells were mated and diploids selected by growth on SC-LEU-TRP solid medium. Individual colonies were grown to early log phase to OD₆₀₀ 0.2 and then 5 μ l were spotted onto medium to select for the plasmids (SC-LEU-TRP) or onto medium to select for expression of the reporter *HIS3* gene (SC-LEU-TRP-HIS) indicating an interaction. Plates were incubated for two days at 30°C and photographed. The experiments were done in triplicate.

2.3.4 Homology searching and phylogenetics

Yeast Shu2 homologues from fungi were retrieved from the non-redundant amino acid sequence database at NCBI using PSI-BLAST. Hits with E-values below 0.005 were used for subsequent iterations. An additional PSI-BLAST search beginning with the human SWS1 (ZSWIM7) protein led to hits across many eukaryotic taxa and in archaea after 3 iterations. While Shu2-homologues

were found in hundreds of species, a selection representing major lineages and model organisms is shown in Figure 4. Protein sequence phylogenies were inferred in PhyML using the LG substitution model with 4 rate classes (120). Branch support values were generated with the approximate likelihood ratio test (aLRT).

2.3.5 Evolutionary rate covariation of Shu2 and fly SWS1 with meiotic and mitotic proteins

Values of evolutionary rate covariation (ERC) were calculated using previously described methods (102). Briefly, orthologous protein sequences were collected from species with sequenced genomes and aligned in *muscle* (18 fungal species and 12 *Drosophila* species for their corresponding datasets) (102,106,121). For each protein we then estimated amino acid branch lengths using a fixed tree topology and the *aaml* program of the PAML package. Branch lengths were then transformed to relative rates using a projection operator (122,123). The ERC value between any two proteins was calculated as the correlation coefficient between their evolutionary rates.

The elevation of Shu complex ERC values as a group was tested by comparison to 100,000 random sets of genes of the same size ($N = 4$ proteins). A p -value was estimated from the number of random protein sets with mean ERC values equal to or greater than the mean ERC between Shu complex proteins. Sets of mitotic, meiotic, and “recombinase activity” proteins were obtained from Gene Ontology annotation through the Yeast Mine and FlyBase Query Builder web tools for yeast and *Drosophila*, respectively (124,125). Statistical significance for ERC

between Shu2 and these functional groups was performed by comparing their ERC distributions to the whole-proteome background (all genes) through Wilcoxon rank sum tests.

2.3.6 Spore viability assay

Diploid yeast strains where both copies of the indicated genotype had been disrupted or mutated at their endogenous locus were sporulated at 30°C. The individual spores were tetrad dissected onto rich medium and spore viability ascertained. A plate of twenty-two individual tetrads was analyzed in triplicate with standard deviations calculated.

2.3.7 Mitotic recombination assays

Mitotic recombination rates were calculated from WT, *shu1*Δ, and *shu2*Δ cells containing the *leu2*-ΔEcoRI::*URA3*::*leu2*-ΔBstEII direct repeat recombination assay as described in (101). Gene conversion (GC) events are measured by Leu+ Ura+ colonies and single-strand annealing (SSA) recombinants are measured by Leu+ Ura- colonies. Nine individual colonies were analyzed of each genotype and the experiment was performed in triplicate. The mitotic recombination rate and standard deviation was calculated as described (126).

2.4 ACKNOWLEDGEMENTS

This chapter is modified from the following collaborative published work:

Godin, S.K., Meslin, C., Kabbinavar, F., Bratton-Palmer, D.S., Hornack, C., Mihalevic, M.J., Yoshida, K., Sullivan, M., Clark, N.L. and Bernstein, K.A. (2015) Evolutionary and functional analysis of the invariant SWIM domain in the conserved Shu2/SWS1 protein family from *Saccharomyces cerevisiae* to *Homo sapiens*. *Genetics*, **199**, 1023-1033.

All authors contributed to the experimental design and planning of the manuscript. C.M. and N.L.C. performed all ERC and phylogentic experiments presented. M.S., S.K.G., K.Y., and D.S.B. performed the Y2Hs. F.K. and S.K.G. performed the recombination assays and tetrad dissection. S.K.G. performed the serial dilutions and strain construction.

3.0 THE SHU COMPLEX INTERACTS WITH THE RAD51 NUCLEOPROTEIN FILAMENT TO MEDIATE ERROR-FREE RECOMBINATION

3.1 INTRODUCTION

DNA double-strand breaks (DSBs) are cytotoxic lesions whose improper repair can lead to mutations, genomic rearrangements, or cell death. Faced with a DSB, eukaryotic cells can differentially utilize non-homologous end joining (NHEJ) or homologous recombination (HR) to repair the lesion. Misregulation of these pathways is both a hallmark of, and a driving force behind, cancer development. Recent work in the budding yeast *Saccharomyces cerevisiae* has characterized a novel regulator of HR, the Shu complex, which is also conserved in humans (62,64,66). Loss of the Shu complex leads to misregulation of HR resulting in a higher mutation rate and increased genome rearrangements (62,64,66,99). Therefore, the Shu complex is likely an important regulator to suppress the chromosomal rearrangements and mutations observed in tumor cells although the mechanism is largely unknown.

In budding yeast, the primary method of repairing a DSB is through Rad51-mediated HR [Reviewed in (2,127)]. Following recognition of a DSB break by the cell, the 5' end of the break is resected leading to 3' single-stranded DNA (ssDNA) overhangs that are coated by the ssDNA binding complex RPA. RPA on the nucleoprotein filament is displaced by Rad51 in a Rad52-dependent fashion. Formation of the Rad51 nucleoprotein filament is required for the homology search and strand invasion steps of HR. Resolution of the HR intermediates can be achieved through a multistep process leading to either crossover or non-crossover products.

Since formation of the Rad51 filament is essential for all recombination events that require strand invasion, Rad51 loading onto the DNA is tightly regulated. Srs2 is a DNA helicase referred to as an “anti-recombinase” since it functions to destabilize Rad51 filaments by translocating along ssDNA mediating Rad51 removal from DNA ends (33,34). Additional proteins promote Rad51 filament formation, for example Rad52, which displaces RPA to facilitate Rad51 loading (128,129). At the same time, the Rad51 paralogues, the heterodimer Rad55-Rad57, integrate into and stabilize the Rad51 filament, block the progression of Srs2, and allow improved Rad51 nucleation and elongation (24,35,130-132). Failure to form Rad51 filaments shifts repair of DSBs away from HR towards Rad51-independent repair pathways such as single-strand annealing (SSA) (133-135). In SSA the ends of a break are resected to reveal distal homologous stretches of DNA that base pair to one another, a process that can result in the loss of the intervening genetic sequences.

The Shu complex, comprised of Shu1, Shu2, Csm2, and Psy3 was previously identified in a genetic screen to identify mutants that suppress the slow growth phenotype of *top3Δ* mutants (62). Further analysis revealed that the Shu complex promotes Rad51-dependent HR (65,107). Subsequently, it was found in *Schizosaccharomyces pombe* that the Shu2 homologue, Sws1, physically interacts with Srs2, and that loss of the Shu complex suppresses the camptothecin-sensitivity of *srs2Δ* cells (64). More recently, it was demonstrated in *S. cerevisiae* that the Shu complex suppresses Srs2 recruitment to DSBs (107). This suggests a model whereby the Shu complex promotes Rad51-dependent HR by inhibiting the anti-recombinase Srs2.

Sequence homology between the Shu complex proteins, Shu1 and Psy3, and the human RAD51 paralogues, XRCC2 and RAD51D, respectively, has suggested that this yeast complex is composed of additional Rad51 paralogues (64). Consistent with this hypothesis, recent structural

information has revealed that both Psy3 and Csm2 adopt a similar alpha-beta sandwich fold structurally homologous to the ATPase core domain of Rad51 and RecA (67,68). Two independent crystallization studies demonstrate that the Shu complex is able to bind to DNA through the activity of the L2 loops in Psy3 and Csm2 (67,68). Importantly, Shu1 and Shu2 are dispensable for DNA binding *in vitro*, suggesting that recruitment of the Shu complex to DNA is mediated by Psy3 and Csm2 under endogenous conditions (68). However, both studies analyzed the DNA-binding capability of the Shu complex for either ssDNA or dsDNA substrates, both of which are not the DNA structures typically used during HR, therefore the biological substrates for these proteins are currently unclear. Additionally, it remains unknown if the Shu complex functions similarly to the other Rad51 paralogues, Rad55 and Rad57, which are incorporated into the Rad51 filament to mediate Rad51 filament nucleation and elongation.

Here we show that the Shu complex acts during DSB repair, shifting the balance towards error-free DNA repair through gene conversion and away from other error-prone repair pathways, such as SSA. We report that similar to the other Rad51 paralogues, Csm2 interacts with Rad51 as well as Rad55 and Rad57, and functions epistatically to Rad55-Rad57. Interestingly, we show by fluorescent microscopy that loss of the Shu complex results in impaired Rad55 focus formation indicating that Csm2 and Psy3 are needed for efficient recruitment of Rad55 to DSB sites. Finally, we find that the loss of the Shu complex alters the balance of HR outcomes away from the Rad51-dependent gene conversion and towards the Rad51-independent SSA pathway. Together our work describes a model whereby the Shu complex, controlled by the DNA-binding activity of the Csm2 and Psy3 heterodimer, interacts with the Rad51 filament to stabilize it.

3.2 RESULTS

3.2.1 Csm2 and Psy2 preferentially bind forked and 3' overhang DNA substrates

Recently the co-structure of two Shu complex members, Csm2 and Psy3, has been solved and biochemical analysis has revealed that the heterodimer of Csm2 and Psy3 is responsible for binding of the Shu complex to DNA *in vitro* (67,68). However, the preferred physiological DNA substrates for these proteins has yet to be identified. To understand the function of the Shu complex during HR, we sought to characterize the preferred DNA substrates for these proteins. First, we co-purified Csm2 and Psy3 as a 1:1 heterodimer to homogeneity (Figure 8A). Since the Shu complex was previously found to function during post-replicative repair (60), we first examined the ability of a Csm2-Psy3 complex to bind a forked DNA substrate. Csm2-Psy3 complex was titrated against a fluorescein labeled forked DNA substrate and binding measured by fluorescence anisotropy (Figure 8B).

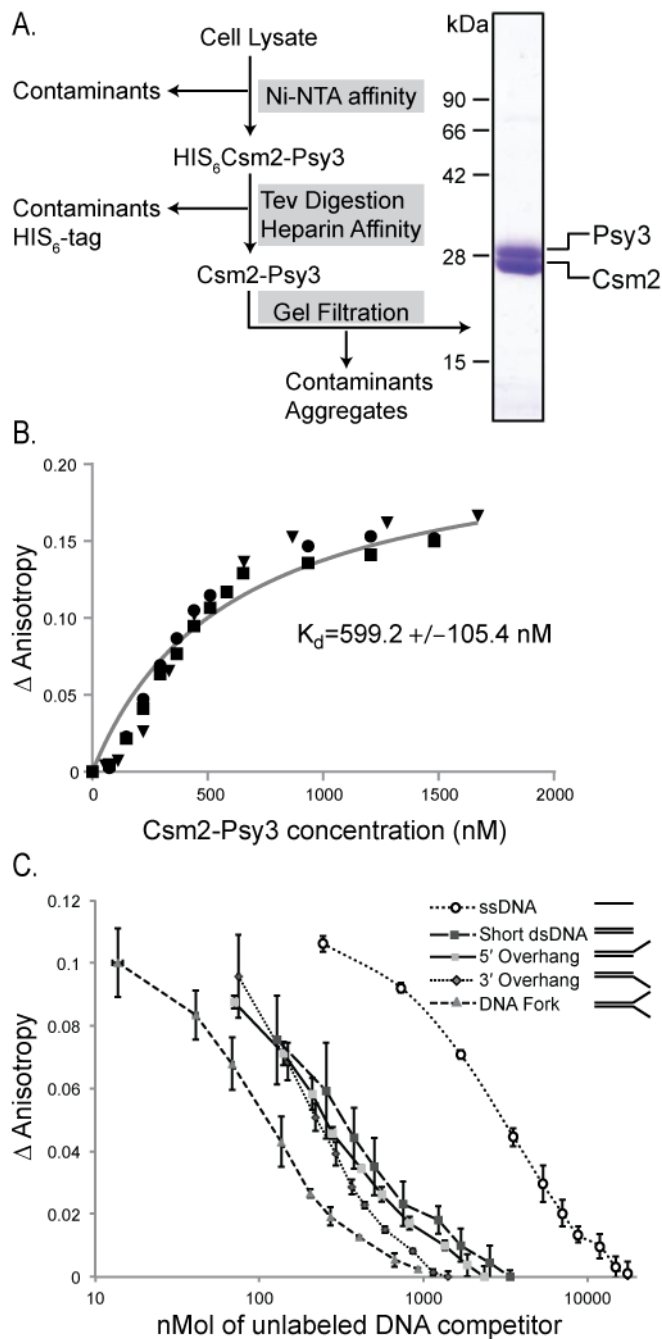


Figure 8. The Csm2 and Psy3 heterodimer preferentially bind forked and 3' overhang DNA substrates.

A. Csm2-Psy3 was purified using the schematic presented in conditions outlined in the MATERIALS AND METHODS section. Coomassie stained Csm2-Psy3 heterodimer (2.4 micrograms) is shown. Csm2 is 25 kDa and Psy3 is 28 kDa. B. The Csm2-Psy3 heterodimer was assayed for DNA binding. Increasing concentrations of Csm2-Psy3 was added to a reaction mixture containing 25 nM fluorescein-labeled DNA fork in a fluorescence spectrophotometer. The experiment was done in triplicate and the standard deviation is plotted.

An estimate of the equilibrium dissociation constant, K_d , is 200 nM. C. Fluorescein-labeled fork (25 nM) was allowed to bind to 546.6 nMol of Psy3-Csm2 and then competed off with increasing concentrations of unlabeled DNA substrates in a fluorescence spectrophotometer. Compared to the fluorescein labeled fork, the 3' overhang, 5' overhang, dsDNA, and ssDNA require a greater than 1.5, 2, 3, and 26-fold higher concentration, respectively, to exhibit 50% competition. The experiment was done in triplicate and the standard deviation is plotted.

To define the best binding substrate for the Csm2-Psy3 heterodimer, we added sufficient protein to obtain ~80% binding to the fluorescently labeled fork substrate and then added unlabeled DNA competitors, such single-stranded DNA (ssDNA), short double-stranded DNA (dsDNA), 5' DNA overhang, 3' DNA overhang, or a forked DNA substrate (Table 3; Figure 8C). Our results show that the forked DNA substrate and to a lesser extent the 3' DNA overhang, effectively compete for Csm2-Psy3 binding, while 5'-overhang DNA, dsDNA, and ssDNA requires a greater than 2, 3, and 26-fold higher concentration, respectively, than forked DNA to show 50% inhibition (Figure 8C). Importantly, forked DNA and 3' overhangs are DNA structures utilized by the homologous recombination pathway. We then verified these results by performing electrophoretic mobility shift assays (EMSA) using the substrates illustrated in Table 3. In this assay, a mobility shift in the DNA substrate would be observed if the competing DNA substrate bound to Csm2-Psy3 heterodimer. We find that the forked DNA and, to a lesser extent the 3' overhang substrates, are the best DNA binding competitors for Csm2-Psy3 (Figure 23). Together our results show that the Csm2-Psy3 complex can specifically recognize and bind DNA substrates used by the homologous recombination pathway.

3.2.2 Csm2 interacts with Rad51 and the Rad51 paralogues Rad55-Rad57

Two of the human components of the Shu complex, XRCC2 and RAD51D, are RAD51 paralogues, which are proteins that have structural similarity to RAD51 (64,92). Consistent with this finding, the crystal structure of the yeast Shu proteins, Csm2 and Psy3, also reveal structural similarity to Rad51 (67,68). These results strongly suggest that, like the mammalian Shu complex, Csm2 and Psy3 are also Rad51 paralogues. Other Rad51 paralogues in yeast, such as the Rad55-Rad57 heterodimer, are incorporated into the Rad51 filament, thus stabilizing and promoting Rad51 filament formation and elongation (35,130,131). Since Csm2 and Psy3 bind to similar DNA substrates utilized by Rad51 during HR, we assessed whether they could interact with Rad51 or the other Rad51 paralogues, Rad55 or Rad57, by yeast-two-hybrid (Y2H). We obtained plasmids harboring fusions of the GAL4 activation domain with *RAD51*, *RAD55*, or *RAD57* (pGAD) or of the *GAL4*-DNA binding domain with *PSY3* or *CSM2* (pGBD) (Figure 9). Growth of yeast cells transformed with the respective combination of plasmids was assessed on medium lacking leucine and tryptophan (Control) or additionally lacking histidine (Interaction). Using this assay, we observe that Csm2 interacts with both Rad51 and Rad55 as well as weakly with Rad57 (Figure 9). In contrast, Psy3 does not interact with Rad51, Rad55, or Rad57 (Figure 9). These results are consistent with the model that Csm2 mediates binding of the Shu complex to DNA perhaps through its physical interaction with Rad51 or the other Rad51 paralogues.

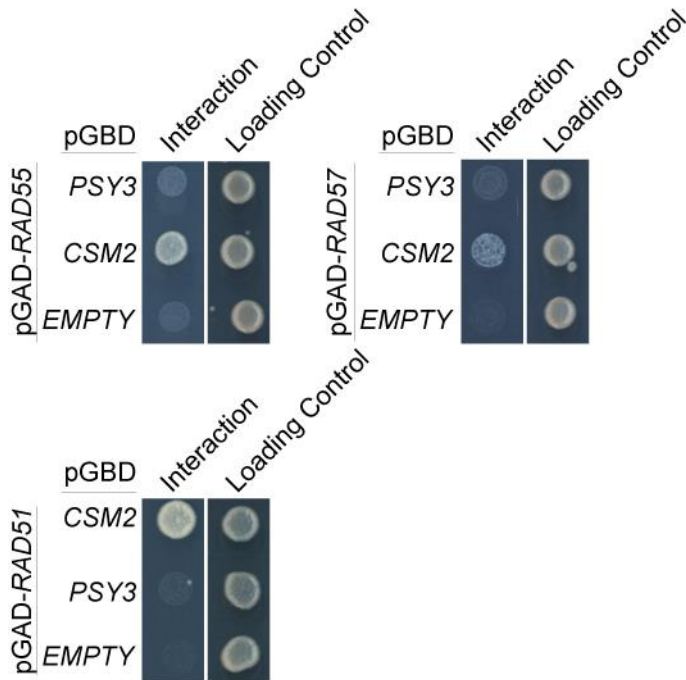


Figure 9. Csm2 physically interacts with Rad51, Rad55, and Rad57 by yeast-2-hybrid.

Csm2 or Psy3 cloned into the pGAD (containing a GAL4-activating domain) plasmid were assayed for interaction with Rad55, Rad57 or Rad51, which were individually cloned into the pGBD plasmid (containing a GAL4-binding domain), by yeast-two-hybrid. Growth on minimal medium lacking histidine indicates a yeast-two-hybrid interaction as *HIS3* is the downstream reporter gene activated by interaction between the queried plasmids (Interaction). Equal cell plating was determined by growth on minimal media lacking leucine and tryptophan, which selects for the two plasmids (Loading Control).

3.2.3 The Shu complex and Rad55-Rad57 function in the same epistasis group

Similar to other Rad51 paralogues, we find that Csm2 interacts with Rad51. Therefore, we asked whether Csm2 functions in the same epistasis group as Rad55-Rad57. To address this question, we compared *csm2Δ* and *rad55Δ* single and double mutants for sensitivity to DNA damaging agents such as methyl methanesulfonate (MMS, a DNA alkylating agent) or ionizing radiation (IR,

which induces DSBs) (Figure 10A). Since *rad55* Δ cells were previously found to be cold sensitive, we analyzed these mutants for growth at both 23°C and 30°C (24,136,137) (Figure 10A). We observe that both a *rad55* Δ single mutant and *rad55* Δ *csm2* Δ double mutants are equally sensitive to both MMS and IR treatments when compared to the wild-type (WT) or a *csm2* Δ single mutant, suggesting that Rad55 is epistatic to Csm2 with respect for DNA damage (Figure 10A). These results show that Rad55 and Csm2 likely function in the same epistasis group. Interestingly, *csm2* Δ cells were only sensitive to 0.006% MMS at lower temperatures (Figure 10A; 23°C panel) suggesting that like Rad55-Rad57, the Shu complex is likely involved in formation or stabilization of a larger complex.

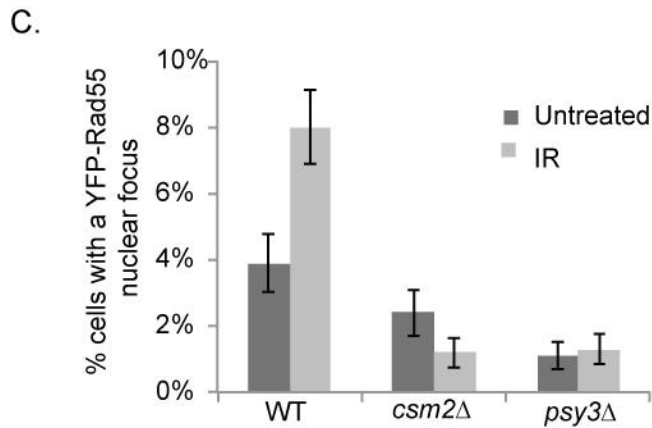
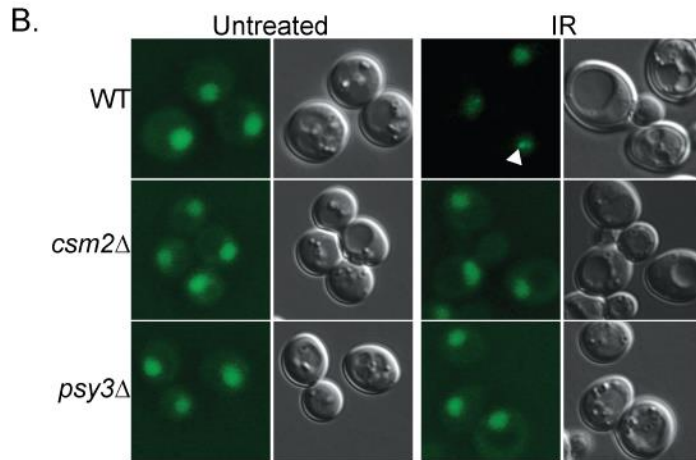
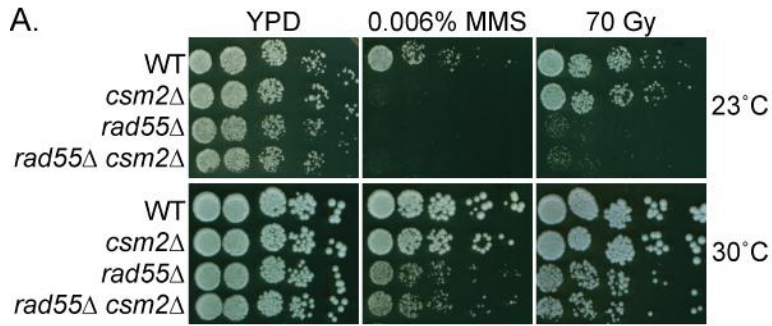


Figure 10. Csm2 is in the same epistasis group as Rad55 and regulated Rad55 recruitment to DNA damage sites.

A. WT, *csm2*Δ, *rad55*Δ, and *rad55*Δ *csm2*Δ cells were five-fold serially diluted onto YPD medium or YPD medium containing 0.006% MMS or exposed to 60 Gy IR and incubated at 23°C or 30°C for two days. B. YFP-Rad55 expressing strains were analyzed for the percentage of cells with nuclear Rad55 foci before (untreated) or after IR (40 Gy). Images of Rad55 are shown and a fluorescent Rad55 focus is indicated with

a white arrowhead. Each experiment was done in triplicate with a total of 400-800 total cells analyzed with standard errors plotted.

3.2.4 Csm2 is necessary for the recruitment of Rad55 to DNA damage sites

Since Csm2 and Rad55 function in the same epistasis group in response to DNA damaging agents, we wondered if Csm2 or Psy3 would be necessary for Rad55 recruitment to DSB sites. We analyzed cells with fluorescently tagged Rad55 (YFP-Rad55) for formation of fluorescent foci, which indicates their redistribution to a DNA damage site, before and after exposure to IR (Figure 10B and 10C). In WT cells, we observe a Rad55 focus in approximately 4% of cells before DNA damage (untreated) and this percentage increases to 8% following IR exposure, suggesting that Rad55 is redistributed to DNA damage sites (Figure 10B and 10C). In contrast, in cells where either *CSM2* or *PSY3* are deleted, we do not see an increase in Rad55 recruitment into DNA repair foci, and we observe fewer cells with a Rad55 focus after IR (Figure 10C). Therefore, Csm2 and Psy3 are needed for efficient recruitment of Rad55 to DNA damage sites caused by IR.

3.2.5 Unlike *rad55*Δ, the cold sensitivity of *csm2*Δ cells exposed to MMS is not suppressed by over-expression of Rad55-Rad57 or Rad51

Previously it was reported that the cold-sensitivity of *rad55*Δ cells exposed to IR could be suppressed by either over-expressing Rad55, Rad55-Rad57 together, or Rad51 using a CEN or 2μ plasmid (132,138,139). Therefore we asked if the slow growth of *csm2*Δ cells exposed to MMS would similarly be suppressed by Rad55-Rad57 or Rad51 over-expression. Akin to what was previously observed with IR, the cold sensitivity of *rad55*Δ cells exposed to MMS could be

partially suppressed by expressing Rad55-Rad57 or Rad51 from a CEN plasmid (Figure 11). In contrast, the slow growth of *csm2Δ* upon MMS exposure was not suppressed by either Rad55-Rad57 co-expression or Rad51 at 23°C (Figure 11). Therefore, it is possible that Csm2 and Rad55 have different roles with respect to their function during repair of MMS induced lesions. Alternatively, greater expression levels of Rad51 might be needed in order to observe suppression of this phenotype.

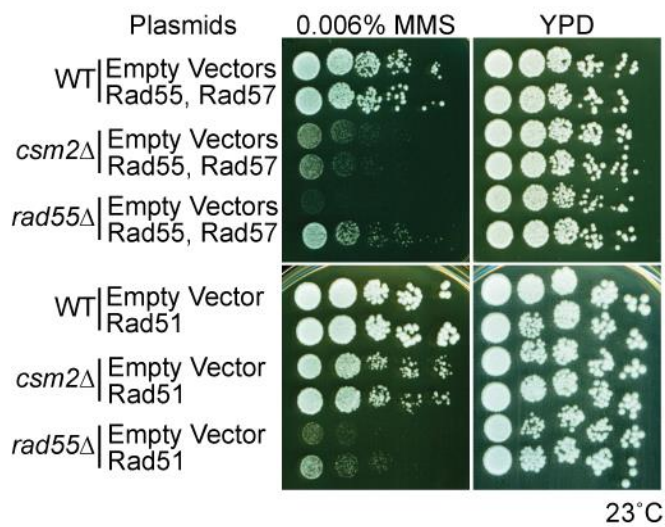


Figure 11. Over-expression of Rad55-Rad57 or Rad51 does not suppress the MMS sensitivity of *csm2Δ* cells at 23°C.

WT, *csm2Δ*, and *rad55Δ* cells were either co-transformed with both a Rad55 and Rad57 plasmid, a Rad51 plasmid, or their respective empty vectors. Cells were grown to early log phase in minimal medium with selection for the plasmids and then five-fold serially diluted onto YPD or YPD with 0.006% MMS. After three or four days of growth at 23°C, the plates were photographed.

3.2.6 The Shu complex promotes Rad51-dependent recombination events

Previously, we hypothesized that the Shu complex promotes Rad51 filament formation since fewer spontaneous Rad51 fluorescent foci are observed when the Shu complex is disrupted in yeast or mammalian cells (64,107). Since Rad51 filaments are essential for HR, we asked whether disruption of the Shu complex might alter repair pathway choice if Rad51 filament formation is limited. To address this question, we utilized a heteroallelic recombination assay that can distinguish between direct repeat recombination mediated by sister chromatid gene conversion (GC, a Rad51-mediated event) and intrachromosomal single-strand annealing (SSA, a Rad51-independent event) (Figure 12A). In this assay a recombination event can generate a functional *LEU2* allele between two *leu2* heteroalleles. The intervening *URA3* marker between the *leu2* alleles enables us to differentiate between sister chromatid GC (Leu⁺ Ura⁺) and SSA (Leu⁺ Ura⁻) recombinants (Figure 12A). Using this assay, wild-type *PSY3* cells exhibit similar rates of GC and SSA (Figure 12B). In contrast, disruption of *PSY3* or *CSM2* results in significantly more SSA events ($p \leq 0.05$ and $p \leq 0.01$, respectively) where GC events are modestly, but significantly, reduced ($p \leq 0.001$) (Figure 12B). Since more SSA recombinants are observed with *PSY3* or *CSM2* disruption, these results are consistent with the model where inhibiting the Shu complex shifts the repair of spontaneous DSBs towards a Rad51-independent repair process.

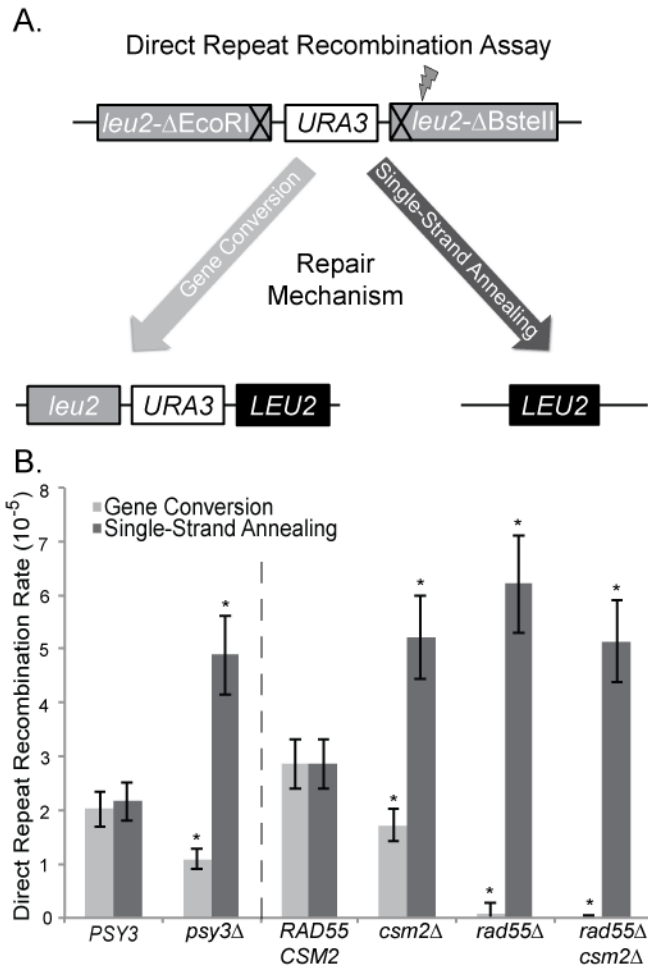


Figure 12. Disruption of *CSM2* or *PSY3* leads to more Rad51-independent recombination events.

A. Strains harboring a direct repeat recombination assay (*leu2-ΔEcoRI::URA3::leu2-ΔBstEII*) were used to simultaneously measure rates of direct repeat recombination by gene conversion or intra-chromosomal single-strand annealing that result in a *LEU2*⁺ allele. Generation of a function *LEU2* gene can occur either through a gene conversion event in which the other *leu2* allele is used as a template for repair (Rad51-dependent, left side of cartoon) resulting in Leu⁺Ura⁺ colonies. Alternatively, repair can also occur by single-strand annealing where the intervening regions are resected until a region of homology is exposed and religated (Rad51-independent, right side of cartoon) resulting in Leu⁺Ura⁻ colonies. B. The rates of gene conversion and single-strand annealing events in *psy3Δ*, *csm2Δ*, *rad55Δ*, or *rad55Δ csm2Δ* strains were compared to control cells (*PSY3* or *RAD55 CSM2*) where equal rates of gene conversion and single-strand annealing events are observed. The dashed line indicates that these strains were analyzed independently.

Since Rad55 interacts with Csm2 and functions in the same epistasis group in response to DNA damage, we furthermore assessed whether disrupting Rad55 would have a similar effect on recombination rates using this assay. We assayed *csm2Δ* and *rad55Δ* single mutants and compared their recombination rates to the double *rad55Δ csm2Δ* mutant or *RAD55 CSM2* cells (Figure 12B). As expected, disruption of *RAD55* resulted in very few detectable GC events (recombination rate less than 6.7×10^{-7}) and SSA rates were increased to a level similar to a *csm2Δ* single mutant (Figure 12B). These results show that Rad55 has a more prominent role in mediating gene conversion when compared to disruption of either *PSY3* or *CSM2*. Furthermore, the increased SSA event observed in either a *rad55Δ* or *csm2Δ* single or double mutants were similar, again suggesting that Rad55 and Csm2 are epistatic.

3.3 DISCUSSION

After a DSB occurs, cells can commit to multiple repair pathways to repair the lesion. An important complex in committing the cell to error-free DNA repair is the Shu complex. Recently the crystal structures of two components of the Shu complex, Csm2 and Psy3, have been solved (67,68). These proteins bind DNA and are structural paralogues of Rad51. With this in mind, we examined the preferred binding substrates of purified Csm2-Psy3 heterodimer and find that these proteins preferentially bind to forked DNA and, to a lesser extent, 3' over-hang DNA substrates (Figure 8 and Figure 23). Importantly these DNA structures are utilized by the HR pathway and are coated by Rad51 nucleoprotein filaments to perform the essential homology search and strand invasion HR steps. Since Csm2 and Psy3 exhibit structural similarity to Rad51, we examined whether they interact with Rad51 or the other known Rad51 paralogues in yeast, Rad55-Rad57. Importantly, by

yeast-2-hybrid we detected an interaction between Csm2 and Rad51 as well as Rad55-Rad57 (Figure 9). Subsequently, we found that Csm2 is epistatic to Rad55, suggesting that they function in the same pathway (Figure 10). Importantly, by fluorescent microscopy we find that Csm2 and Psy3 are necessary for Rad55 recruitment to DSB sites induced by ionizing radiation (Figure 11). Finally, we discovered, using recombination assays, that both Csm2 and Psy3 are important in Rad51-mediated repair at the expense of error-prone DNA repair mechanisms such as SSA (Figure 12). Together our results point to a model where the Shu complex, which consists of Rad51 paralogues, is likely recruited to HR substrates through its DNA binding activity where it can interact with Rad51 and Rad55-Rad57 to mediate Rad51 filament formation and commitment to error-free DNA repair (Figure 13).

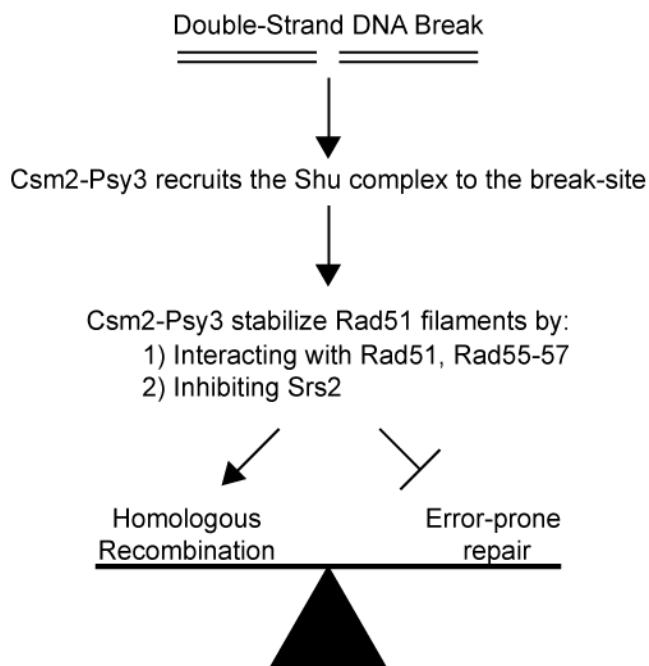


Figure 13. Schematic of the role of the Shu complex during error-free HR.

After a double-strand DNA break occurs, Csm2-Psy3 heterodimer recruits the Shu complex to the break-site which can either be at a replication fork or a 3' DNA overhang. At the break-site, Csm2-Psy3 can promote Rad51 filament formation and stabilization; 1) through a direct interaction with Rad51 and Rad55-Rad57

and/or 2) by inhibiting Srs2 recruitment to DSB sites. Stabilization of Rad51 filaments promotes DSB repair by error-free HR pathway while inhibiting other error-prone DNA repair mechanisms such as SSA.

One of the key steps in HR is the formation of Rad51 filaments. Importantly, there are proteins that mediate Rad51 filament formation, such as Rad52 and its epistasis group of proteins including the Rad51 paralogues, Rad55-Rad57 (24,129,137,140-142). How do the Rad51 paralogues promote Rad51 nucleofilament formation? Both Rad55-Rad57 are RecA-like proteins with structural similarity to Rad51 (130,131) and are needed for Rad51 mediated recombination events (24). Since disruption of either *RAD55* or *RAD57* leads to slower and reduced recruitment of Rad51 to DSB sites and dimmer Rad51 foci (23,143,144), it has been proposed that Rad55-Rad57 nucleate Rad51 filaments where they stabilize Rad51 on the ssDNA end leading to longer Rad51 filament tracks (24,145). In support of this model, the IR sensitivity of *rad55Δ* or *rad57Δ* can be suppressed by over-expressing Rad51 (132,138,139). Furthermore, the cold sensitivity of *rad55Δ* and *rad57Δ* suggests that they are important for stabilization of larger complexes such as the Rad51 presynaptic filament (136,137).

There are several lines of evidence that suggest that the Shu complex also consists of Rad51 paralogues. First, like the other Rad51 paralogues, the structure of Csm2 and Psy3 shows similarity to Rad51 (67,68). Secondly, similar to Rad55 and Rad57, the Shu genes are also needed for Rad51 recruitment to DNA damage sites in both yeast and human cells (64,66,107). Additionally, Csm2 interacts with Rad51 and the other Rad51 paralogues (Figure 9) and its disruption leads to decreases in Rad51-mediated DNA repair processes (Figure 12). Finally, Csm2 is in the same epistasis group as Rad55 in response to DNA damaging agents MMS and IR (Figure 10A). Together, we provide further genetic evidence that the Shu complex consists of Rad51 paralogues that is consistent with the structural homology observed by She *et al* and Tao *et al* (67,68).

In addition to the Rad51 paralogues stabilizing Rad51 on the DNA, there are also factors that mediate Rad51 filament disassembly such as the DNA helicase Srs2. ATP-bound Rad51 frequently binds ssDNA, although with limited extension. In contrast, ADP-bound Rad51 can be readily disassociated from DNA (127,145,146). Srs2 promotes ATP hydrolysis of DNA bound Rad51 and then subsequently uses its helicase activity to translocate along the DNA filament where it can interact with the next available Rad51-ATP substrate (147-149). In humans there are multiple proteins that have overlapping functions to Srs2 such as RECQL5, PARI, and RTEL (150-153). Recently, the Rad51 paralogues Rad55-Rad57 have been shown to physically interact with Srs2 in a 1:1 ratio (35). Further biochemical analysis has revealed that Rad55-Rad57 has an additional function in mediating Rad51 filament formation through its interaction with Srs2 where it inhibits Srs2 translocation activity and thus prevents removal of Rad51 from ssDNA substrates (35).

The Shu complex also has a role in regulating Srs2. Shu2 physically interacts with Srs2 in both budding and fission yeast (63,64). Disruption of either *SHU1* or *SHU2* results in more fluorescently tagged Srs2 recruited into spontaneous DNA repair foci and increased recruitment of Srs2 to inducible DSB sites (107). Therefore, it is possible that the interaction between Rad51 paralogues in promoting Rad51 filament assembly by inhibiting Srs2 may be a shared function. However, it remains unknown if the Shu complex is incorporated into the Rad51 filament like the other paralogues.

One puzzling observation made here is that Csm2 and Psy3 both promote Rad55 focus formation after IR but are not IR sensitive when disrupted (Figure 10). This is consistent with a reduction in Rad51 foci observed in *shu1Δ* cells (107). Although fewer Rad55 foci are observed, perhaps enough Rad55 is recruited to these lesions to enable cell viability after IR treatment in the

absence of *PSY3* or *CSM2*. Alternatively, there may be a delay in the kinetics of Rad55 focus assembly at DNA repair sites that would not result in a growth defect in IR exposed *csm2Δ* cells.

How are the roles of the Shu complex different from Rad55-Rad57 during HR? Previously we proposed a model where the function of the Shu complex was to inhibit Srs2 recruitment to DNA repair sites, thus promoting error-free Rad51 mediated recombination. We find that disruption of either *RAD55* or *RAD57* leads to a more pronounced defect in HR and increased sensitivity to a broader range of DNA damaging agents. Furthermore, unlike Rad55-Rad57, the Shu genes likely have a more specialized function with respect to HR, perhaps a more dominant role at the replication fork or in response to specific types of DNA lesions. Consistent with this idea, the Shu complex was shown to have a role in post-replicative repair and to influence use of error-free DNA polymerases in response to MMS induced lesions (60,62). Furthermore, disruption of the Shu complex members leads to sensitivity to MMS specifically but not other DNA damaging agents (i.e. IR, UV, HU, etc.) (60,62,64,65). Unlike the other Rad51 paralogues, *csm2Δ* cold sensitivity upon exposure to MMS is not suppressed by Rad51 over-expression (Figure 11). These results may explain why *csm2Δ* or *psy3Δ* cells do not have a more dramatic effect on gene conversion rates like those observed in *rad55Δ* cells. Regardless, the interaction between the Shu complex and the other key players in mediating HR (such as Rad51, Rad55, Rad57, Srs2), underscore the importance of understanding the unique roles these proteins play during Rad51 filament formation.

3.4 MATERIALS AND METHODS

3.4.1 Strains, plasmids and media

The strains used in this study are listed in Table 4 and are isogenic with W303 and derived from the *RAD5+* strains W1588-4C and W5909-1B (116,117) except for PJ69-4A and PJ69-4 α strains used during the yeast-2-hybrid experiments (118). Standard protocols were used for crosses, tetrad dissection, and yeast transformation (LiOAc method) (119). The media was prepared as described, except with twice the amount of leucine (119).

3.4.2 Purification of Csm2 and Psy3

Full length *S. cerevisiae* Csm2 and Psy3 were amplified from genomic DNA by PCR and cloned into the bacterial co-expression plasmid pCDF Duet-1 (cloning described in Table 4; EMD Millipore). Protein expression was performed in *E.coli* BL21 (DE3) Codon+(pRIL) via IPTG induction. Cells were harvested by centrifugation, lysed in 20 mM Tris (pH 8.0), 300 mM NaCl, 10% glycerol, 5 mM imidazole, 1 mM β -mercaptoethanol, and the lysates cleared by centrifugation at 30,000xg. Csm2 and Psy3 were co-purified by nickel affinity chromatography (Qiagen) via the His₆ tag on Csm2, followed by an overnight digestion with TEV. The Csm2-Psy3 complex was then further purified using HiTrap Heparin HP (GE Healthcare) affinity chromatography and size exclusion chromatography using a Sephacryl S-200 column (GE Healthcare) with peak fractions eluting as an apparent heterodimer verified by SDS-PAGE. The peak fractions were dialyzed into a buffer containing 20 mM Tris (pH 8.0), 300 mM NaCl, 8% glycerol, and 1 mM dithiothreitol and concentrated to 1.6 mg/ml using a Vivaspin concentrator (Millipore).

3.4.3 Competition electrophoretic mobility shift assay (EMSA)

Fluorescein-labeled DNA fork (260 nM), detailed in Table 5, with or without an unlabeled competitor DNA oligonucleotide (1300 nM), was incubated on ice for 30 minutes with purified Csm2-Psy3 complex (3.0 μ M) in EMSA reaction buffer (10 mM Tris pH 8.0, 50 mM NaCl, 2 mM DTT, 4 mM $MgCl_2$) in a reaction volume of 10 μ l. Equilibrated samples were loaded on a pre-cooled and pre-run 5% native polyacrylamide gel containing 0.5X TBE and run at 200 volts for 2 hours at 4°C. The resulting gel was visualized by fluorescence using a FLA-5100 Fluorescent Image Analyzer (FujiFilm).

3.4.4 Fluorescence anisotropy assays for DNA binding

The basic protocol and mathematical rationale for this technique is outlined in Hey et al (154). All experiments were performed using a Cary Eclipse Fluorescence Spectrophotometer (Varian) fitted with a peltier thermostatted multicell holder and automated polarizer. Fluorescent anisotropy/polarization measurements were collected with the excitation wavelength of 498 nm (slit-width 5 nm) and the emission wavelength at 520 nm (slit-width 5 nm), with a photomultiplier tube (PMT) voltage of 780V. Reactions were carried out at 30°C in a standard reaction buffer (20 mM Tris pH 8, 100 mM NaCl) with a total volume of 400 μ L. A fluorescein-labeled DNA fork substrate (Table 5) was used in each of the experiments. For the DNA binding isotherms, anisotropy measurements were collected using three fluorescein-labeled fork concentrations (25 nM). Purified Csm2-Psy3 was titrated into the reaction volume to the indicated concentration and allowed 7.5 minutes of equilibration prior to the anisotropy measurement. Protein was titrated until the anisotropy signal plateaued, indicating saturation of the labeled probe. For the competition

curves, fluorescence experiments were carried out with 25 nM fluorescein-labeled DNA fork and 546.6 nM Csm2-Psy3. The different unlabeled competitors (Table 5) were added at increasing concentrations and allowed 7.5 minutes equilibration time before each measurement. Unlabeled DNA probe was added until polarized fluorescence stabilized, indicating saturation of the reaction with unlabeled DNA probe. Experiments were done in triplicate.

3.4.5 Yeast-2-Hybrids

The yeast-two-hybrid plasmid pGAD was used to express a fusion of GAL4 activation domain and pGBD was used to express a fusion of the GAL4 DNA binding domain. pGAD expressing plasmids (Csm2, Psy3, and empty vector) were transformed into PJ69-4A (118) and positive colonies were selected on SC-LEU medium. pGBD expressing plasmids (Rad55, Rad57, Rad51) were transformed in PJ69-4 α (118) and recombinants were selected on SC-TRP medium. PJ69-4A and PJ69-4 α haploid yeast cells harboring their respective plasmids were mated and diploids were selected on SC-LEU-TRP solid medium. Individual diploid cells were grown to early log phase OD₆₀₀ 0.2 and then 5 μ l were spotted onto medium to select for the plasmids (SC-LEU-TRP) or onto medium to select for expression of the reporter *HIS3* gene (SC-LEU-TRP-HIS) indicating a yeast-2-hybrid interaction. Plates were incubated for two days at 30°C and subsequently photographed. Each experiment was done in triplicate.

3.4.6 Serial dilutions

The indicated strains were grown to early log phase, diluted to an OD₆₀₀ of 0.2 and subsequently five-fold serially diluted onto rich medium or rich medium exposed to 70 Gy or 0.006% methyl methanesulfonate (MMS) and incubated for two days at either 23°C or 30°C.

3.4.7 Fluorescent microscopy

Cells were grown overnight at 30°C in 3 ml cultures of SC with adenine (100 mg/ml) and harvested for microscopy as previously described (155). A YFP-Rad55 integrated at its endogenous locus was introduced by mating into WT, *csm2Δ*, and *psy3Δ* cells and was visualized before and after 40 Gy of ionizing radiation using a Nikon TiE inverted live cell system with a 100X oil immersion objective (1.45 numerical aperture) with a Photometrics HQ2 camera and motorized Prior Z-stage. Stacks of 11 0.3μm sections were captured using the following exposure times: differential interference contrast (60 ms) and YFP-Rad55 (4000 ms). The images were deconvolved using Elements imaging software (Nikon). All images were processed and enhanced identically and experiments were performed in triplicate with 400-800 total cells analyzed.

3.4.8 Mitotic recombination assays

Mitotic recombination rates were calculated from haploid cells with the indicated mutations and the *leu2-ΔEcoRI::URA3::leu2-ΔBstEII* direct repeat recombination assay as described in (101). Single-strand annealing (SSA) recombinants were measured as Leu⁺ Ura⁻ colonies and gene conversion (GC) events were measured as Leu⁺ Ura⁺ colonies. For each genotype, nine individual

colonies were analyzed and the experiment was performed in triplicate. The average mitotic recombination rate and standard deviation was calculated as described by (126).

3.5 ACKNOWLEDGEMENTS

This chapter is modified from the following collaborative published work:

Godin, S., Wier, A., Kabbinavar, F., Bratton-Palmer, D.S., Ghodke, H., Van Houten, B., VanDemark, A.P. and Bernstein, K.A. (2013) The Shu complex interacts with Rad51 through the Rad51 paralogues Rad55-Rad57 to mediate error-free recombination. *Nucleic Acids Res*, **41**, 4525-4534

All authors contributed to the planning and experimental design. A.W. purified the Csm2-Psy3 used in these experiments and performed the EMSA. A.W. and S.G. performed the fluorescence anisotropy experiments. D.S.B. performed the wild type Y2H's, while S.G. performed the Rad51 and Rad55 knockout Y2H. F.K. performed the recombination assays. S.G. performed all serial dilutions and fluorescence work.

4.0 PROMOTION OF RAD51 PRESYNAPTIC FILAMENT ASSEMBLY BY THE ENSEMBLE OF S. CEREVISIAE RAD51 PARALOGUES WITH RAD52

4.1 INTRODUCTION

HR represents a major tool for repairing injured replication forks, chromosomes with DNA double-strand breaks (DSBs), telomere lengthening, and ensuring the accurate disjunction of homologous chromosomes in meiosis I (156,157). Defective HR underlies human diseases including cancer and Fanconi anemia (71,92-94,98). An important conserved HR step is the formation of a Rad51-ssDNA nucleoprotein filament, also called the presynaptic filament, at DNA damage. In yeast, Rad51 presynaptic filament assembly on ssDNA pre-occupied by RPA, the ubiquitous single-strand DNA binding protein, is facilitated by Rad52 (or by BRCA2 in humans) and a heterodimeric complex of the Rad51 paralogues Rad55 and Rad57 (150,157). In conjunction with the DNA motor protein Rad54, the presynaptic filament mediates homology search and strand invasion, and the resultant DNA joint, the D-loop, is resolved through mechanistically distinct pathways to a crossover or non-crossover product.

Recent studies identified the yeast Shu complex as a novel factor that promotes Rad51-dependent repair through an undefined mechanism (60,62,64,65,107). The Shu complex consists of four subunits that include two Rad51 paralogues (Csm2 and Psy3), Shu1, and Shu2 (62) and is conserved in humans (64,66,158). The Shu complex was originally identified during a screen for mutants that suppress the slow growth of *top3Δ* cells and it was shown to act in the *RAD52* epistasis group to promote HR (62,65). The Shu complex similarly suppresses the HU and MMS sensitivity of *sgs1Δ* cells, placing it at an early step of HR (62). Here we present the first biochemical evidence

for a synergistic role of the Shu complex with Rad55-Rad57 and Rad52 to promote Rad51 presynaptic filament formation on RPA-coated ssDNA. Our data support a model wherein Csm2 and Rad55 bridge interactions among the Rad55-Rad57 heterodimer, the Shu complex, and Rad52 to promote Rad51-dependent homology-directed DNA repair.

4.2 RESULTS

4.2.1 The Shu complex interacts with the regulators of Rad51 filament formation and acts upstream of Rad51 filament formation

We first focused on the purified Csm2-Psy3 heterodimer (Figure 24), as the known protein interaction and DNA binding activities occur through these subunits, including our previous findings that Csm2 associates with Rad55 in the yeast two-hybrid (Y2H) system (89). Indeed, we found by affinity pull-down that Csm2-Psy3 interacts with Rad55-Rad57 (Figure 14A and Figure 25A). Similarly, the Shu complex (Csm2-Psy3-Shu1-Shu2) interacts with Rad55-Rad57 by pull-down (data not shown). We next asked whether Csm2 would interact with Rad52 by Y2H analysis (Figure 14B). As shown before, association of Csm2 with Rad55 and self-interaction of Rad52 were seen (61,89,159), and, importantly, Csm2 and Rad55 interacted with Rad52 (Figure 14B). While the Csm2-Rad52 interaction was abolished in *rad55* Δ cells, the Rad52-Rad55 interaction remained without *CSM2* (Figure 14C, D). We employed biochemical pull-down to validate these interactions and found that, consistent with the Y2H results above, while GST-tagged Rad52 could interact with Rad55-Rad57 (Figure 14E), its interaction with the Shu complex was negligible. We attempted to validate that Rad55-Rad57 bridges Rad52 to Shu

complex by performing the GST pull-down on a mixture of GST-Rad52, Rad55-Rad57, and Shu complex. However, the degree to which Shu complex is pulled down by Rad52 is either not affected or only modestly affected by the presence of Rad55-Rad57 (data not shown), perhaps because the associations are too labile for the tripartite assembly to persist through washing steps. In agreement with prior Y2H results (61,89), pull-down analysis revealed that Rad55-Rad57 interacts with Rad51 while Csm2-Psy3 does so only weakly (Figure 25B). Addition of Csm2-Psy3 does not attenuate Rad55-Rad57 interaction with Rad51, suggesting the interactions are non-competitive (data not shown). We have additionally tested RPA in pull-downs and find that it may interact weakly with Rad55-Rad57 (data not shown).

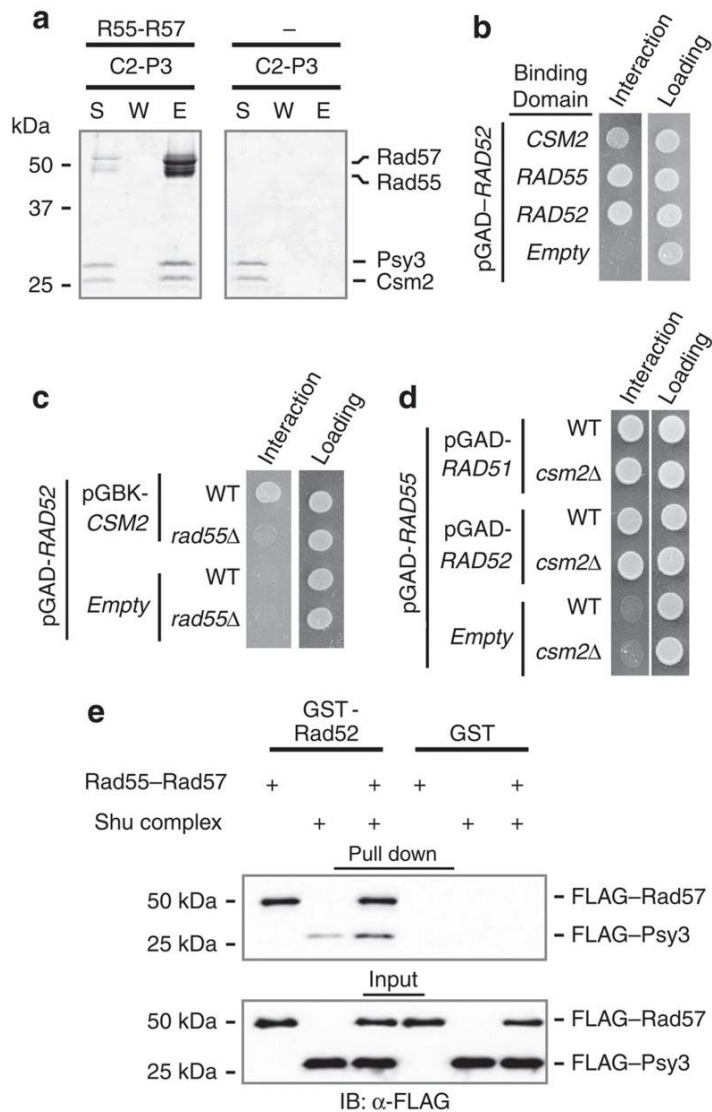


Figure 14. Interactions of Rad55-Rad57 with the Shu complex and Rad52.

A. Rad55-Rad57 was incubated with Csm2-Psy3 and the protein complex was captured through the (His)₆ tag on Rad55 using Ni²⁺ resin. S, supernatant containing unbound proteins; W, wash of the resin; E, eluate from the resin. B. Rad52 was tested for Y2H interaction with the indicated proteins. C. The Y2H interaction between Rad52 and Csm2 was examined in wild type or *rad55Δ* cells. D. The Y2H interaction between Rad52 and Rad55 was examined in wild type or *csm2Δ* cells. E. GST-tagged Rad52 was mixed with Rad55-Rad57 or Shu complex, and protein complexes were captured on glutathione resin. Immunoblotting for the FLAG tag on Rad57 and Psy3 was used to identify Rad55-Rad57 and Shu complex retained on the resin.

It has been proposed that the Shu complex and Rad55-Rad57 act to promote Rad51 presynaptic filament formation by antagonizing the Srs2 helicase (35), which negatively regulates HR by disrupting the presynaptic filament (33,34). Cells lacking Srs2 therefore accumulate ssDNA-bound Rad51. Since Rad54 enhances the ability of the Rad51 presynaptic filament to catalyze DNA strand invasion (40), *srs2Δ rad54Δ* double mutants are inviable, likely because they accumulate long-lived presynaptic filaments. Thus, *srs2Δ rad54Δ* inviability is suppressed by disruption of *RAD52*, which limits presynaptic filament formation (160). Similarly, disruption of *RAD55* or *CSM2* suppresses *srs2Δ rad54Δ* inviability (161). To expand upon these findings, we asked whether disruption of *RAD55* or *CSM2* suppresses *srs2Δ rad54Δ* inviability to the same extent as *RAD52* deletion by tetrad dissection and spore analysis, and indeed it does (Figure 26, p-value < 0.05). Thus, the Shu complex and Rad55-Rad57 do not act solely as negative regulators of Srs2 and can function independently of Rad54.

4.2.2 The Shu complex acts with Rad55-Rad57 and Rad52 to stimulate Rad51 filament formation

We used several complementary approaches to assess the role of the Shu complex in Rad51 presynaptic filament assembly (Figure 15A, B, Figure 27). Specifically, we monitored Rad51 loading onto RPA-coated ssDNA bound to magnetic beads (Figure 15A) and also examined homologous DNA strand exchange activity (Figure 15B). In the absence of RPA, Rad51 readily gained access to the bead-immobilized ssDNA and efficiently catalyzed the exchange of homologous DNA strands (Figure 15A, B, lane 2). However, RPA on ssDNA strongly attenuated

Rad51 loading efficiency and DNA strand exchange (Figure 15A, B, lane 3). Under the reaction conditions, the Shu complex and Rad55-Rad57 alone or together were insufficient to overcome the inhibitory effect of RPA (Figure 15A, B, lanes 4-6). The addition of Rad52 permitted Rad51 loading onto RPA-coated ssDNA, but, because of the limiting conditions employed, the amount of ssDNA-associated Rad51 was only a fraction of that achieved when RPA was absent (Figure 15A, B, lane 7 compared to 2). Rad51 loading in the presence of Rad52 was stimulated by the addition of Rad55-Rad57 but not the Shu complex (Figure 15A, B, lanes 7 compared to 8 and 9). Importantly, adding Shu complex together with Rad52 and Rad55-Rad57 led to a marked stimulation of Rad51 loading and DNA strand exchange activity (Figure 15A, B, lane 10). The enhancement of Rad51 loading by Rad55-Rad57 and the Shu complex is most prominent at both 18°C and 23°C and less pronounced at 30°C (Figure 15B and Figure 28A, B). This is consistent with *rad55Δ* cells exhibiting a more severe DNA damage sensitivity at lower temperatures (35,136). Since we found that Shu complex stimulates Rad51 filament assembly, we next visualized the nucleoprotein products of Rad51 loading using electron microscopy (EM). Consistent with our biochemical data, we observed a significantly greater number of Rad51 filaments in reactions where Rad55-Rad57 and Shu complex were added together with Rad52 (Figure 27). Collectively, these results reveal a synergistic action of Rad52 and the two Rad51 paralogue complexes in enabling utilization of RPA-coated ssDNA for presynaptic filament assembly.

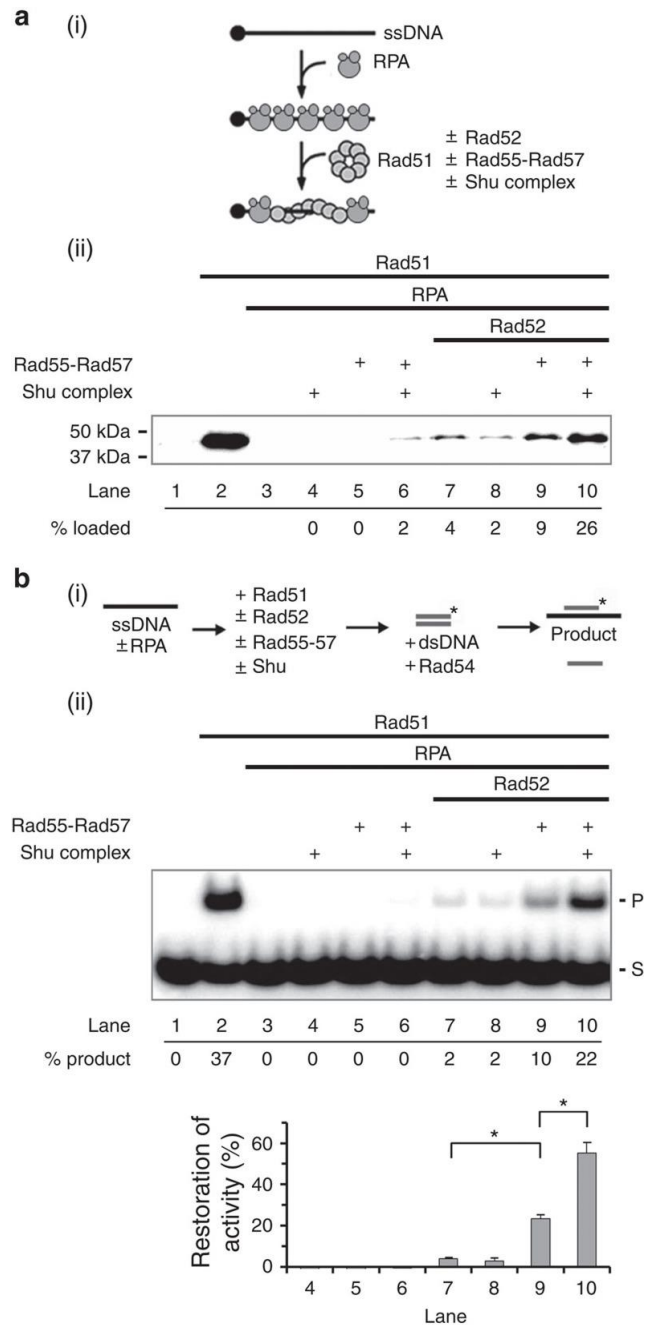


Figure 15. Enhancement of Rad51 loading onto RPA-coated ssDNA by the Shu complex and Rad55-Rad57.

A. (i) Schematic of the Rad51 loading assay. A. (ii) Magnetic bead resin with immobilized ssDNA was pre-incubated with RPA, then Rad51 was added along with combinations of Rad52, Shu complex, and Rad55-Rad57. The amount of Rad51 retained on the ssDNA was determined by immunoblotting. B. (i) Schematic

of the DNA strand exchange assay. B. (ii) RPA-coated ssDNA was incubated with Rad51 and combinations of Rad52, Shu complex, and Rad55-Rad57, mixed with radiolabeled homologous dsDNA and Rad54, and then analyzed. S, dsDNA substrate; P, DNA strand exchange product. Standard deviations are plotted and (*) indicates significance.

We found that the Csm2-Psy3 heterodimer is just as adept as the full Shu complex in the enhancement of presynaptic filament assembly in the presence of Rad55-Rad57, suggesting that Shu1 and Shu2, which are not Rad51 paralogues, may not be directly involved in presynaptic filament assembly (Figure 29A). The DNA strand exchange reactions performed in Figure 15B contained Rad54 to accelerate the rate of product formation (162), but similar results were obtained without Rad54 (Figure 29B). Rad55-Rad57 and the Shu complex do not appear to directly enhance the activities of Rad51 or Rad54 since DNA strand exchange reactions lacking RPA are not stimulated by addition of Rad55-Rad57 and Shu complex (Figure 29C). When Rad51 loading incubations were shortened to 45 min, similar results were obtained (data not shown).

4.2.3 Csm2's interaction with Rad55-Rad57 is essential for its function *in vitro* and *in vivo*

By X-ray crystallography, several groups have determined the structure of Csm2-Psy3 (67,68,90). We searched for solvent exposed residues that could participate in interaction with a partner molecule such as Rad55. We applied surface triplet propensity analysis (163) to this structure (68) to reveal a potential protein interaction surface on Csm2 (Figure 30A), which is highly conserved in numerous fungal homologues (Figure 30B). The phenylalanine 46 to alanine (F46A) (Figure 16A and Figure 30) mutation was made, as changing this surface residue is

unlikely to affect the stability or folding of Csm2. Importantly, we found that the F46A mutation disrupts the Y2H interaction of Csm2 with Rad55 but not Psy3 (Figure 16B).

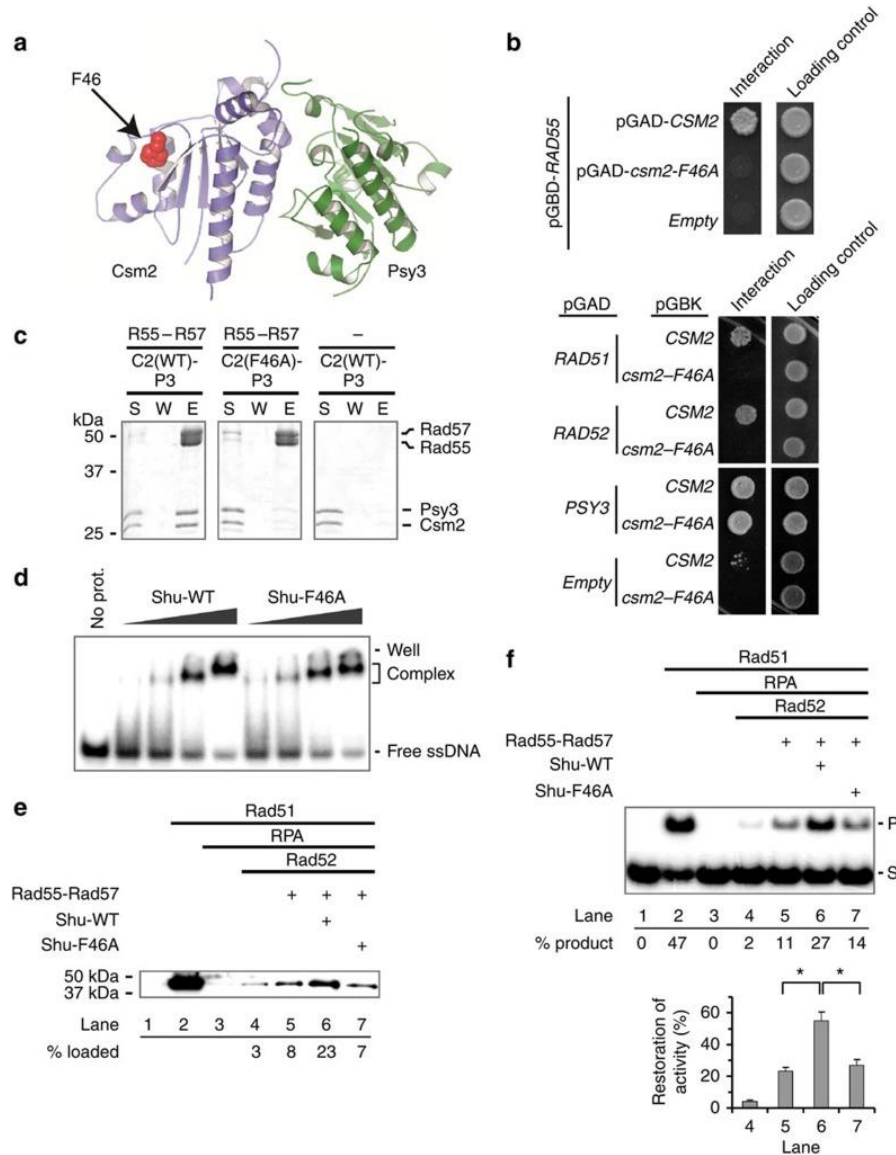


Figure 16. Impairment of physical interaction and functional synergy of the Shu complex with Rad55-Rad57 by the *csm2-F46A* mutation.

A. Cartoon view of the Csm2-Psy3 heterodimer(68), with Csm2 in blue and Psy3 in green. Csm2-F46 is highlighted in red. B. Y2H analysis for interaction of Csm2 and *csm2-F46A* with Rad55, Rad51, Rad52, and Psy3. C. Pull-down assay (as in Fig. 1a) to examine interaction of (His)₆-Rad55-Rad57 with Csm2-Psy3 harboring *csm2-F46A*. D. Analysis of the DNA binding activity of Shu complex harboring *csm2-*

F46A. E. Rad51 loading and F. DNA strand exchange assays were carried out as in Figure 15 to evaluate the efficacy of Shu complex harboring *csm2-F46A* in the promotion of presynaptic filament assembly. Standard deviations are plotted and (*) indicates significance.

We purified Csm2-Psy3 containing the *csm2-F46A* mutant and verified that it is impaired for Rad55-Rad57 interaction (Figure 16C) but is proficient in DNA binding (Shu-F46A; Figure 16D) and complex formation with Shu1-Shu2 (Figure 24). Consistent with Rad55 bridging the interactions between Csm2 with Rad51 and Rad52, we found that the mutant Csm2 does not interact with Rad51 or Rad52 (Figure 16B), and, importantly, that Shu-F46A is unable to enhance Rad51 presynaptic filament assembly in the bead-based Rad51 loading assay or DNA strand exchange reaction (Figure 16E, F, compare lane 6 to 7). These results provide the first evidence that the physical interaction between Csm2 and Rad55-Rad57 is functionally significant and are congruent with our finding that the Shu complex synergizes with Rad55-Rad57 in Rad51 presynaptic filament assembly.

To determine if the Csm2-Rad55 interaction is important for HR, we integrated *csm2-F46A* into the endogenous *CSM2* locus and found that the mutant cells are almost as sensitive to MMS as *csm2Δ* cells (Figure 17A). Furthermore, since previous studies demonstrated that the Shu complex acts upstream of Sgs1, we tested if the *csm2-F46A* mutation suppresses the MMS and HU sensitivity of an *sgs1Δ* mutant like *csm2Δ* and found that it does (Figure 17B). We next employed a direct repeat recombination assay (89,164) to reveal that *csm2-F46A* cells are as impaired as the *csm2Δ* mutant in Rad51-mediated gene conversion (Figure 17C), with a corresponding increase in Rad51-independent single-strand annealing events (Figure 17C; (89), p -value < 0.02). Consistent with disruption of other HR factors (99), using a canavanine mutagenesis assay we found that *csm2-F46A* cells accumulate spontaneous mutations like *csm2Δ* (60,62)

(Figure 17D). Together, our results demonstrate that the interaction between Csm2 and Rad55 is indispensable for the biological efficacy of the Shu complex.

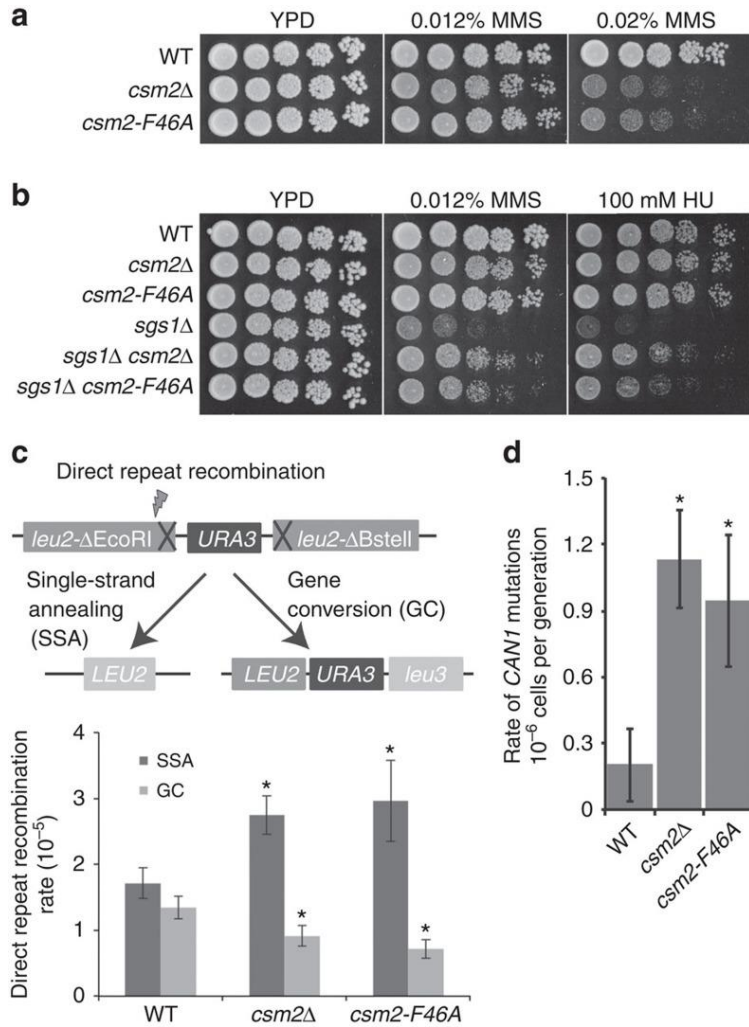


Figure 17. Impairment of homologous recombination by the *csm2-F46A* mutation.

A. *csm2-F46A* cells are as sensitive to MMS as a *csm2Δ* mutant. Cultures were five-fold serially diluted onto YPD medium with the indicated dose of MMS and incubated for 2 days at 30°C. B. Similar to *csm2Δ*, *csm2-F46A* alleviates the MMS and HU sensitivity of an *sgs1Δ* mutant. Cells of the indicated genotypes were five-fold serially diluted and tested for sensitivity to 0.012% MMS or 100 mM HU. C. WT, *csm2Δ*, or *csm2-F46A* cells harboring a direct repeat HR reporter (*leu2-ΔEcoRI::URA3::leu2-ΔBstEII*) were tested for spontaneous rates of Rad51-dependent gene conversion (GC) and Rad51-independent single-strand annealing (SSA) as

described (89). The rates of GC are significantly decreased in both *csm2-F46A* and *csm2Δ* strains ($p < 0.01$) with a corresponding increase in SSA relative to WT strains ($p < 0.02$). Standard deviations are plotted and (*) indicates significance. D. Like *csm2Δ* cells, *csm2-F46A* cells exhibit an elevated mutation rate in a canavanine mutagenesis assay. Standard deviations are plotted and (*) indicates significance.

4.3 DISCUSSION

Regulation of Rad51 presynaptic filament formation is essential for HR-mediated repair of damaged DNA and stalled replication forks. Mutations in human mediators of Rad51 presynaptic filament assembly, viz, the hRAD51 paralogues (RAD51B, RAD51C, RAD51D, XRCC2, XRCC3) or BRCA2, can result in a predisposition to numerous cancers (71,92-94,98). Whether the Rad51 mediators function independently or in a cooperative fashion has remained unknown (27,165,166). In budding yeast, Rad52 and the Rad55-Rad57 complex have been shown biochemically to promote presynaptic filament formation in isolation. We have furnished evidence that while the Shu complex is devoid of recombination mediator activity, it synergizes with Rad55-Rad57 and Rad52 to mediate the assembly of Rad51 on RPA-coated ssDNA (Figure 18, see chapter 5 discussion). Our work supports a model in which Rad55-Rad57 bridges an interaction between Rad52 and the Shu complex (Figure 14) that is functionally important for Rad51 presynaptic filament assembly (Figure 15, Figures 27 and 29). Our study represents the first *in vitro* reconstitution of Rad51 presynaptic filament assembly being mediated by an ensemble of seven proteins (Rad52, Rad55-Rad57, and Shu1-Shu2-Csm2-Psy3). Furthermore, we have revealed the importance of the Csm2-Rad55 interaction in promoting HR in cells (Figure 17) and in the facilitation of Rad51 presynaptic filament assembly and homologous DNA

pairing and strand exchange *in vitro* (Figure 16). Genetic evidence suggests that the Shu complex acts primarily in the repair of stalled replication forks (60), and while Shu1 and Shu2 are required for efficient fork repair *in vivo*, they are dispensable for Rad51 loading *in vitro* (Figure 29A). One possibility is that the Shu complex interaction with Rad55-Rad57 enables its association with replication fork derived DNA intermediates and subsequently Shu1 and Shu2 would be necessary for DNA repair progression. Although the function of Shu1-Shu2 remains elusive, previous work suggested that they may regulate Shu complex binding to complex DNA structures produced during HR (68), or Shu complex interactions with other HR regulators, such as Srs2 (35,63,150). Intriguingly, the arrangement of the human BCDX2 RAD51 paralogue complex is similar to the Shu complex with Rad55-Rad57 (Figure 31). Given the conservation of the HR machinery, mechanistic insights into the yeast Rad51 paralogues will provide a model for understanding how the human paralogues promote HR. For example, the human RAD51 paralogues may work with BRCA2, the functional equivalent of yeast Rad52, in presynaptic filament assembly (167). This postulated function of the human RAD51 paralogues is likely important for cancer avoidance (71,92-94,98).

4.4 MATERIALS AND METHODS

4.4.1 Strains, plasmids, and media

The strains used are listed in Table 6. Yeast crosses, transformations, tetrad dissections, and media preparation were carried out as described (89). The *csm2-F46A* mutation was introduced into integration, Y2H, and expression vectors by site-directed mutagenesis using primers

Csm2.F46A.Forward (GATGCCACAAGCTCAGCTCCGCTAAGTCAATTCC) and Csm2.F46A.Reverse (GGAATTGACTTAGCGGAGCTGAGCTTGTGGCATC). The integration vector was made using primers Csm2.Integration.HindIII (CCCAAGCTTAACAATTCCTCTCTGAGTTGAAA) and Csm2.Integration.MfeI (CCCCAATTGTATCCTTTAAATAAAACCTGTTTTTCCC) to amplify *CSM2* with promoter and terminator from genomic DNA. The amplified DNA was cut with HindIII and MfeI and ligated into yiPLAC211 cut with HindIII and EcoRI.

4.4.2 Yeast-2-Hybrid analysis

Y2H experiments were carried out as described in chapters 2 and 3.

4.4.3 Serial dilutions

Five-fold serial dilutions were performed with a starting OD₆₀₀ of 0.5, as described in chapters 2 and 3.

4.4.4 Mitotic recombination assay

Mitotic recombination assays were performed as described in chapters 2 and 3 (164) and recombination rates and standard deviations calculated (126). Each experiment was performed in quadruplicate with standard deviations plotted and significance determined by t-test.

4.4.5 Canavanine mutagenesis assay

For each trial, individual *CAN1* colonies from WT, *csm2* Δ , and *csm2-F46A* cells were grown in 5 ml YPD medium overnight at 30°C, diluted 1:10, and 250 μ l were plated onto SC-ARG+CAN plates. To determine the number of cells plated, the culture was further diluted 1:10,000 and 120 μ l were plated onto YPD plates. The plates were incubated at 30°C for two days before colonies were counted. The relative rate of *CAN1* inactivation for each strain is reported as an average of five experiments with standard deviations plotted.

4.4.6 Suppression of *rad54* Δ *srs2* Δ synthetic lethality

To analyze the suppression of *rad54* Δ *srs2* Δ synthetic lethality, a diploid yeast strain heterozygous for the indicated genes was sporulated for 72 hrs and tetrad dissected onto rich medium and incubated for two days at 30°C. Three hundred and sixty one tetrads were genotyped and assessed for viability. Chi squared analysis was used to determine significance for which genotypes were associated with inviability.

4.4.7 Protein expression and purification

Rad51, Rad52, RPA, and Rad54 proteins were prepared as previously described (168-170). The Rad55-Rad57 complex was expressed in *S. cerevisiae* strain JEL1 (171) by using the pESC-URA vector (Agilent) harboring (His)₆-tagged *RAD55* and FLAG-tagged *RAD57* genes; the affinity tags are fused to the N-termini of Rad55 and Rad57 proteins. Cells were grown at 30°C until OD₆₆₀ of 0.7 then induced for protein expression by the addition of galactose to 2%, cultured

for an additional 18 hrs, and harvested by centrifugation. All the subsequent steps were carried out at 4°C in Buffer T (25 mM Tris-HCl, pH 7.4, 10% glycerol, 0.5 mM EDTA, 0.01% IGEPAL CA-630 (Sigma), 1 mM DTT) was used throughout protein purification. Importantly, the inclusion of ATP and Mg²⁺ during lysis (with 5 mM ATP and 2 mM Mg²⁺) and purification steps (with 2 mM of each) helps minimize the aggregation of Rad55-Rad57 and precipitation. To prepare cell lysate, a 40 g cell pellet was resuspended in 160 ml of buffer with 500 mM KCl, 10% sucrose, 0.1% IGEPAL, and protease inhibitors (1 mM phenylmethylsulfonyl fluoride and 5 µg/ml each of aprotinin, chymostatin, leupeptin, and pepstatin) then lysed by grinding with dry ice followed by sonication. After ultracentrifugation (100,000 X g for 1 hr), the clarified lysate was incubated with 2 ml of Ni²⁺-NTA affinity resin (Qiagen) for 30 min with gentle mixing. The resin was poured into a column and washed using buffer with 500 mM KCl and 20 mM imidazole, followed by elution using wash buffer supplemented with 250 mM imidazole. The eluate was then mixed with 0.5 ml anti-FLAG affinity resin (Sigma) for 2 hrs with gentle mixing. The resin was poured into a column and washed using buffer with 200 mM KCl, followed by elution using wash buffer supplemented with 0.3 mg/ml FLAG peptide. The protein pool was diluted with an equal volume of buffer T and fractionated in a 1 ml Mono Q column with a 30 ml gradient of 100-700 mM KCl, collecting 0.5 ml fractions. The peak fractions of Rad55-Rad57 (eluting at ~290 mM KCl) were pooled, concentrated in an Amicon Ultra micro-concentrator (Millipore) to 0.6 ml, and fractionated in a 24 ml SuperDex 200 size exclusion column (GE Healthcare) in buffer with 300 mM KCl, collecting 0.5 ml fractions. The peak fractions of Rad55-Rad57 (eluting at appropriate position for monodisperse, heterodimeric complex) were pooled, concentrated in an Amicon Ultra micro-concentrator to 150 µl, snap-frozen in liquid nitrogen, and stored at -80°C. The yield of highly purified Rad55-Rad57 was ~150 µg.

The Shu complex was expressed in *E. coli* (Rosetta [DE3]) by co-transforming cells with the pET-Duet vector harboring (His)₆-tagged Shu1 and MBP-tagged Shu2 and the pRSF-Duet vector harboring Strep-tagged Csm2 and FLAG-tagged Psy3. All the affinity tags are fused to the N-terminus of proteins. Cells were grown in 2xLB broth supplemented with 0.1 mM ZnCl₂ at 37°C until OD₆₀₀ of 0.8 and protein expression was induced by the addition of IPTG to 0.2 mM and shifted to growth at 16°C for 16 hrs. Cells were harvested by centrifugation. All the subsequent steps were conducted at 4°C in buffer T. For lysate preparation, a 40 g cell pellet was resuspended in 200 ml of buffer with 300 mM KCl and protease inhibitors as above then lysed by sonication. After ultracentrifugation (100,000 X g for 1 hr), the clarified lysate was incubated with 2 ml of Ni²⁺-NTA affinity resin (Qiagen) for 30 min with gentle mixing. The resin was poured into a column and washed using buffer with 150 mM KCl and 10 mM imidazole, followed by elution using wash buffer supplemented with 200 mM imidazole. The eluate was then mixed with 2 ml amylose affinity resin (NEB) for 2 hrs with gentle mixing. The resin was poured into a column and washed with buffer with 150 mM KCl. Tobacco etch virus (TEV) protease (10 µg) was mixed with the resin to cleave at the linker between MBP and Shu2 and thus permit release of the Shu complex from the amylose resin; this incubation was performed overnight at 4°C. The released Shu complex was mixed with 0.7 ml anti-FLAG affinity resin (Sigma) for 2 hrs with gentle mixing. The resin was poured into a column and washed using buffer with 150 mM KCl, followed by elution using wash buffer supplemented with 0.3 mg/ml FLAG peptide. The eluate was concentrated in an Amicon Ultra micro-concentrator to 0.6 ml and fractionated in a 24 ml SuperDex 200 column in buffer with 150 mM KCl, collecting 0.5 ml

fractions. For both WT and F46A forms, Shu complex eluted at the position for monodisperse tetrameric protein complex. The peak fractions were pooled, concentrated in an Amicon Ultra micro-concentrator to 100 μ l, snap-frozen in liquid nitrogen, and stored at -80°C. The yield of highly purified Shu complex was 65 μ g.

4.4.8 Affinity pull-down assays

Csm2-Psy3 (0.5 μ g) was incubated with or without His-tagged Rad55-Rad57 (0.5 μ g) in 30 μ l of buffer C (20 mM MOPS, pH 7.2, 150 mM KCl, 10% glycerol, 0.01% IGEPAL, 1 mM DTT, 1 mM ATP, 2 mM MgCl₂, 15 mM imidazole) for 60 min at 4°C. The reactions were mixed with 4 μ l of Ni²⁺-NTA resin for 30 min at 4°C. After washing the resin five times with 150 μ l of buffer C with 200 mM KCl, bound proteins were eluted with 2% SDS. The supernatant (S), elution (E), and wash (W) fractions were analyzed by 15% SDS-PAGE followed by Coomassie Blue staining. For pull-down via GST-Rad52, proteins were captured on glutathione resin using the same procedure as above but using buffer with 100 mM KCl and no imidazole, then the various fractions were immunoblotted with α -FLAG antibody (Sigma Aldrich, catalog # A8592) to detect the FLAG-tagged Shu complex and Rad55-Rad57. The input samples shown represent 1/30th of the total input.

4.4.9 Rad51 loading onto ssDNA immobilized on magnetic beads

RPA (0.4 μM) was added to biotinylated dT 83-mer ssDNA (1.4 μM nucleotides) coupled to magnetic streptavidin beads (Roche) in 10 μl of buffer A (35 mM MOPS, pH 7.2, 50 mM KCl, 1 mM DTT, 2 mM ATP, 5 mM MgCl_2 , 100 $\mu\text{g/ml}$ BSA) at 37°C for 10 min. Excess RPA was removed by magnetic separation. Then, a mixture consisting of the indicated combination of Rad51, Rad52, Rad55-Rad57, and Shu complex was added to the RPA-coated ssDNA resin in 10 μl buffer A. The protein concentrations used were 0.75 μM Rad51, 0.06 μM Rad52, 0.11 μM Rad55-Rad57, and 0.23 μM Shu complex. The reactions were incubated at 18°C (except where stated otherwise) for 90 min with periodic agitation. The beads were briefly washed twice with 10 μl buffer A. Proteins were eluted with 2% SDS and Rad51 amount was determined by immunoblotting with α -Rad51 antibody (144).

4.4.10 Homologous DNA pairing and strand exchange reaction

Oligonucleotide-based DNA pairing and strand exchange assay was conducted as described previously (172) with slight modifications. The 80-mer ssDNA oligonucleotide (1.6 μM nucleotides) was incubated with RPA (0.13 μM) in buffer A at 37°C for 10 min. Then, a mixture consisting of the indicated combination of Rad51, Rad52, Rad55-Rad57, and Shu complex was incorporated. The protein concentrations used were 0.64 μM Rad51, 0.05 μM Rad52, 0.14 μM Rad55-Rad57, and 0.14 μM Shu complex. The reactions were incubated at 18°C (except where stated otherwise) for 90 min, then spermidine (4 mM final concentration) and ^{32}P -labeled

homologous 40-mer dsDNA (0.8 μM base pairs final concentration) with Rad54 (0.035 μM final concentration) and an ATP regenerating system (20 mM creatine phosphate, 30 $\mu\text{g/ml}$ creatine kinase) were added to complete the reaction (final volume of 12.5 μl). The reactions were incubated for 30 min at 18°C, deproteinized by treatment with 1% SDS and 1 mg/ml proteinase K for 5 min at 37°C, and then subjected to electrophoresis in a 10% polyacrylamide gel in TAE buffer (40 mM Tris acetate, pH 7.4, 0.5 mM EDTA). Radiolabeled DNA species were visualized and quantified by phosphorimaging.

4.4.11 Electron microscopy

The reactions were set up similarly to the DNA strand exchange assay for examining Rad51 loading efficiency, except that a longer ssDNA substrate (150-mer) was used and BSA was not included in buffer A. After a 1.5 hr incubation at 18°C, the reaction was applied to a glow-discharged, carbon-coated EM grid (Ted Pella, Inc.) and stained with 2% uranyl acetate. The EM images were acquired on an FEI Tecnai T12 transmission electron microscope at magnification of 30,000 with 20 images sampled per grid. 200 to 400 nucleoprotein particles were counted for each reaction condition.

4.4.12 DNA binding assay

The Shu complex (0.05, 0.10, 0.20, and 0.40 μM) was incubated with radiolabeled 83-mer ssDNA (1 μM nucleotides) in buffer B (20 mM MOPS, pH 7.2, 1 mM DTT, 150 mM KCl, 5 mM

MgCl₂, 2.5 mM ATP) for 10 min at 30°C. DNA species were resolved by electrophoresis in an 8% polyacrylamide gel run in TA buffer (40 mM Tris acetate, pH 7.4) and then visualized and quantified by phosphorimaging.

4.5 ACKNOWLEDGEMENTS

This chapter is modified from the following collaborative published work:

Gaines, W.A., Godin, S.K., Kabbinavar, F.F., Rao, T., VanDemark, A.P., Sung, P. and Bernstein, K.A. (2015) Promotion of presynaptic filament assembly by the ensemble of *S. cerevisiae* Rad51 paralogues with Rad52. *Nat Commun*, **6**, 7834.

All authors conceived of and planned the experiments. W.A.G. purified all proteins and performed all *in vitro* assays. W.A.G. and T.R. performed the electron microscopy experiments. A.P.V. performed all surface triplet propensity analysis. F.F.K. and S.K.G. performed the Y2Hs and performed the tetrad dissections. S.K.G. performed all serial dilutions, recombination assays, and mutagenesis assays.

5.0 DISCUSSION

Here we describe how the Shu complex has been conserved from budding yeast to humans, and provide evidence that it functions primarily to stimulate Rad51 filament formation during DNA damage as summarized in Figure 18. These findings have important implications for the study of homologous recombination and for understanding cancer development and treatment, as described in the preceding chapters. As the field turns its attention to the function of the human Rad51 paralogues, we believe the findings we have outlined here for the budding yeast Shu complex will serve as a framework for understanding the mechanistic function of the human Shu complex.

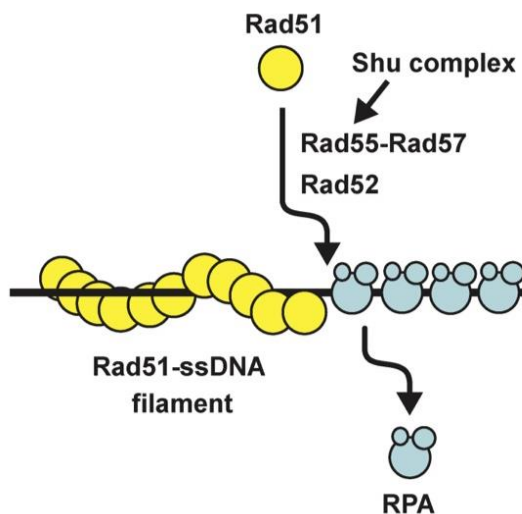


Figure 18. Model for Shu complex function in presynaptic filament assembly.

Rad52 and Rad55-Rad57 together promote the nucleation of Rad51 onto RPA-coated DNA to seed the assembly of the Rad51 presynaptic filament. Our results have revealed that the Shu complex, via its interaction with Rad55-Rad57, enhances the efficiency of the filament assembly process.

The observation a decade ago that Shu2 is well conserved from budding yeast to humans indicated that a mechanistic understanding of the Shu complex in yeast might be functionally

relevant to humans. Other groups have found physical interactions between Shu2/SWS1 with Rad51 paralogues in budding yeast, fission yeast, and humans, but no group had conclusively determined whether the Shu complex has an orthologous complex in higher eukaryotes. Our finding that every eukaryotic lineage has a clear Shu2 orthologue, and that this orthologue shows strong co-evolutionary signatures with Rad51 paralogues, strongly supports the idea that every eukaryotic lineage contains a Shu complex comprised of a Shu2/SWS1 orthologue interacting with Rad51 paralogues. Indeed, after identifying the Shu2 orthologue in *C. elegans*, other members of the laboratory were able to detect physical interactions between *C. elegans Sws-1* and the *C. elegans* Rad51 paralogues Rip-1 and Rfs-1 ((173), McClendon and Sullivan et al, unpublished work). This conservation of a Shu complex throughout eukaryotes means that moving forward, our understanding of the *in vivo* and *in vitro* functionality of the Shu complex in lower eukaryotes, such as budding yeast and *C. elegans*, will provide a framework for studying the human Shu complex and its role in human health.

The fact that the Shu complex responds only to specific forms of replication fork damage makes the Shu complex a compelling target for selective therapies. While inhibition of HR, such as in patients with mutations in *BRCA2*, dramatically sensitizes cells to different chemotherapeutic interventions, such as PARP inhibitors, chemical inhibition of central HR proteins such as *BRCA2* or *RAD51* are likely to cause serious side effects and be poorly tolerated in patients. The Shu complex, with its more specialized function and less severe phenotype when deleted when compared to the Rad51 paralogues Rad55-Rad57, may prove to be an effective target in the treatment of human disease. Why deletion of the Shu complex gives a minor phenotype relative to its binding partners Rad55-Rad57 remains unknown, but likely stems from its more specialized response to specific lesions and the possibility of Shu complex-independent HR pathways as

discussed below. Given the conservation of Shu2/SWS1 and its relatively minor phenotype compared to disruption of the Rad51 paralogues, inhibition of SWS1, perhaps by blocking its association with its obligate binding partner SWSAP1, may be an effective chemotherapeutic target. Disruption of the Shu complex will likely be effective at sensitizing tumors to alkylating agents, but not to other chemotherapeutics or endogenous damage, likely minimizing unwanted side effects compared to other targets in the HR pathway. Similarly, chemical inhibition of the Shu complex may prove useful for treating patients with Bloom, Werner, and Rothmund-Thomson syndromes. The Shu complex was originally characterized as mutants which rescue the defects created by Top3 and its binding partner, Sgs1, the homologue of the proteins mutated in Bloom, Werner, and Rothmund-Thomson syndromes (62). Disruption of the Shu complex rescues the severe hyper-recombination and mutation rates of cells without *SGS1*, and it will be important to determine if disruption of the human Shu complex will be able to rescue the phenotypes of cells without the Sgs1 homologues, indicating that the Shu complex could be a potent clinical target for these patients.

We feel that this study provides a reasonable framework in which to evaluate the function of the human Shu complex, but this work also raises numerous questions that should be addressed in budding yeast to more fully characterize the Shu complex. What follows are several of the major questions that these studies have generated, and several experimental approaches that will help to clarify the role of the budding yeast Shu complex in HR.

5.1 DOES THE SHU COMPLEX REMAIN ASSOCIATED WITH THE RAD51 FILAMENT?

The finding that the Shu complex acts to stimulate Rad51 filament formation, accounting for half of the total Rad51 filament formation *in vitro*, raises several questions about its function *in vivo* (chapter 4). For instance, how the Shu complex associates with the Rad51 filament remains unknown. The Shu complex could be integrated throughout the Rad51 filament, or it could bind to the surface of the filament as has been proposed for Rad52 (Summarized in Figure 19 and (27)). Alternatively, the Shu complex could act to “cap” a Rad51 filament, and direct Rad51 filaments to expand unidirectionally, as was suggested in a paper investigating the meiotic function of the Shu complex (90). Given these unanswered questions, it will be essential to look directly at Rad51 filaments by electron microscopy or dual atomic force microscopy in the presence or absence of the Shu complex, Rad55-Rad57, and Rad52 to determine if/how these proteins are interacting with the Rad51 filament. If the Shu complex remains associated with the Rad51 filament, it will be important to determine if it can impact downstream steps of HR, such as the recruitment of strand invasion factors, e.g. Rad54, Rdh54, or the inhibition of Srs2 during Rad51 filament formation.

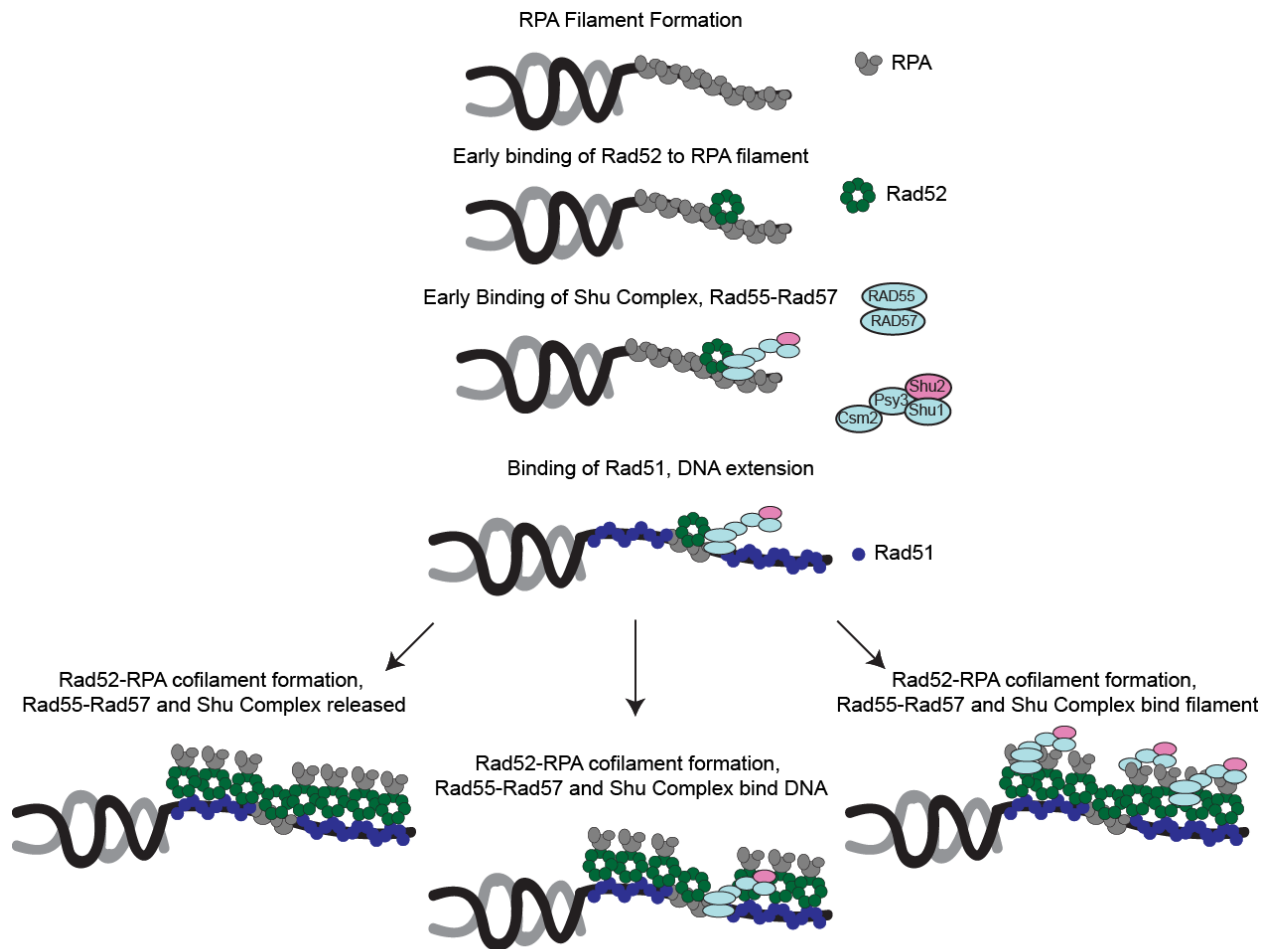


Figure 19. Models of how the Shu complex and Rad55-Rad57 may interact with the Rad51 filament.

The first, critical experiment to determine if the Shu complex remains bound to Rad51 filaments would be to directly visualize these filaments, such as by EM, AFM or as recently demonstrated in Claire Wyman's laboratory, using combined total internal reflection fluorescence and scanning force microscopy (TIRF-SFM, (36)). In general, during these kinds of experiments Rad51 coated ssDNA is placed onto a thin piece of mica or glass and visualized as a clearly visible nucleoprotein filament, similar to the EM images of Rad51 in chapter 4. Depending on the type of assay being used, proteins such as the Shu complex would be labeled by quantum-dot, gold particle, or fluorescent tags and co-incubated with the Rad51 filament and visualized for their ability to interact with the filament. A clear possibility in this assay is that the Shu complex would

need as its binding partners, Rad55-Rad57 and Rad52, to effectively or efficiently integrate into and/or interact with the Rad51 filament (Figures 18 and 19). Alternatively, the Shu complex may simply dissociate from the DNA as Rad51 filaments form (Figure 19, left). In an opposing model, the Shu complex may coat the Rad51 filament like its binding partner Rad52 (Figure 19, right). To investigate these models, the easiest approach would be to use the TIRF-SFM set up. In this assay, different fluorophores could be conjugated to Rad55, Rad52, and Csm2 to allow simultaneous visualization of each protein's localization patterns on Rad51 filaments. Alternatively, in an AFM or EM system, a single protein such as Csm2 could be labeled with a gold particle or quantum dot and evaluated for integration into the Rad51 filament with and without either Rad55 or Rad52. These experiments would likely provide exciting data on whether Csm2, as well as Rad55 and Rad52, could integrate into the Rad51 filament, and if that integration, or the location of the integration in the filament, depended upon the other proteins being evaluated.

Data from these kinds of experiments would likely be invaluable to our understanding of both the structure and contents of the Rad51 filament, as well the mechanistic function of the Shu complex itself. For instance, formation of Rad51 filaments on structured DNA, such as a forked DNA, may alter integration of the Shu complex into the filament, which could help inform the role of the Shu complex at MMS-induced replication damage (Discussed further in section 5.2). If the Shu complex integrates into the Rad51 filament, it may change the localization of other proteins known to interact with the filament, such as Rdh54, a potential binding partner for the Shu complex, which is discussed more in section 5.4. Additionally, the Shu complex is known to physical interact with Srs2 in both budding and fission yeast (63,64), and if the Shu complex was present inside the filament it may provide mechanistic clues to the significance of this interaction, which is the focus of section 5.3. Finally, the Shu complex has also been found to have an

important function in meiotic HR, so understanding how the Shu complex may differentially interact with a Rad51 filament, a filament of Dmc1, the meiosis-specific Rad51 homologue, or a co-filament of Rad51 and Dmc1 could yield functionally useful insights into the Shu complex's meiotic role which is discussed further in section 5.6.

5.2 WHAT UNDERLIES THE SPECIFIC ROLE OF THE SHU COMPLEX IN THE REPAIR OF MMS-INDUCED DNA DAMAGE?

With such a central function in HR as stimulating 50-70% of the total amount of Rad51 filament formation *in vitro* (chapter 4), an important question in the field is why the Shu complex mutants are only sensitive to such a discrete set of damaging agents, e.g. MMS and cisplatin induced replication damage, while the Shu complex's binding partners Rad52, Rad55, and Rad51 have much broader DNA damage sensitivities, including other replicative blocking agents such as UV or hydroxyurea (HU) treatment (Godin et al unpublished).

5.2.1 Lesion specificity of the Shu complex

One possible explanation is that the Shu complex may respond only to discrete lesions at a replication fork, such as methylated DNA, abasic sites, or ssDNA breaks. However, by blocking the repair of methylated DNA by base excision repair at different steps so that cells would accumulate different levels of these lesions, we were unable to see any lesion specificity for the Shu complex in the repair of MMS-induced damage (Godin et al, unpublished). In fact, this analysis broadened the substrate specificity for the Shu complex to include methylated DNA,

ssDNA breaks, abasic sites, and the intermediates produced by *rad27* Δ cells, which may include both the replication intermediates (e.g. unprocessed okazaki fragments) or the unrepaired 5'-dRPs normally processed by Rad27 during BER (Godin et al, unpublished). Together, this analysis suggests that the Shu complex is responding to many types of lesions that challenge replication forks and thus lesion-specificity may not fully explain the modest phenotype of a Shu complex mutant. Alternatively, these data may support a model wherein the Shu complex promotes a specific pathway in HR, e.g. replication fork protection as discussed in section 5.3.

This analysis raised even further questions about the Shu complex's specificity for DNA damage beyond MMS. We found that disruption of any member of the Shu complex results in sensitivity to cisplatin, which can induce replication fork blocking lesions. These include intra-strand DNA crosslinks and protein-DNA crosslinks, in addition to the more severe ICLs that block DNA unwinding. Because of the broad spectrum of lesions produced during cisplatin treatment, it will be important to determine if the Shu complex has a direct role in ICL repair. Moving forward, this should be addressed by testing the Shu complex mutants for sensitivity to other crosslinking agents, such as psoralen or mitomycin C. If the Shu mutants are sensitive to other sources of ICLs, genetic analysis with other components of ICL repair, e.g. Rad1-Rad10 in NER, or Rev3 in TLS, will be informative. Our unpublished data has demonstrated that the Shu complex mutants are not normally sensitive to UV, and that deletion of Rad1 does not significantly sensitize Shu complex mutants to MMS. If the Shu complex mutants display no synthetic sickness with Rad1 upon UV treatment or MMS treatment, but do display synthetic sickness with Rad1 upon psoralen or cisplatin treatment, it would strongly implicate the Shu complex in ICL repair.

Studying the potential role for the Shu complex in ICL repair will also generate useful data for another unanswered question about the Shu complex's lesion specificity, which is why the Shu

complex is not sensitive to UV radiation. Our unpublished data, as well as other groups, have clearly implicated other HR proteins such as Rad55 in the repair and/or bypass of UV damage (61). However, the Shu complex mutants display no sensitivity beyond WT, even at doses of UV near the lethal range for WT cells. In order to verify that the Shu complex has no role in the replication fork blocking lesions produced by UV, several experiments would be highly informative. An obvious hypothesis is that, in the absence of the Shu complex, the cell is able to reliably use TLS polymerases to efficiently bypass these photoproducts. To determine if the Shu complex functions only in a back-up capacity, single and double mutants between Shu complex mutants, such as *csm2Δ*, and TLS mutants, such as *rev3Δ*, should be evaluated for UV sensitivity. Excitingly, a recent report has used this kind of analysis and found that the double mutants exhibit synergistic UV sensitivity, suggesting a role for the Shu complex in the bypass of UV photoproducts when TLS polymerases are inhibited (61). Building off of these findings, it would be straightforward to perform mutagenesis and recombination assays in WT, *rev3Δ*, *csm2Δ*, and *rad55Δ* combination cells to determine the importance of the Shu complex in promoting repair/tolerance of these lesions by HR. For example, treatment with UV would be predicted to induce either recombination (Bypass by HR) or bypass by TLS polymerases. Looking at the balance of repair by mutation vs. recombination in each single, double, and triple mutant would be informative for determining the preferred repair pathways in a WT cell, and for learning why the Shu complex mutants are only sensitive to UV when TLS polymerases are disrupted. Additionally, determining the difference between a *rad55Δ* mutant, which is sensitive to UV even when TLS polymerases are functional, and a *csm2* mutant, which is not sensitive to UV when TLS polymerases are present, may shed light on the differences between Shu complex-dependent and independent HR.

5.2.2 Regulation of the Shu complex activity by post-translational modifications

One explanation for the differences in Shu complex-dependent and independent HR is that post-translational modifications of some components of the HR machinery may be necessary for recruitment of the Shu complex to sites of damage. There are several promising, non-exclusive possibilities as to what these post-translation modifications may be. For example, Rad55 is phosphorylated in response to DNA damage, specifically after treatment with MMS (29), and, interestingly mutations in Rad55 that prevent Rad55 phosphorylation give a hypomorphic phenotype. These Rad55-phosphorylation mutants are primarily sensitive to MMS, but not IR, and display a reduced MMS sensitivity when compared to a full deletion of *RAD55*. This phenotype is remarkably similar to the deletion of any member of the Shu complex, raising the possibility that Rad55 phosphorylation is required to stimulate its interaction with the Shu complex. In order to test this hypothesis, several experiments would be important. First, Y2H analysis comparing the Rad55 phosphorylation-null mutant's interaction with Csm2 to the WT Rad55 would be highly informative, where loss of this interaction would support the hypothesis that Rad55 phosphorylation regulates binding to the Shu complex. Additionally, since all *in vitro* work on Rad55-Rad57 uses proteins purified from yeast, it is possible that a fraction of the Rad55-Rad57 being used are phosphorylated and they may be responsible for the interaction levels observed (chapter 4). These *in vitro* pull down assays should be repeated in the presence or absence of a phosphatase, which will remove the endogenous phosphorylation of Rad55-Rad57, or the kinase Rad53, which phosphorylates Rad55-Rad57, to determine if phosphorylation is important for this interaction. Finally, evaluating the epistatic relationship between a Rad55 phosphorylation-null mutant and *CSM2* for MMS resistance or ability to perform HR would determine if the Shu complex requires Rad55's phosphorylation in order to exert its function.

Beyond Rad55, posttranslational modifications of other factors, such as SUMOylation of Rad52, could also regulate the Shu complex. Previous reports find that deletion of *SHU1* can inhibit Rad52-dependent HR at rDNA (32), but this inhibition largely depends on the ability of Rad52 to be SUMOylated. One possible explanation for this finding is that SUMOylated Rad52 triggers a Shu complex-dependent form of HR, but non-SUMOylatable Rad52 is incapable of effectively initiating Shu complex-dependent HR. These experiments that found this relation with SUMO status of Rad52 were performed exclusively on rDNA, so it would be informative to determine if non-SUMOylatable Rad52 has any other HR defects outside of the rDNA. These could include impaired HR, as measured by the direct repeat recombination assay, or sensitivity to MMS. Both potential phenotypes could be due to reduced Shu complex functionality. Alternatively, the non-SUMOylatable form of Rad52 may actually suppress a Shu complex mutant's MMS sensitivity if an alternative form of HR is being reliably initiated. Determining if the SUMO status of Rad52 alters a Shu complex mutant's phenotype would clarify the role of post-translational modifications on regulating the function of the Shu complex.

5.3 WHAT DIFFERENTIATES THE ROLE OF THE SHU COMPLEX AT AN HU-INDUCED STALLED FORK FROM AN MMS-INDUCED STALLED FORK

One of the major questions regarding the Shu (Suppresses HU sensitivity) complex is why deletion of the Shu complex is able to rescue both the severe MMS and HU sensitivity of an *sgs1Δ* cell, while disruption of the Shu complex itself only leads to increased sensitivity to MMS but not HU. The fact that loss of the Shu complex rescues an HU-treated *sgs1Δ* cell strongly suggests that a major function of the Shu complex is to generate the kinds of toxic DNA intermediates, e.g. double

Holliday junctions, that are normally processed by Sgs1 following HU exposure. However, the observation that Shu complex mutants display no HU sensitivity, whereas other HR mutants such as *rad55Δ* cells are sensitive to HU, suggest there is a Shu complex-independent role for HR proteins at the replication fork that does not necessitate the formation of complex, HR intermediates that are toxic in *sgs1Δ* cells (61,62). Excitingly, several recent reports suggest possible clues as to what these Shu complex independent roles might be as well as methods to test these models.

In humans, RAD51 has functions independent of HR in regulating HU-stalled replication forks (84). This work found that RAD51 interacts with FANCD2 and RAD18 to ensure mono-ubiquitination of PCNA. Mono-ubiquitinated PCNA results in Pol eta recruitment to HU-stalled replication forks, which promotes survival of HU-treated cells through an as yet undetermined mechanism. Critically, this function for RAD51 persisted when RAD51 was pharmacologically inhibited from performing HR or in cells lacking BRCA2, a critical factor for HR, which suggests RAD51's function at HU-treated forks is independent of HR. One hypothesis for why Shu complex mutants are not HU sensitive is that in the absence of Shu complex-dependent HR, cells can readily utilize a similar kind of pathway where TLS polymerases are able to promote viability in HU treated cells. In support of this model, previous work has uncovered that simultaneous disruption of *REV3*, yeast pol zeta, with the Shu complex can uncover a previously unobserved role for the Shu complex at UV-damaged replication forks, so a similar phenomena may occur in HU-treated cells (61). However, in the absence of Rad51-stabilizing proteins such as Rad55, this Rad51-dependent recruitment of TLS polymerases may not occur as readily, giving rise to the HU sensitivity seen in *rad55Δ* cells. Moving forwards, it will be informative to evaluate the recruitment and function of the TLS polymerases at HU-stalled replication forks in the presence

or absence of the Shu complex or other members of the HR machinery using chromatin immunoprecipitations and the kinds of genetic assays described in chapters 3 and 4.

While evaluating the genetic dependencies for the Shu complex at HU-stalled forks will be informative, recent work has generated a new method to directly evaluate the role of the Shu complex at purified, HU-stalled forks. A recent paper from Dana Brnzei's group purified the HR intermediates produced at an MMS-damaged replication fork and directly evaluated these structure by EM (59). They found these cells generate multiple kinds of structures proposed to form during HR at a replication fork (Figure 2). These intermediates include double Holliday junctions, single Holliday junctions, and hemi-catenanes formed by Sgs1-mediated dissolution of double Holliday junctions. Critically, they also found that the lesion at a fork that initiates HR are likely gaps of ssDNA and not free ssDNA ends (Figure 2). Using this system, *sgs1*Δ cells accumulated more intermediates, as predicted. In order to determine why the Shu complex mutants display MMS but not HU sensitivity, use of this assay will be highly informative. In this assay, will there be differences in the kinds of replication fork intermediates that occur in HU vs. MMS treated cells? Or, will the different types of damage result in a similar kind of repair by HR? If the Shu complex is disrupted in these HU and MMS-treated cells, how are the kinds of DNA intermediates formed after each damaging agent different? Finally, will replication forks form different repair intermediates in an HU-treated Shu complex mutant compared to an HR mutant that is HU sensitive, such as a *rad55*Δ cell? The ability to now directly visualize stalled and broken replication forks by EM clearly has wide-ranging implications in the study of the Shu complex and its differential response to different sources of replication fork stress.

5.4 WHAT IS THE IMPORTANCE OF THE PHYSICAL ASSOCIATION BETWEEN SHU2 AND SRS2?

One of the enduring questions about the Shu complex centers on the function of Shu2's conserved interaction with Srs2. Before the Shu complex was characterized in 2005, it was identified in a high-throughput Y2H screen as a protein that physically interacts with Srs2, whose mechanistic function *in vitro* is to disassemble Rad51 filaments and to regulate polymerase interactions with PCNA during replication (33,34,62,63). In 2006, when the fission yeast Shu complex was characterized, Shu2's orthologue Sws1 was also found to interact with Srs2 (64). However, the function of this conserved interaction has remained elusive. An obvious hypothesis is that the Shu complex, like Rad55-Rad57, could act to inhibit Srs2's ability to destabilize Rad51 filaments (35). In support of this model, previous work has suggested that disruption of the Shu complex causes an elevation in Srs2 foci by fluorescent microscopy (107). In addition, unpublished work from our laboratory finds that, in regards to MMS treatment, Srs2 is epistatic to the Shu complex, suggesting the Shu complex's primary role may relate to Srs2. Arguing against this model, however, is the finding that the Shu complex contains at least some Srs2-independent roles in HR since we find that the lethality of an *srs2Δ rad54Δ* cell is fully suppressed by further deletion of Csm2 (Chapter 4). As an alternative, Srs2 is known to interact with PCNA and prevent polymerases from interacting with PCNA. Thus the Shu complex's interaction with Srs2 may reflect a previously unknown role for the Shu complex in replication fork stability. In order to fully determine the mechanistic function of the interaction between Srs2 and Shu2, significantly more work is required.

The first step in understanding the significance of the interaction between Srs2 and Shu2 is to verify this interaction, originally found by Y2H, through several different approaches such as

Co-IP or by *in vitro* pull downs using purified proteins. It is entirely plausible that these two proteins may only interact in the presence of DNA as both are avid DNA binding proteins, and any Co-IP interaction observed with these proteins should be tested in the presence and absence of a DNase such as benzonase to determine the importance of DNA for this interaction. Additionally, since the Shu complex has been found to require its binding partner Rad55-Rad57 for essentially all of its mitotic functionality (chapter 4), it is possible the Shu complex may only interact with Srs2 via Rad55. This hypothesis could be tested by repeating the Y2H analysis between Srs2 and Shu2 using strains in which the endogenous Rad55 has been disrupted. If Shu2's interaction with Srs2 is dependent upon Rad55, the likely function of the Shu complex may be to further stimulate or regulate the observed ability of Rad55 to inhibit Srs2, which can readily be tested *in vitro* by repeating the experiments performed in (35) to include the Shu complex, or by modifying the *in vitro* assays in chapter 4 to include Srs2.

If, however, Shu2's interaction with Srs2 is independent of Rad55, use of separation-of-interaction alleles will likely prove to be the most useful way to study this interaction. Using site-directed mutagenesis in Shu2, it should be possible to perform a Y2H screen to find mutations that block or reduce the binding of Shu2 to Srs2. Shu2 likely represents an easier candidate in which to find mutations, as it is a significantly smaller protein (223 vs. 1174 amino acids) to mutagenize. Alternatively, if the Y2H screen fails, the analysis could be repeated with the well-conserved fission yeast proteins Srs2 and Sws1, which may give a stronger Y2H signal. Alternatively the interaction domain between Srs2 and Shu2 can be identified using *in vitro* pull-downs of one full-length protein with different domains of the other protein, e.g. full length Shu2 with the Rad51-interacting domain of Srs2. Finding the specific regions of each protein that physically interact with one another will enable a more directed mutagenesis screen to determine how mutations in

each domain alter this interaction. Regardless of the method used, identification of Shu2 alleles that block the interaction with Srs2 will be essential for determining the Srs2-specific functions of the Shu complex in promoting resistance to MMS, reducing mutations, and promoting recombination as determined using the kinds of genetic and *in vitro* assays outlined in chapters 3 and 4.

5.5 DOES THE SHU COMPLEX HAVE A ROLE DOWNSTREAM OF RAD51 FILAMENT FORMATION?

In addition to Shu2's observed interaction with Srs2, we have also found that every member of the Shu complex will strongly interact with Rdh54 by Y2H (Godin et al. unpublished), which suggests a role for the Shu complex in the later steps of HR where Rdh54 (human RAD54B) acts to stimulate strand invasion of Rad51 nucleoprotein filaments into homologous dsDNA. Unfortunately, if the Shu complex does act at later steps of HR, these functions would likely be masked in a full deletion of the Shu complex due to its early function in Rad51 filament formation. To determine a potential function of the Shu complex at these later steps, specific mutations in the Shu complex and/or its binding partner Rdh54 will need to be made to block this interaction. Using these mutants, Rad51 filaments should form normally, but the downstream roles of the Shu complex should be apparent and could be screened for by MMS sensitivity and HR pathway choice using different recombination assays.

There are, however, practical difficulties in studying the interaction between Rdh54 and the Shu complex. Rdh54 appears to interact with multiple components of the Shu complex, which is supported by Y2H analysis finding these interactions persist in cells where *SHU1*, *SHU2*, *CSM2*,

or *PSY3* have been individually deleted (Godin et al. unpublished). Thus, generating a strain where the interactions between the Shu complex and Rdh54 are fully ablated may be difficult. In an ideal scenario, Rdh54 may interact with all of the Shu complex members through the same interface, such that identification of a mutant in Rdh54 that blocks an interaction with one member of the Shu complex will block interactions with the other members of the Shu complex. However, if each member of the Shu complex interacts with Rdh54 through a separate domain, a Y2H screen of each member of the Shu complex for disruptions in the Rdh54 interaction will be necessary, and subsequent analysis of this interaction will necessitate combining multiple separation-of-interaction mutations for the four Shu complex members into one strain to completely inhibit this interaction.

If the practical limitations of these studies are overcome, however, there are several approaches to take to study the function of the interaction with Rdh54. First, using whichever separation-of-interaction approach proved viable, those strains could be evaluated for MMS resistance, mutagenesis, and HR levels as described in chapters 3 and 4. Defects in the recruitment of Rdh54 to a Rad51 filament could manifest as impaired recombination and reduced gene conversion, or it could cause persistent Rad51 filaments *in vivo* as measured by fluorescent microscopy. Alternatively, as Rdh54 has previously been implicated in regulating Rad51-independent BIR (55), perhaps use of these alleles in a BIR recombination assay, such as that developed by Lorraine Symington (54), would uncover a novel role for the Shu complex in preventing the use of this alternative HR pathway. Use of these alleles would also enable informative chromatin immunoprecipitation experiments (ChIP) to determine if the interaction between Rdh54 and the Shu complex is essential for Rdh54's recruitment to DSBs or stalled replication forks. Additionally, in each case described above, a powerful control would be to repeat

the experiments in a strain containing a form of Rad51 developed in Doug Bishop's laboratory that is entirely defective for strand invasion and that is epistatic to all defects in the recruitment of downstream factors such as Rdh54 (174).

5.6 HOW DOES THE FUNCTION OF THE SHU COMPLEX IN MEIOSIS DIFFER FROM MITOSIS?

An important aspect of the Shu complex that was not the central focus of this dissertation is its critical role in promoting HR during meiosis. Our work raises many questions about the mechanistic function of the Shu complex in meiosis, and how that function may differ from its role in mitotically cycling cells. Previous work from Akira Shinohara's group has determined that disruption of any member of the Shu complex causes a significant decrease in viable spores produced during meiosis (90). Critically, disruption of Shu1 or Shu2 gives a more modest phenotype (~75% viability) compared to disruption of Csm2 or Psy3 (~40% viability), suggesting the Shu complex in meiosis may not be functioning as an obligate heterotetramer as in mitosis ((90,175) and chapter 2). Importantly, Csm2 and Psy3 are epistatic to Shu1 and Shu2 in all experiments tested in meiotic cells. In meiosis, loss of the Shu complex results in reduced inter-homologue bias, and poor chromosomal segregation, all consistent with a role for the Shu complex in promoting Rad51 filament formation. However, disruption of the interaction between Csm2 and Rad55 by *csm2-F46A* as reported in chapter 4 does not cause a meiotic defect (Godin et al. unpublished data), suggesting the Shu complex may have a function independent of Rad55, and perhaps even Rad51, during meiosis.

To more fully explore the role of the Shu complex in meiosis, it is important to first verify that the defect caused by disruption of the Shu complex is due to impaired Rad51 filament formation. In meiosis, Rad51's recombinase activity is inhibited by Hed1, which allows the meiosis-specific Rad51 homologue Dmc1 to carry out the recombinase activity during the repair of Spo11-induced DSBs (176,177). If the defects in the Shu complex mutants are caused by impaired Rad51 filament formation, and not by any defects in Dmc1, then deletion of *HED1* will not be predicted to rescue the Shu complex mutants. If, however, *HED1* disruption rescues the phenotype of Shu complex disrupted meiotic cells, it would argue the Shu complex has a role beyond Rad51 filament formation, which is supported by the lack of a defect in the *csm2-F46A* cells. The likely role of the Shu complex would then be regulation of Dmc1, which is functionally and structurally very similar to Rad51. To test this hypothesis, it would be necessary to screen for interactions between the Shu complex and Dmc1 and its regulators, Mei5-Sae3 which excitingly interact with forked DNA structures and Rad51 filaments, just like the Shu complex ((178) chapters 3 and 4)), and additionally stimulate Dmc1 filament formation. If the Shu complex is capable of interacting with any of these proteins, it will be important to use similar *in vitro* assays discussed in chapter 4 to look for a role of the Shu complex in promoting Dmc1 filament formation.

Additionally, when investigating the function of the Shu complex in meiosis, it is important to note that essentially all interacting partners of the Shu complex have roles in meiosis. As a genetic interaction partner, Sgs1 is known to function in crossover regulation in meiosis, but whether the Shu complex has a role in regulating Sgs1 during meiosis is unknown. Similarly, Srs2's role in meiosis has only recently been investigated, but it seems to function to promote HR in potentially the same pathway as the Shu complex (175). Due to the potentially new role for Srs2 in promoting HR in meiosis, it is possible that the interaction observed between Srs2 and Shu2,

discussed in section 5.3, may indicate a cooperative role for these two proteins in meiosis, rather than the Shu complex inhibiting Srs2 as has been hypothesized in mitotic cells. Finally, even if the Shu complex's function in meiosis is to promote Rad51 filament formation, new models will need to be drawn to address why the interaction between the Shu complex and Rad55 seems dispensable for this function in meiotic but not mitotic cells.

5.7 CONCLUDING REMARKS

Together, this thesis helps to establish that the Shu complex is a conserved regulator of HR at specific kinds of replication fork damage and that the Shu complex primarily functions to promote Rad51 filament formation. While there are many open questions regarding the function of the Shu complex, it is our hope that the models and data presented in this work will provide a framework for the study of both the human and budding yeast Shu complexes moving forwards, and will contribute significantly to our understanding of the role of the Shu complex in human health and disease.

APPENDIX A

CHAPTER 2 SUPPLEMENTAL DATA

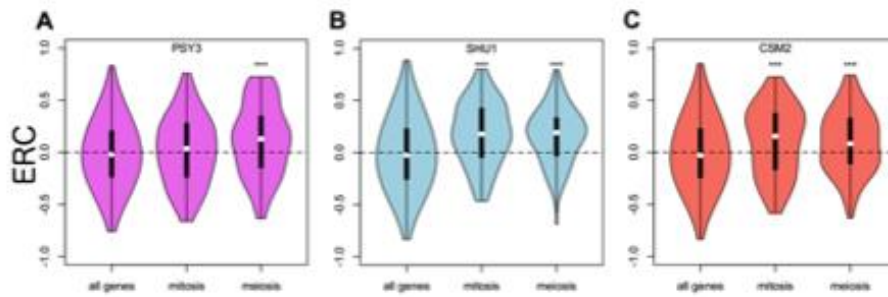


Figure 20. Distributions of ERC with Shu complex members PSY3.

A., SHU1 B., and CSM2 C. Violin plots show the median (dot) and upper and lower quartiles (black box) of ERC values of meiosis and mitosis proteins versus Shu complex members. Similarly, the violin curves depict the density of observed values. Both mitosis and meiosis groups were tested for their departure from the null (all genes) distribution. For these tests “***” indicates a P-value less than 0.001.

Saccharomyces cerevisiae	WFCSC EEFCKY---KVCC S HLLAF S ILL
Candida glabrata	WLC S CEEY T EI---KLLCP H LLAYS I ILL
Eremothecium gossypii	WFC S CT E FAAT---KLM C E H LF A FAILL
Kluyveromyces lactis	WFC S CN E YTKC---KV I C Q HLLAA A ILL
Vanderwaltozyma polyspora	WFC S CD E F N SY---KLMCP H LLAYS I ILL
Lachancea thermotolerans	WFC S CD E Y N TL---I I MC P HLLAF A ILL
Candida albicans	W Y CD C A E Y Q EC---VPV C S H ILAV L I I K
Clavispora lusitaniae	WFC S CE P FS R A---LPV C M H LLAL V LS A
Debaryomyces hansenii	W Y CS C DE F Q A S---LP I CC H L I AL S IA A
Yarrowia lipolytica	M F CT C H D Y A VA--- Q G I CK H LV A V Y IR K
Aspergillus oryzae	W N CT C P T FT L A--- H PV C K H LL A C V LA E
Aspergillus niger	W N CT C P T FT L N---P P V C K H LL A C C LA V
Schizosaccharomyces pombe	W Y CS C S Q FS Y N---P T IC S H I LA A S I LR
Coprinopsis cinerea	F Y CS C PA F S Y S--- H IM C K H LL A T L I A R
Tribolium castaneum	N F C Q C Q AF Q L Q --- S L T CK H V L AL K L N Q
Culex quinquefasciatus	N Y CT C K S Y R FW--- Q AL C K H LL A T R L A P
Dendroctonus ponderosae	N F CH C K F F E DK--- C IT C K H V L AV Y L A K
Drosophila melanogaster	S FC K CE F F Q CH--- S Y T C Q H I L A L R L H Q
Drosophila pseudoobscura	N Y CK C DF F Q S H--- S Y T CP H V L AL K L H Q
Daphnia pulex	F TCT C P S FR H N---N L W C K H LL A L Q LS L
Homo sapiens	H YCS C PA F AF S --- S IL C K H LL A V Y LS Q
Gallus gallus	H FCT C PA F GF T --- S LL C K H IL A V Y LS Q
Xenopus tropicalis	H YCS C PA F S F S--- N ML C K H IL A I Y LS Q
Danio rerio	H YCP C PA F S F T--- S LM C K H LL A V I LS Q
Strongylocentrotus purpuratus	G YCP C L F FS F A---V P M C K H ML A ILL S
Caenorhabditis elegans	H YCT C P Y F Q ST--- N W I CV H IL A Y F AK
Nematostella vectensis	D YCT C PS Y TY T --- S IL C K H LL A A H LA E
Arabidopsis thaliana	D YCG C YS F F Y D--- H PC C K H Q L AAR L AS
Oryza sativa	H LCT C YS F F Y D--- Q LC C K H Q L AAR L AE
Giardia lamblia	G YCS C CH S L R L--- R TF C R H LL A V Q IA I

Figure 21. A deep evolutionary alignment of Shu2/SWS1 orthologues clearly reveals conserved residues of the SWIM domain.

The first block contains the invariant and canonical CXC motif and the highly conserved F/Y residue just upstream. The second block contains the expanded CXHXXA motif.

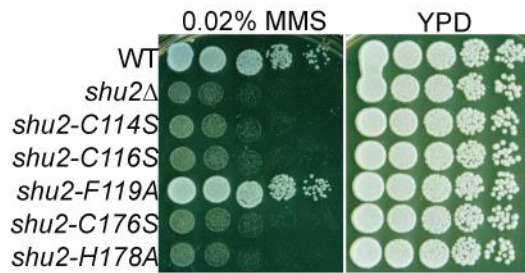


Figure 22. The SWIM domain is important for Shu2's function.

Canonical SWIM domain mutants are non-functional. The indicated mutants were stably integrated into the endogenous *SHU2* locus and 5-fold serially diluted onto YPD medium or YPD medium containing 0.02% MMS and incubated at 30°C for 2 days.

Table 2. Chapter 2 Strains and Plasmids

Name	Description
W9100-2D	<i>MATα ADE2 leu2-3,112 his3-11,15 ura3-1 TRP1 lys2Δ RAD5</i>
KBY159-1C	<i>MATα LYS2 shu1::HphNT1</i>
KBY162-7C	<i>MATα trp1-1 lys2Δ shu2::NatNT2</i>
KBY107-5C	<i>MATα leu2-3,112 trp1-1 LYS2 csm2::KanMX4</i>
KBY108-1C	<i>MATα bar1::LEU2 trp1-1 LYS2 psy3::KanMX4</i>
KBY213-2A	<i>MATα rad55::NatMX</i>
PJ69-4A	<i>MATα trp1-901 leu2-3,112 ura3-52 his3-200 gal4Δ gal80Δ GAL2-ADE2 LYS2::GAL1-HIS3 met2::GAL7-lacZ</i>
PJ69-4	<i>MATα trp1-901 leu2-3,112 ura3-52 his3-200 gal4Δ gal80Δ GAL2-ADE2 LYS2::GAL1-HIS3 met2::GAL7-lacZ</i>

KBY403 *MATa trp1-901 leu2-3,112 ura3-52 his3-200 gal4Δ gal80Δ GAL2-ADE2 LYS2::GAL1-HIS3 met2::GAL7-lacZ shu1::natMX4*
 KBY475 *MATa trp1-901 leu2-3,112 ura3-52 his3-200 gal4Δ gal80Δ GAL2-ADE2 LYS2::GAL1-HIS3 met2::GAL7-lacZ shu1::natMX4*
 W3770-4D *MATa leu2-ΔEcoRI::URA3::leu2-ΔBstEII*
 KBY13-2C *MATa leu2-ΔEcoRI::URA3-HO::leu2-ΔBstEII shu1::HIS3*
 KBY90 *MATa leu2-ΔEcoRI::URA3-HO::leu2-ΔBstEII shu2::TRP1*
 KBY469 *MATa shu2-C114S*
 KBY834-6A *MATa shu2-C116S trp1-1 LYS2 sgs1::HIS3*
 KBY835-3B *MATa shu2-F119A trp1-1 lys2Δ sgs1::HIS3*
 KBY836-5C *MATa shu2-C176S sgs1::HIS3 trp1-1 LYS2*
 KBY856-1C *MATa shu2-H178A sgs1::HIS3 trp1-1 LYS2*
 KBY161-2A *MATa trp1-1 LYS2 shu2::HphNT1*
 KBY51-3B *MATa sgs1::HIS3 trp1-1 LYS2 MET22*
 KBY484-2B *MATa sgs1::HIS3 shu2::NatMX4*
 KBY483-1B *MATa sgs1::HIS3 trp1-1 shu2-C114S*
 KBY138 *MATa/MATa ade2-1/ADE2 TRP1/trp1-1 lys2Δ/LYS2*
 W9100-11B *MATa ade2-1*
 W9100-12C *MATa ADE2 trp1-1 LYS2*
 KBY457 *MATa/MATa ade2-n/ade2-I-SceI shu1::HIS3/shu1::HIS3 met22::KLURA3/MET22 his3::NatMX4/his3::hphMX4 LYS2/lys2::GAL-Iscel*
 KBY21-3D *MATa ade2-n shu1::HIS3 LYS2 met22::KLURA3 his3::NatMX4 RAD5*

KBY24-13A *MAT α ade2-IsceI shu1::HIS3 lys2::GAL-IsceI ura3-1 MET22 his3::hphMX4*
 KBY341 *MAT α /MAT α shu2::TRP1/shu2::TRP1 leu2 Δ EcoRI::URA3-HO::leu2 Δ BstEII/ura3-1 LYS2/LYS2 trp1-1/trp1-1 ade2/ADE2*
 KBY92-1A *MAT α shu2::TRP1 LYS2 trp1-1*
 KBY488 *MAT α /mat α ade2-1/ADE2 trp1-1/TRP1 LYS2/lys2 Δ leu2 Δ EcoRI::URA3-HO::leu2 Δ BstEII/ura3-1 shu2-C114S/shu2-C114S*
 KBY474-1B *MAT α ade2-1 trp1-1 LYS2 leu2 Δ EcoRI::URA3-HO::leu2 Δ BstEII shu2-C114S*
 KBY474-1A *MAT α ADE2 TRP1 lys2 Δ ura3-1 shu2-C114S*
 KBY342 *MAT α ADE2/ade2-1 bar1::LEU2/leu2-3,112 TRP1/trp1-1 csm2::KanMX4/csm2::KanMX4 ura3-1/leu2 Δ EcoRI::URA3-HO::leu2 Δ BstEII*
 KBY107-2C *MAT α ADE2 bar1::LEU2 TRP1 csm2::KanMX4 ura3-1*
 KBY38-6D *MAT α csm2::KanMX4 leu2 Δ EcoRI::URA3-HO::leu2 Δ BstEII his3-11 trp1-1 ade2-1*
 KBY343 *MAT α psy3::KanMX4/psy3::KanMX4 leu2 Δ EcoRI::URA3-HO::leu2 Δ BstEII his3-11/ura3-1 ade2-1/ADE2 trp1-1/trp1-1 LYS2/LYS2*
 KBY57-1B *MAT α psy3::KanMX4 leu2 Δ EcoRI::URA3-HO::leu2 Δ BstEII ade2-1 trp1-1 LYS2*
 KBY106-12B *MAT α trp1-1 LYS2 psy3::KanMX4*
 KBY875 *MAT α / α ADE2/ADE2 TRP1/trp1-1 lys2 Δ /LYS2 shu2-C116S/shu2-C116S*
 KBY861-2C *MAT α ADE2 TRP1 lys2 Δ shu2-C116S*
 KBY861-1D *MAT α ADE2 trp1-1 LYS2 shu2-C116S*
 KBY886 *MAT α / α ADE2/ADE2 trp1-1/trp1-1 lys2 Δ /LYS2 shu1u2-F119A/shu1-F119A*

KBY835-3D	<i>MATa ADE2 trp1-1 lys2Δ shu2-F119A</i>
KBY835-5B	<i>MATα trp1-1 LYS2 shu2-F119A</i>
KBY878	<i>MATa/α ade2-1/ADE2 TRP1/trp1-1 LYS2/LYS2 shu2-C176S/shu2-C176S</i>
KBY863-5A	<i>MATa ade2-1 TRP1 LYS2 shu2-C176S</i>
KBY863-5C	<i>MATα ADE2 trp1-1 LYS2 shu2-C176S</i>
KBY876	<i>MATa/α ade2-1/ADE2 TRP1/trp1-1 lys2Δ/LYS2 shu2-H178A/shu2-H178A</i>
KBY864-1A	<i>MATa ade2-1 TRP1 lys2Δ shu2-H178A</i>
KBY864-1D	<i>MATα ade2-1 trp1-1 LYS2 shu2-H178A</i>
pWJ1479	<i>pGBDK-SHU2 (TRP, KAN^R)</i>
pWJ1474	<i>pGAD-SHU1 (LEU, AMP^R)</i>
pWJ1477	<i>pGAD-CSM2 (LEU, AMP^R)</i>
pWJ1476	<i>pGAD-PSY3 (LEU, AMP^R)</i>
pGAD-C2	<i>pGAD-C2 (LEU, AMP^R)</i>
pKB108	<i>pGBK-Shu2-C114S (TRP, KAN^R)</i>
pKB318	<i>pGBK-Shu2-C116S (TRP, KAN^R)</i>
pKB330	<i>pGBK-Shu2-F119A (TRP, KAN^R)</i>
pKB319	<i>pGBK-Shu2-C176S (TRP, KAN^R)</i>
pKB320	<i>pGBK-Shu2-H178A (TRP, KAN^R)</i>
pKB321	<i>pGBK-Shu2-A181T (TRP, KAN^R)</i>
pKB52	<i>pGAD-SWSAP1 (LEU, AMP^R)</i>
pKB78	<i>pGBD-SWS1 (TRP, AMP^R)</i>
pKB93	<i>pGBD-Sws1-C85S (TRP, AMP^R)</i>

pKB94	<i>pGBD-Sws1-C87S (TRP, AMP^R)</i>
pKB322	<i>pGBD-Sws1-F90A (TRP, AMP^R)</i>
pKB316	<i>pGBD-Sws1-C103S (TRP, AMP^R)</i>
pKB317	<i>pGBD-Sws1-H105A (TRP, AMP^R)</i>
pKB142	<i>pGBD-Sws1-A108T (TRP, AMP^R)</i>
pGBD-C1	<i>pGBD-C1 (TRP, AMP^R)</i>
pKB13	yiPLAC211-Shu2-C114S
pKB315	yiPLAC211-Shu2
pKB327	yiPLAC211-Shu2-C116S
pKB323	yiPLAC211-Shu2-F119A
pKB328	yiPLAC211-Shu2-C176S
pKB324	yiPLAC211-Shu2-H178A

All yeast strains are W303 background derivatives and *RAD5* (116) W1588 (117) except for PJ69-4A and PJ69-4 (118). The KBY403 and KBY475 strains were constructed in PJ69-4 and PJ69-4A backgrounds, respectively. The strains are listed in the order they appear in the figures and text.

Table 3. Chapter 2 Primers

Name	Sequence
hSWS1.F	GCGGAATTCATGGCCGTAGTGTTGCCGGCGGTTG
hSWS1.R	GCGGTCGACCTACTTAAAGGTGGACTGCAGCTC
SWSAP1.F	GCGGAATTCATGCCTGCCGCCGGACCGCCTTTG
SWSAP1.R	GCGGTCGACTCAGGGCTGGCCTCCAGAGCTTGAAC
hSWS1.C85S.F	GCTTCTTGTCATTACTCTTCATGTCCTGCATTTG
hSWS1.C85S.R	CAAATGCAGGACATGAAGAGTAATGACAAGAAGC
hSWS1.C87S.F	CTTGTCATTACTGTTTCATCTCCTGCATTTGCATTCTC
hSWS1.C87S.R	GAGAATGCAAATGCAGGAGATGAACAGTAATGACAAG
hSWS1.F90A.F	CTGTTTCATGTCCTGCAGCCGCATTCTCAGTGCTAC
hSWS1.F90A.R	GTAGCACTGAGAATGCGGCTGCAGGACATGAACAG
hSWS1.C103S.F	GACAGCATCCTGTCCAAGCATCTCTTGG
hSWS1.C103S.R	CCAAGAGATGCTTGGACAGGATGCTGTC
hSWS1.H105A.F	CAGCATCCTGTGCAAGGCCCTCTTGGCAGTTTAC
hSWS1.H105A	GTAAACTGCCAAGAGGGCCTTGACACAGGATGCTG
hSWS1.A108T.F	GCAAGCATCTCTTGACAGTTTACCTGAGTC
hSWS1.A108T.R	GACTCAGGTAAACTGTCAAGAGATGCTTGC
Shu2.C114S.F	CGCACACTGGTTCTCCTCATGTGAAGAG
Shu2.C114S.R	CTCTTCACATGAGGAGAACCAGTGTGCG
Shu2.S114C.F	CGCACACTGGTTCTGCTCATGTGAAGAG
Shu2.S114C.R	CTCTTCACATGAGCAGAACCAGTGTGCG
Shu2.C116S.F	CACACTGGTTCTGCTCATCCGAAGAGTTTTGTAAATAC

Shu2.C116S.R	GTATTTACAAAACCTCTTCGGATGAGCAGAACCAGTGTG
Shu2.F119A.F	GGTTCTGCTCATGTGAAGAGGCCTGTAAATACTTTCATGAAG
Shu2.F119A.R	CTTCATGAAAGTATTTACAGGCCTCTTCACATGAGCAGAACC
Shu2.C176S.F	CAAATTTGATAAAGTTTGTTCCTCGCATCTACTGGCGTTCTC
Shu2.C176S.R	GAGAACGCCAGTAGATGCGAGGAACAACTTTATCAAATTT
Shu2.H178A.F	GTTTGTGTTGTTCTCGGCTCTACTGGCGTTC
Shu2.H178A.	GAACGCCAGTAGAGCCGAACAACAAAC
Shu2.A181T.F	GTTTCGCATCTACTGACGTTCTCCATTTTGC
Shu2.A181T.R	GCAAAATGGAGAACGTCAGTAGATGCGAAC

APPENDIX B

CHAPTER 3 SUPPLEMENTAL DATA

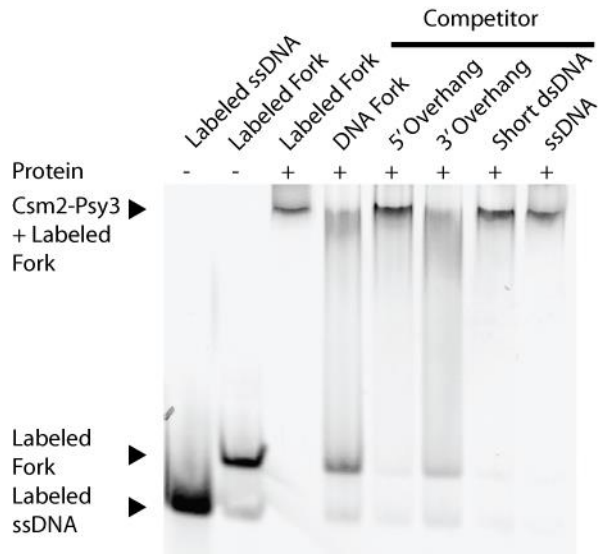


Figure 23. Competition electrophoretic mobility shift assay (EMSA).

Fluorescein-labeled DNA fork (260 nM), detailed in Table 3, with or without an unlabeled competitor DNA oligonucleotide (1300 nM), was incubated on ice for 30 minutes with purified Csm2-Psy3 complex (3.0 μ M) in EMSA reaction buffer (10 mM Tris pH 8.0, 50 mM NaCl, 2 mM DTT, 4 mM $MgCl_2$) in a reaction volume of 10 μ l. Equilibrated samples were loaded on a pre-cooled and pre-run 5% native polyacrylamide gel containing 0.5X TBE and run at 200 volts for 2 hours at 4°C. The resulting gel was visualized by fluorescence using a FLA-5100 Fluorescent Image Analyzer (FujiFilm).

Table 4. Chapter 3 Strains and Plasmids

Name	Description
W1588-4A	MAT α ade2-1 can1-100 his3-11,15 leu2-3,112 trp1-1 ura3-1 RAD5
W5909-1B	<i>MATα ADE2 TRP1 lys2Δ</i>
PJ69-4A	<i>MATα trp1-901 leu2-3,112 ura3-52 his3-200 gal4Δ gal80Δ GAL2-ADE2 LYS2::<i>GAL1-HIS3</i> met2::<i>GAL7-lacZ</i></i>
PJ69-4 α	<i>MATα trp1-901 leu2-3,112 ura3-52 his3-200 gal4Δ gal80Δ GAL2-ADE2 LYS2::<i>GAL1-HIS3</i> met2::<i>GAL7-lacZ</i></i>
KBY 217	<i>MATα trp1-901 leu2-3,112 ura3-52 his3-200 gal4Δ gal80Δ GAL2-ADE2 LYS2::<i>GAL1-HIS3</i> met2::<i>GAL7-lacZ</i> rad51::<i>natMX4</i></i>
KBY 222	<i>MATα trp1-901 leu2-3,112 ura3-52 his3-200 gal4Δ gal80Δ GAL2-ADE2 LYS2::<i>GAL1-HIS3</i> met2::<i>GAL7-lacZ</i> rad51::<i>natMX4</i></i>
KBY 212	<i>MATα trp1-901 leu2-3,112 ura3-52 his3-200 gal4Δ gal80Δ GAL2-ADE2 LYS2::<i>GAL1-HIS3</i> met2::<i>GAL7-lacZ</i> rad55::<i>natMX4</i></i>
KBY 221	<i>MATα trp1-901 leu2-3,112 ura3-52 his3-200 gal4Δ gal80Δ GAL2-ADE2 LYS2::<i>GAL1-HIS3</i> met2::<i>GAL7-lacZ</i> rad55::<i>hphMX4</i></i>
W3770-4D	<i>MATα leu2-ΔEcoRI::<i>URA3::leu2-ΔBstEII</i></i>
KBY57-1B	<i>MATα leu2-ΔEcoRI::<i>URA3-HO::leu2-ΔBstEII psy3::<i>KanMX4</i></i></i>

KBY38-3B	<i>MATa leu2-ΔEcoRI::URA3-HO::leu2-ΔBstEII csm2::KanMX4</i>
KBY65-21C	<i>MATa leu2-ΔEcoRI::URA3-HO::leu2-ΔBstEII rad55Δ</i>
KBY65-1C	<i>MATa leu2-ΔEcoRI::URA3-HO::leu2-ΔBstEII csm2::KanMX4 rad55Δ</i>
KBY65-12B	<i>MATa csm2::KanMX rad55Δ leu2-ΔEcoRI::URA3-HO::leu2-ΔBstEII</i>
KBY15-2A	<i>MATa csm2::KanMX</i>
KBY89-2B	<i>MATα rad51::LEU2 ade2-n::TRP1::ade2-I-SceI lys2::GAL-I-SceI</i>
W4121-9B	<i>MATa rad55Δ bar1::LEU2</i>
W3791-2B	<i>MATa rad57::LEU2 YFP-8ala-RAD55 bar1::LEU2</i>
KBY107-5C	<i>MATa csm2::KanMX</i>
KBY108-1C	<i>MATa psy3::KanMX bar1::LEU2</i>
W9100-2D	<i>MATα ADE2 leu2-3,112 his3-11,15 ura3-1 TRP1 lys2Δ</i>
W3778-2B	<i>MATa YFP-8ala-RAD55 bar1::LEU2</i>
KBY108-5A	<i>MATα psy3::KanMX4 YFP-8ala-Rad55</i>
KBY107-4A	<i>MATα csm2::KanMX YFP-8ala-Rad55</i>
pWJ1481	<i>pGBD-CSM2 (TRP, KAN^R)</i>
pKBB5	<i>pGBD-PSY3 (TRP, KAN^R)</i>
pGBD-C1	<i>pGBD-C1 (TRP, KAN^R)</i>
pGAD-C2	<i>pGAD-C2 (LEU, AMP^R)</i>
pGAD-RAD51	<i>pGAD-C2-RAD51 (cloned SmaI to Sall; LEU, AMP^R)</i>
pGAD-RAD55	<i>pGAD-RAD55 (LEU, AMP^R)</i>
pGAD-RAD57	<i>pGAD-RAD57 (LEU, AMP^R)</i>
pWJ1921	<i>pCDF-DUET1 with CSM2-TEV in MCS1 (PstI to HindIII) and TEV-PSY3 in MCS2 (BglII to KpnI)</i>
pRS313-RAD51	<i>pRS313-RAD51 (CEN, HIS, AMP^R)</i>
pRS416	<i>pRS416 (CEN, URA, AMP^R)</i>
pRS413	<i>pRS413 (CEN, HIS, AMP^R)</i>
pRS313-RAD57	<i>pRS313-RAD57 (CEN, HIS, AMP^R)</i>
pRS316-RAD55	<i>pRS316-RAD55 (CEN, URA, AMP^R)</i>

Table 5. Chapter 3 Primers used

DNA Substrate	Sequence
Single Stranded	3'-GACGCTCGAGCTTAAGTGACCTCACTGGAG-5'
Short dsDNA	5'-CTGCGAGCTCGAATTCACCTGGAGTGACCTC-3' 3'-GACGCTCGAGCTTAAGTGACCTCACTGGAG-5'
5' Overhang	5'-TCAAAGTCACGACCTAGACACTGCGAGCTCGAATTCACCTGGAGTGACCTC-3' 3'-GACGCTCGAGCTTAAGTGACCTCACTGGAG-5'
3' Overhang	5'-CTGCGAGCTCGAATTCACCTGGAGTGACCTC-3' 3'-AGTTTCAGTGCTGGATCTGTGACGCTCGAGCTTAAGTGACCTCACTGGAG-5'
Fork ^a	5'-TTTTTTTTTTTTTTTTTTTTTCTTGACAAGCTTGCGCACT-3' 3'-TTTTTTTTTTTTTTTTTTCACGGAAGTTCGAACGCGTGA-5'

^a The fluorescein-labeled fork is identical to the fork substrate with a single fluorescein molecule attached to the 3' end of the top strand

APPENDIX C

CHAPTER 4 SUPPLEMENTAL DATA

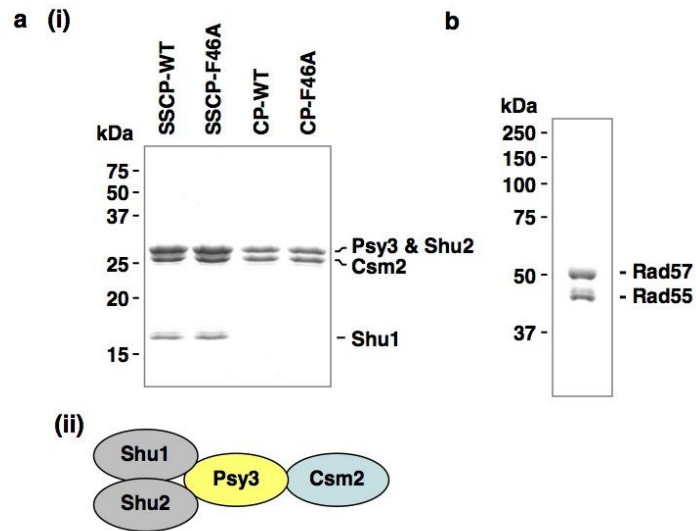


Figure 24. Purity analysis of Shu complex and Rad55-Rad57.

(i) SDS-PAGE analysis of purified Shu (SSCP; Shu1-Shu2-Csm2-Psy3) complex and Csm2-Psy3 (CP; Csm2-Psy3) complex with either wild-type Csm2 or the Csm2-F46A mutant. A. (ii) Schematic depiction of the arrangement of subunits within the Shu complex. B. SDS-PAGE analysis of purified Rad55-Rad57 complex.

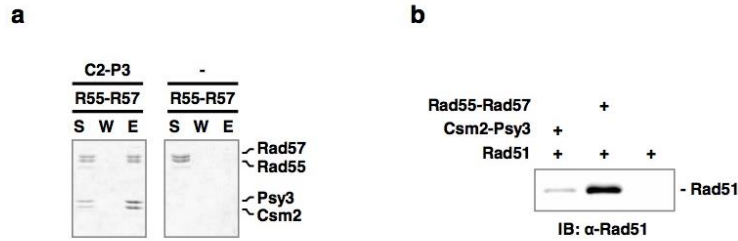


Figure 25. Interactions of Rad55-Rad57 with the Shu complex and Rad51.

A. Physical interaction of Csm2-Psy3 with Rad55-Rad57 was revealed by pull-down in which Strep-tagged Csm2-Psy3 was captured on Steptactin resin. Analysis followed the procedure described. B. Interaction of Rad51 with Rad55-Rad57 or Csm2-Psy3 was assessed by pull-down. Complexes were captured on anti-FLAG resin via the FLAG tag on Psy3 or Rad57. The elution fractions were immunoblotted for Rad51.

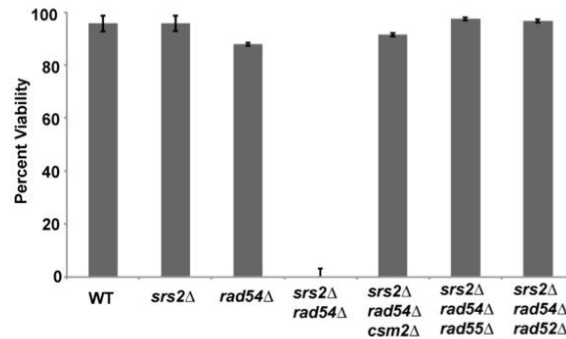


Figure 26. Genetic analyses of *csm2*Δ for functions independent of *RAD54* and *SRS2*.

Deletion of *CSM2*, *RAD55*, or, *RAD52* suppresses the synthetic lethality of *srs2*Δ *rad54*Δ.

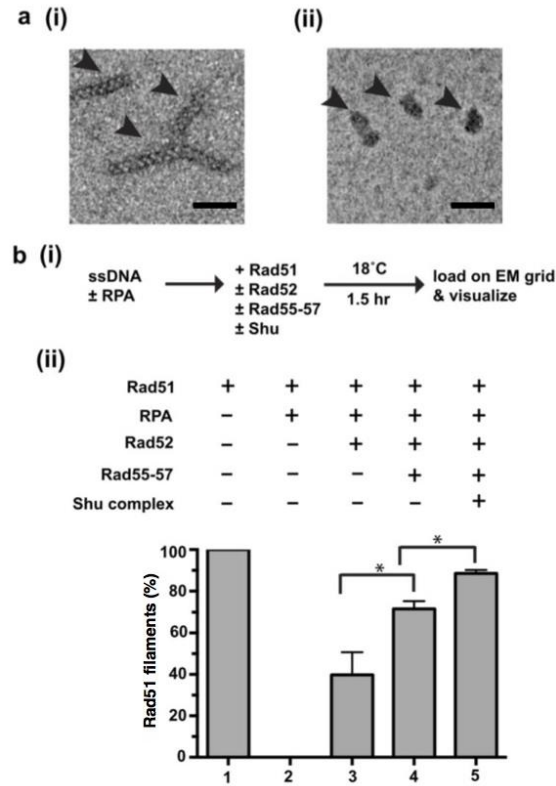


Figure 27. Electron microscopy visualization of the nucleoprotein complexes formed via Shu complex and Rad55-Rad57 facilitated loading of Rad51.

A. Representative images of Rad51 (i) and RPA (ii) nucleoprotein complexes with ssDNA as visualized by negatively stained EM (Scale bars: 50 nm) B. (i) Schematic of the Rad51 loading assay employed for EM visualization. B. (ii) RPA-coated ssDNA was incubated with Rad51 and combinations of Rad52, Shu complex, and Rad55-Rad57, then analyzed by EM. The graphed values represent the portion of all nucleoprotein complex observed (Both Rad51 and RPA) that were identified as Rad51 filaments under each condition. Standard deviations are plotted and (*) indicates significance.

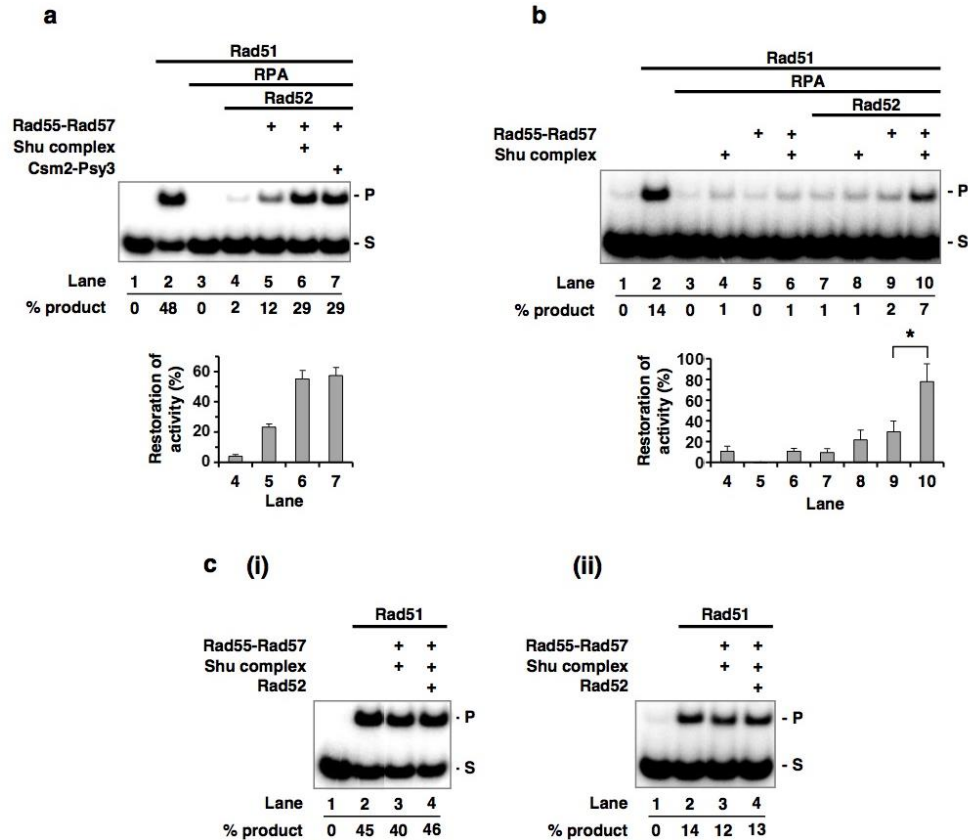


Figure 29. Analysis of Shu complex and Csm2-Psy3 complex in Rad51-mediated DNA strand exchange.

A. Results showing that Csm2-Psy3 is just as adept as Shu complex in enabling Rad51 to utilize an RPA-coated ssDNA substrate for DNA strand exchange. Reactions were carried out as in Figure 15 (i.e. at 18°C with Rad54 present). B. Results showing that omission of Rad54 does not affect the ability of Rad55-Rad57 and Shu complex to promote DNA strand exchange with an RPA-coated ssDNA substrate. The reactions were carried out as in Figure 15B, except that Rad54 was omitted and the reaction time upon dsDNA addition extended to 10 hrs. C. Results showing that Rad55-Rad57 and Shu complex do not stimulate DNA strand exchange activity of Rad51 when free ssDNA is used as substrate. DNA strand exchange activity of Rad51 when free ssDNA is used as substrate. DNA strand exchange reactions were performed without RPA present. In (i) Rad54 was added to the reactions and a reaction time of 30 min was used, similarly to Figure 15B. In (ii), Rad54 was omitted and a reaction time of 10 hours was used as in panel B.

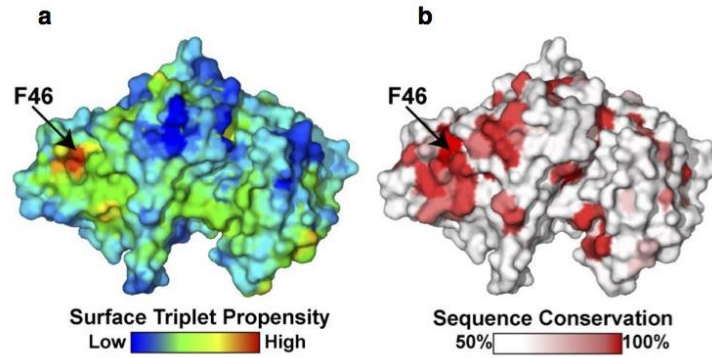


Figure 30. Analysis of the Csm2-Psy3 structure to identify potential protein-protein interaction surfaces.

A. Surface triplet propensity mapped onto the surface of the Csm2-Psy3 heterodimer. Values were calculated as described in (163) and colored as a heat map with residues having a higher predicted score in red. The location of Csm2 F46A is indicated. B. Sequence conservation from an alignment of 21 fungal orthologues was mapped onto the surface of the Csm2-Psy3 heterodimer. Invariant residues (including Csm2 F46A) are shown in red while positions with less than 50% identity are colored white.

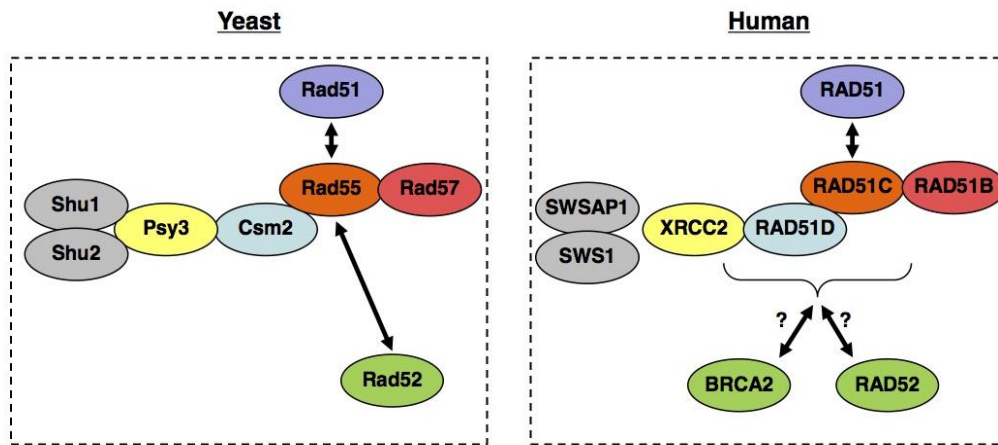


Figure 31. Comparison of human and yeast Rad51 paralogue complexes.

The RAD51 paralogs form the BCDX2 complex consisting of the RAD51B-RAD51C heterodimer associated with the RAD51D-XRCC2 heterodimer. Likewise, we have found that the yeast Rad51 paralogs associate in a similar higher order structure. Both human and yeast Rad51 paralogs interact with and functionally regulate Rad51. Given that the yeast Rad51 paralogs function with Rad52, it seems likely that the human RAD51 paralogs function in a similar manner with human RAD52 and/or BRCA2 in presynaptic filament assembly.

Table 6. Chapter 4 Strains and Plasmids

Name	Description
PJ69-4A	<i>MATa trp1-901 leu2-3,112 ura3-52 his3-200 gal4Δ gal80Δ GAL2-ADE2 LYS2::GAL1-HIS3 met2::GAL7-lacZ</i>
PJ69-4 α	<i>MATα trp1-901 leu2-3,112 ura3-52 his3-200 gal4Δ gal80Δ GAL2-ADE2 LYS2::GAL1-HIS3 met2::GAL7-lacZ</i>
KBY 212	<i>MATa trp1-901 leu2-3,112 ura3-52 his3-200 gal4Δ gal80Δ GAL2-ADE2 LYS2::GAL1-HIS3 met2::GAL7-lacZ rad55::natMX4</i>
KBY 221	<i>MATα trp1-901 leu2-3,112 ura3-52 his3-200 gal4Δ gal80Δ GAL2-ADE2 LYS2::GAL1-HIS3 met2::GAL7-lacZ rad55::hphMX4</i>
W9100-2D	<i>MATα ADE2 leu2-3,112 his3-11,15 ura3-1 TRP1 lys2Δ</i>
KBY619-7C	<i>MATα csm2::KanMX4 LYS2 trp1-1</i>
KBY804-17D	<i>MATa LYS2 srs2::HIS3 csm2::kanMX4 rad55::NatNt2 rad52::URA3</i>
KBY363-3C	<i>MATα trp1-1 LYS2 rad54::LEU2</i>
KBY107-2D	<i>MATa lys2Δ csm2::KanMX4</i>
KBY551	<i>MATα csm2-F46A</i>
KBY51-3B	<i>MATa sgs1::HIS3 trp1-1 LYS2</i>
KBY707-2A	<i>MATa sgs1::HIS3 bar1::LEU2 LYS2 csm2::KanMX4</i>
KBY611-1B	<i>MATα csm2-F46A sgs1::HIS3 LYS2</i>
KBY225-5B	<i>MATa leu2ΔEcoRI::URA3-HO::leu2ΔBsteII LYS2 trp1-1</i>

KBY225-8D	<i>MATα leu2ΔEcoRI::URA3-HO::leu2ΔBstEII csm2::kanMX LYS2 trp1-1</i>
KBY650-5C	<i>MATα csm2-F46A trp1-1 LYS2 leu2ΔEcoRI::URA3-HO::leu2ΔBstEII</i>
KBY233-6D	<i>MATα trp1-1 CAN1</i>
KBY614-3D	<i>MATα LYS2 trp1-1 csm2::KanMX4 CAN1</i>
KBY613-1B	<i>MATα trp1-1 LYS2 CAN1 Csm2-F46A</i>
ZOO347	pGAD-RAD52 (LEU, AMP ^R)
pWJ1481	pGBK-CSM2 (TRP, KAN ^R)
pGBD-RAD52	pGBD-RAD52 (TRP, KAN ^R)
pGBD-C1	pGBD-C1 (TRP, KAN ^R)
pGAD-C2	pGAD-C2 (LEU, AMP ^R)
pGAD-RAD51	pGAD-C2-RAD51 (cloned SmaI to SalI; LEU, AMP ^R)
pGBD-RAD55	pGAD-RAD55 (LEU, AMP ^R)
MH34	ADH-RAD52 (LEU, AMP ^R)
pRS424	pRS424 (TRP, AMP ^R)
pWJ1476	<i>pGAD-CSM2 (LEU, AMP^R)</i>
pKB212	<i>pGAD-csm2-F46A (LEU, AMP^R)</i>
pKB44	<i>pGBK-csm2-F46A (TRP, KAN^R)</i>
pKB139	yiPLAC211-Csm2-F46A
pET-DUET-S1S2	Co-expression of Shu1 and Shu2 (AMP ^R)
pRSF-DUET-C2P3	Co-expression of Csm2 and Psy3 (KAN ^R)
pESC-R55R57	Co-expression of Rad55 and Rad57 (URA)

BIBLIOGRAPHY

1. Hoeijmakers, J.H. (2001) Genome maintenance mechanisms for preventing cancer. *Nature*, **411**, 366-374.
2. Heyer, W.D., Ehmsen, K.T. and Liu, J. (2010) Regulation of homologous recombination in eukaryotes. *Annual review of genetics*, **44**, 113-139.
3. Ellis, N.A., Groden, J., Ye, T.Z., Straughen, J., Lennon, D.J., Ciocci, S., Proytcheva, M. and German, J. (1995) The Bloom's syndrome gene product is homologous to RecQ helicases. *Cell*, **83**, 655-666.
4. Kitao, S., Ohsugi, I., Ichikawa, K., Goto, M., Furuichi, Y. and Shimamoto, A. (1998) Cloning of two new human helicase genes of the RecQ family: biological significance of multiple species in higher eukaryotes. *Genomics*, **54**, 443-452.
5. Puranam, K.L. and Blackshear, P.J. (1994) Cloning and characterization of RECQL, a potential human homologue of the Escherichia coli DNA helicase RecQ. *J Biol Chem*, **269**, 29838-29845.
6. Seki, M., Yanagisawa, J., Kohda, T., Sonoyama, T., Ui, M. and Enomoto, T. (1994) Purification of two DNA-dependent adenosinetriphosphatases having DNA helicase activity from HeLa cells and comparison of the properties of the two enzymes. *J Biochem*, **115**, 523-531.
7. Yu, C.E., Oshima, J., Fu, Y.H., Wijsman, E.M., Hisama, F., Alisch, R., Matthews, S., Nakura, J., Miki, T., Ouais, S. *et al.* (1996) Positional cloning of the Werner's syndrome gene. *Science*, **272**, 258-262.
8. Bernstein, K.A., Gangloff, S. and Rothstein, R. (2010) The RecQ DNA helicases in DNA repair. *Annu Rev Genet*, **44**, 393-417.
9. Savitsky, K., Bar-Shira, A., Gilad, S., Rotman, G., Ziv, Y., Vanagaite, L., Tagle, D.A., Smith, S., Uziel, T., Sfez, S. *et al.* (1995) A single ataxia telangiectasia gene with a product similar to PI-3 kinase. *Science*, **268**, 1749-1753.
10. Shiloh, Y. (1997) Ataxia-telangiectasia and the Nijmegen breakage syndrome: related disorders but genes apart. *Annu Rev Genet*, **31**, 635-662.
11. Kolodner, R.D., Putnam, C.D. and Myung, K. (2002) Maintenance of genome stability in *Saccharomyces cerevisiae*. *Science*, **297**, 552-557.
12. Li, X. and Heyer, W.D. (2008) Homologous recombination in DNA repair and DNA damage tolerance. *Cell Res*, **18**, 99-113.

13. Bernstein, K.A. and Rothstein, R. (2009) At loose ends: resecting a double-strand break. *Cell*, **137**, 807-810.
14. Clerici, M., Mantiero, D., Lucchini, G. and Longhese, M.P. (2005) The *Saccharomyces cerevisiae* Sae2 protein promotes resection and bridging of double strand break ends. *J Biol Chem*, **280**, 38631-38638.
15. Kim, H.S., Vijayakumar, S., Reger, M., Harrison, J.C., Haber, J.E., Weil, C. and Petrini, J.H. (2008) Functional interactions between Sae2 and the Mre11 complex. *Genetics*, **178**, 711-723.
16. Lengsfeld, B.M., Rattray, A.J., Bhaskara, V., Ghirlando, R. and Paull, T.T. (2007) Sae2 is an endonuclease that processes hairpin DNA cooperatively with the Mre11/Rad50/Xrs2 complex. *Mol Cell*, **28**, 638-651.
17. Fiorentini, P., Huang, K.N., Tishkoff, D.X., Kolodner, R.D. and Symington, L.S. (1997) Exonuclease I of *Saccharomyces cerevisiae* functions in mitotic recombination in vivo and in vitro. *Mol Cell Biol*, **17**, 2764-2773.
18. Huang, K.N. and Symington, L.S. (1993) A 5'-3' exonuclease from *Saccharomyces cerevisiae* is required for in vitro recombination between linear DNA molecules with overlapping homology. *Mol Cell Biol*, **13**, 3125-3134.
19. Mimitou, E.P. and Symington, L.S. (2008) Sae2, Exo1 and Sgs1 collaborate in DNA double-strand break processing. *Nature*, **455**, 770-774.
20. Zhu, Z., Chung, W.H., Shim, E.Y., Lee, S.E. and Ira, G. (2008) Sgs1 helicase and two nucleases Dna2 and Exo1 resect DNA double-strand break ends. *Cell*, **134**, 981-994.
21. Sung, P. and Klein, H. (2006) Mechanism of homologous recombination: mediators and helicases take on regulatory functions. *Nat Rev Mol Cell Biol*, **7**, 739-750.
22. Wold, M.S. (1997) Replication protein A: a heterotrimeric, single-stranded DNA-binding protein required for eukaryotic DNA metabolism. *Annu Rev Biochem*, **66**, 61-92.
23. Lisby, M., Barlow, J.H., Burgess, R.C. and Rothstein, R. (2004) Choreography of the DNA damage response: spatiotemporal relationships among checkpoint and repair proteins. *Cell*, **118**, 699-713.
24. Sung, P. (1997) Yeast Rad55 and Rad57 proteins form a heterodimer that functions with replication protein A to promote DNA strand exchange by Rad51 recombinase. *Genes Dev*, **11**, 1111-1121.
25. Krogh, B.O. and Symington, L.S. (2004) Recombination proteins in yeast. *Annu Rev Genet*, **38**, 233-271.
26. West, S.C. (2003) Molecular views of recombination proteins and their control. *Nat Rev Mol Cell Biol*, **4**, 435-445.

27. Gibb, B., Ye, L.F., Kwon, Y., Niu, H., Sung, P. and Greene, E.C. (2014) Protein dynamics during presynaptic-complex assembly on individual single-stranded DNA molecules. *Nat Struct Mol Biol*, **21**, 893-900.
28. Bashkirov, V.I., King, J.S., Bashkirova, E.V., Schmuckli-Maurer, J. and Heyer, W.D. (2000) DNA repair protein Rad55 is a terminal substrate of the DNA damage checkpoints. *Mol Cell Biol*, **20**, 4393-4404.
29. Herzberg, K., Bashkirov, V.I., Rolfmeier, M., Haghazari, E., McDonald, W.H., Anderson, S., Bashkirova, E.V., Yates, J.R., 3rd and Heyer, W.D. (2006) Phosphorylation of Rad55 on serines 2, 8, and 14 is required for efficient homologous recombination in the recovery of stalled replication forks. *Mol Cell Biol*, **26**, 8396-8409.
30. Sacher, M., Pfander, B., Hoegge, C. and Jentsch, S. (2006) Control of Rad52 recombination activity by double-strand break-induced SUMO modification. *Nat Cell Biol*, **8**, 1284-1290.
31. Torres-Rosell, J., Sunjevaric, I., De Piccoli, G., Sacher, M., Eckert-Boulet, N., Reid, R., Jentsch, S., Rothstein, R., Aragon, L. and Lisby, M. (2007) The Smc5-Smc6 complex and SUMO modification of Rad52 regulates recombinational repair at the ribosomal gene locus. *Nat Cell Biol*, **9**, 923-931.
32. Bernstein, K.A., Juanchich, A., Sunjevaric, I. and Rothstein, R. (2013) The Shu complex regulates Rad52 localization during rDNA repair. *DNA Repair (Amst)*, **12**, 786-790.
33. Krejci, L., Van Komen, S., Li, Y., Villemain, J., Reddy, M.S., Klein, H., Ellenberger, T. and Sung, P. (2003) DNA helicase Srs2 disrupts the Rad51 presynaptic filament. *Nature*, **423**, 305-309.
34. Veaute, X., Jeusset, J., Soustelle, C., Kowalczykowski, S.C., Le Cam, E. and Fabre, F. (2003) The Srs2 helicase prevents recombination by disrupting Rad51 nucleoprotein filaments. *Nature*, **423**, 309-312.
35. Liu, J., Renault, L., Veaute, X., Fabre, F., Stahlberg, H. and Heyer, W.D. (2011) Rad51 paralogues Rad55-Rad57 balance the antirecombinase Srs2 in Rad51 filament formation. *Nature*, **479**, 245-248.
36. Sanchez, H., Kertokalio, A., van Rossum-Fikkert, S., Kanaar, R. and Wyman, C. (2013) Combined optical and topographic imaging reveals different arrangements of human RAD54 with presynaptic and postsynaptic RAD51-DNA filaments. *Proc Natl Acad Sci U S A*, **110**, 11385-11390.
37. Santa Maria, S.R., Kwon, Y., Sung, P. and Klein, H.L. (2013) Characterization of the interaction between the *Saccharomyces cerevisiae* Rad51 recombinase and the DNA translocase Rdh54. *J Biol Chem*, **288**, 21999-22005.
38. Klein, H.L. (1997) RDH54, a RAD54 homologue in *Saccharomyces cerevisiae*, is required for mitotic diploid-specific recombination and repair and for meiosis. *Genetics*, **147**, 1533-1543.

39. Heyer, W.D., Li, X., Rolfsmeier, M. and Zhang, X.P. (2006) Rad54: the Swiss Army knife of homologous recombination? *Nucleic Acids Res*, **34**, 4115-4125.
40. Petukhova, G., Stratton, S. and Sung, P. (1998) Catalysis of homologous DNA pairing by yeast Rad51 and Rad54 proteins. *Nature*, **393**, 91-94.
41. Qi, Z., Redding, S., Lee, J.Y., Gibb, B., Kwon, Y., Niu, H., Gaines, W.A., Sung, P. and Greene, E.C. (2015) DNA sequence alignment by microhomology sampling during homologous recombination. *Cell*, **160**, 856-869.
42. Wright, W.D. and Heyer, W.D. (2014) Rad54 functions as a heteroduplex DNA pump modulated by its DNA substrates and Rad51 during D loop formation. *Mol Cell*, **53**, 420-432.
43. Li, X. and Heyer, W.D. (2009) RAD54 controls access to the invading 3'-OH end after RAD51-mediated DNA strand invasion in homologous recombination in *Saccharomyces cerevisiae*. *Nucleic acids research*, **37**, 638-646.
44. Li, X., Zhang, X.P., Solinger, J.A., Kiianitsa, K., Yu, X., Egelman, E.H. and Heyer, W.D. (2007) Rad51 and Rad54 ATPase activities are both required to modulate Rad51-dsDNA filament dynamics. *Nucleic Acids Res*, **35**, 4124-4140.
45. Solinger, J.A., Kiianitsa, K. and Heyer, W.D. (2002) Rad54, a Swi2/Snf2-like recombinational repair protein, disassembles Rad51:dsDNA filaments. *Mol Cell*, **10**, 1175-1188.
46. Lo, Y.C., Paffett, K.S., Amit, O., Clikeman, J.A., Sterk, R., Brenneman, M.A. and Nickoloff, J.A. (2006) Sgs1 regulates gene conversion tract lengths and crossovers independently of its helicase activity. *Mol Cell Biol*, **26**, 4086-4094.
47. Janke, C., Magiera, M.M., Rathfelder, N., Taxis, C., Reber, S., Maekawa, H., Moreno-Borchart, A., Doenges, G., Schwob, E., Schiebel, E. *et al.* (2004) A versatile toolbox for PCR-based tagging of yeast genes: new fluorescent proteins, more markers and promoter substitution cassettes. *Yeast*, **21**, 947-962.
48. Ira, G., Malkova, A., Liberi, G., Foiani, M. and Haber, J.E. (2003) Srs2 and Sgs1-Top3 suppress crossovers during double-strand break repair in yeast. *Cell*, **115**, 401-411.
49. Boddy, M.N., Gaillard, P.H., McDonald, W.H., Shanahan, P., Yates, J.R., 3rd and Russell, P. (2001) Mus81-Eme1 are essential components of a Holliday junction resolvase. *Cell*, **107**, 537-548.
50. Fricke, W.M. and Brill, S.J. (2003) Slx1-Slx4 is a second structure-specific endonuclease functionally redundant with Sgs1-Top3. *Genes Dev*, **17**, 1768-1778.
51. Ip, S.C., Rass, U., Blanco, M.G., Flynn, H.R., Skehel, J.M. and West, S.C. (2008) Identification of Holliday junction resolvases from humans and yeast. *Nature*, **456**, 357-361.

52. Schwartz, E.K. and Heyer, W.D. (2011) Processing of joint molecule intermediates by structure-selective endonucleases during homologous recombination in eukaryotes. *Chromosoma*, **120**, 109-127.
53. Costantino, L., Sotiriou, S.K., Rantala, J.K., Magin, S., Mladenov, E., Helleday, T., Haber, J.E., Iliakis, G., Kallioniemi, O.P. and Halazonetis, T.D. (2014) Break-induced replication repair of damaged forks induces genomic duplications in human cells. *Science*, **343**, 88-91.
54. Ho, C.K., Mazon, G., Lam, A.F. and Symington, L.S. (2010) Mus81 and Yen1 promote reciprocal exchange during mitotic recombination to maintain genome integrity in budding yeast. *Mol Cell*, **40**, 988-1000.
55. Signon, L., Malkova, A., Naylor, M.L., Klein, H. and Haber, J.E. (2001) Genetic requirements for RAD51- and RAD54-independent break-induced replication repair of a chromosomal double-strand break. *Mol Cell Biol*, **21**, 2048-2056.
56. Hashimoto, Y., Ray Chaudhuri, A., Lopes, M. and Costanzo, V. (2010) Rad51 protects nascent DNA from Mre11-dependent degradation and promotes continuous DNA synthesis. *Nat Struct Mol Biol*, **17**, 1305-1311.
57. Zellweger, R., Dalcher, D., Mutreja, K., Berti, M., Schmid, J.A., Herrador, R., Vindigni, A. and Lopes, M. (2015) Rad51-mediated replication fork reversal is a global response to genotoxic treatments in human cells. *J Cell Biol*, **208**, 563-579.
58. Iannascoli, C., Palermo, V., Murfun, I., Franchitto, A. and Pichierri, P. (2015) The WRN exonuclease domain protects nascent strands from pathological MRE11/EXO1-dependent degradation. *Nucleic Acids Res*, **43**, 9788-9803.
59. Giannattasio, M., Zwicky, K., Follonier, C., Foiani, M., Lopes, M. and Branzei, D. (2014) Visualization of recombination-mediated damage bypass by template switching. *Nat Struct Mol Biol*, **21**, 884-892.
60. Ball, L.G., Zhang, K., Cobb, J.A., Boone, C. and Xiao, W. (2009) The yeast Shu complex couples error-free post-replication repair to homologous recombination. *Molecular microbiology*, **73**, 89-102.
61. Xu, X., Ball, L., Chen, W., Tian, X., Lambrecht, A., Hanna, M. and Xiao, W. (2013) The yeast Shu complex utilizes homologous recombination machinery for error-free lesion bypass via physical interaction with a Rad51 paralogue. *PLoS One*, **8**, e81371.
62. Shor, E., Weinstein, J. and Rothstein, R. (2005) A genetic screen for top3 suppressors in *Saccharomyces cerevisiae* identifies SHU1, SHU2, PSY3 and CSM2: four genes involved in error-free DNA repair. *Genetics*, **169**, 1275-1289.
63. Ito, T., Chiba, T., Ozawa, R., Yoshida, M., Hattori, M. and Sakaki, Y. (2001) A comprehensive two-hybrid analysis to explore the yeast protein interactome. *Proceedings of the National Academy of Sciences of the United States of America*, **98**, 4569-4574.

64. Martin, V., Chahwan, C., Gao, H., Blais, V., Wohlschlegel, J., Yates, J.R., 3rd, McGowan, C.H. and Russell, P. (2006) Sws1 is a conserved regulator of homologous recombination in eukaryotic cells. *The EMBO journal*, **25**, 2564-2574.
65. Mankouri, H.W., Ngo, H.P. and Hickson, I.D. (2007) Shu proteins promote the formation of homologous recombination intermediates that are processed by Sgs1-Rmi1-Top3. *Molecular biology of the cell*, **18**, 4062-4073.
66. Liu, T., Wan, L., Wu, Y., Chen, J. and Huang, J. (2011) hSWS1.SWSAP1 is an evolutionarily conserved complex required for efficient homologous recombination repair. *The Journal of biological chemistry*, **286**, 41758-41766.
67. She, Z., Gao, Z.Q., Liu, Y., Wang, W.J., Liu, G.F., Shtykova, E.V., Xu, J.H. and Dong, Y.H. (2012) Structural and SAXS analysis of the budding yeast SHU-complex proteins. *FEBS letters*, **586**, 2306-2312.
68. Tao, Y., Li, X., Liu, Y., Ruan, J., Qi, S., Niu, L. and Teng, M. (2012) Structural analysis of Shu proteins reveals a DNA binding role essential for resisting damage. *The Journal of biological chemistry*, **287**, 20231-20239.
69. Compton, S.A., Ozgur, S. and Griffith, J.D. (2010) Ring-shaped Rad51 paralog protein complexes bind Holliday junctions and replication forks as visualized by electron microscopy. *The Journal of biological chemistry*, **285**, 13349-13356.
70. Meindl, A., Hellebrand, H., Wiek, C., Erven, V., Wappenschmidt, B., Niederacher, D., Freund, M., Lichtner, P., Hartmann, L., Schaal, H. *et al.* (2010) Germline mutations in breast and ovarian cancer pedigrees establish RAD51C as a human cancer susceptibility gene. *Nat Genet*, **42**, 410-414.
71. Clague, J., Wilhoite, G., Adamson, A., Bailis, A., Weitzel, J.N. and Neuhausen, S.L. (2011) RAD51C germline mutations in breast and ovarian cancer cases from high-risk families. *PLoS One*, **6**, e25632.
72. Osorio, A., Endt, D., Fernandez, F., Eirich, K., de la Hoya, M., Schmutzler, R., Caldes, T., Meindl, A., Schindler, D. and Benitez, J. (2012) Predominance of pathogenic missense variants in the RAD51C gene occurring in breast and ovarian cancer families. *Hum Mol Genet*, **21**, 2889-2898.
73. Thompson, E.R., Boyle, S.E., Johnson, J., Ryland, G.L., Sawyer, S., Choong, D.Y., kConFab, Chenevix-Trench, G., Trainer, A.H., Lindeman, G.J. *et al.* (2012) Analysis of RAD51C germline mutations in high-risk breast and ovarian cancer families and ovarian cancer patients. *Hum Mutat*, **33**, 95-99.
74. Blanco, A., Gutierrez-Enriquez, S., Santamarina, M., Montalban, G., Bonache, S., Balmana, J., Carracedo, A., Diez, O. and Vega, A. (2014) RAD51C germline mutations found in Spanish site-specific breast cancer and breast-ovarian cancer families. *Breast Cancer Res Treat*, **147**, 133-143.

75. Namazi, A., Abedinzadeh, M., Nourbaksh, P. and Neamatzadeh, H. (2015) Association between the XRCC3 Thr241Met polymorphism and risk of colorectal cancer: a meta analysis of 5,193 cases and 6,645 controls. *Asian Pac J Cancer Prev*, **16**, 2263-2268.
76. Vaz, F., Hanenberg, H., Schuster, B., Barker, K., Wiek, C., Erven, V., Neveling, K., Endt, D., Kesterton, I., Autore, F. *et al.* (2010) Mutation of the RAD51C gene in a Fanconi anemia-like disorder. *Nat Genet*, **42**, 406-409.
77. Shu, Z., Smith, S., Wang, L., Rice, M.C. and Kmiec, E.B. (1999) Disruption of muREC2/RAD51L1 in mice results in early embryonic lethality which can be partially rescued in a p53(-/-) background. *Mol Cell Biol*, **19**, 8686-8693.
78. Deans, B., Griffin, C.S., Maconochie, M. and Thacker, J. (2000) Xrcc2 is required for genetic stability, embryonic neurogenesis and viability in mice. *EMBO J*, **19**, 6675-6685.
79. Pittman, D.L. and Schimenti, J.C. (2000) Midgestation lethality in mice deficient for the RecA-related gene, Rad51d/Rad51l3. *Genesis*, **26**, 167-173.
80. Kuznetsov, S.G., Haines, D.C., Martin, B.K. and Sharan, S.K. (2009) Loss of Rad51c leads to embryonic lethality and modulation of Trp53-dependent tumorigenesis in mice. *Cancer Res*, **69**, 863-872.
81. Miller, K.A., Yoshikawa, D.M., McConnell, I.R., Clark, R., Schild, D. and Albala, J.S. (2002) RAD51C interacts with RAD51B and is central to a larger protein complex in vivo exclusive of RAD51. *J Biol Chem*, **277**, 8406-8411.
82. Wiese, C., Collins, D.W., Albala, J.S., Thompson, L.H., Kronenberg, A. and Schild, D. (2002) Interactions involving the Rad51 paralogs Rad51C and XRCC3 in human cells. *Nucleic Acids Res*, **30**, 1001-1008.
83. Masson, J.Y., Tarsounas, M.C., Stasiak, A.Z., Stasiak, A., Shah, R., McIlwraith, M.J., Benson, F.E. and West, S.C. (2001) Identification and purification of two distinct complexes containing the five RAD51 paralogs. *Genes Dev*, **15**, 3296-3307.
84. Kachroo, A.H., Laurent, J.M., Yellman, C.M., Meyer, A.G., Wilke, C.O. and Marcotte, E.M. (2015) Evolution. Systematic humanization of yeast genes reveals conserved functions and genetic modularity. *Science*, **348**, 921-925.
85. Yokoyama, H., Sarai, N., Kagawa, W., Enomoto, R., Shibata, T., Kurumizaka, H. and Yokoyama, S. (2004) Preferential binding to branched DNA strands and strand-annealing activity of the human Rad51B, Rad51C, Rad51D and Xrcc2 protein complex. *Nucleic Acids Res*, **32**, 2556-2565.
86. Lin, Z., Kong, H., Nei, M. and Ma, H. (2006) Origins and evolution of the recA/RAD51 gene family: evidence for ancient gene duplication and endosymbiotic gene transfer. *Proc Natl Acad Sci U S A*, **103**, 10328-10333.

87. Schild, D., Lio, Y.C., Collins, D.W., Tsomondo, T. and Chen, D.J. (2000) Evidence for simultaneous protein interactions between human Rad51 paralogs. *J. Biol. Chem.*, **275**, 16443-16449.
88. Takata, M., Sasaki, M.S., Tachiiri, S., Fukushima, T., Sonoda, E., Schild, D., Thompson, L.H. and Takeda, S. (2001) Chromosome Instability and Defective Recombinational Repair in Knockout Mutants of the Five Rad51 Paralogs. *Mol. Cell. Biol.*, **21**, 2858-2866.
89. Godin, S., Wier, A., Kabbinavar, F., Bratton-Palmer, D.S., Ghodke, H., Van Houten, B., VanDemark, A.P. and Bernstein, K.A. (2013) The Shu complex interacts with Rad51 through the Rad51 paralogues Rad55-Rad57 to mediate error-free recombination. *Nucleic Acids Res*, **41**, 4525-4534.
90. Sasanuma, H., Tawaramoto, M.S., Lao, J.P., Hosaka, H., Sanda, E., Suzuki, M., Yamashita, E., Hunter, N., Shinohara, M., Nakagawa, A. *et al.* (2013) A new protein complex promoting the assembly of Rad51 filaments. *Nature communications*, **4**, 1676.
91. Kawabata, M., Kawabata, T. and Nishibori, M. (2005) Role of recA/RAD51 family proteins in mammals. *Acta Medica Okayama*, **59**, 1-9.
92. Suwaki, N., Klare, K. and Tarsounas, M. (2011) RAD51 paralogs: roles in DNA damage signalling, recombinational repair and tumorigenesis. *Semin Cell Dev Biol*, **22**, 898-905.
93. Pennington, K.P. and Swisher, E.M. (2012) Hereditary ovarian cancer: beyond the usual suspects. *Gynecol. Oncol.*, **124**, 347-353.
94. Filippini, S.E. and Vega, A. (2013) Breast cancer genes: beyond BRCA1 and BRCA2. *Frontiers in bioscience*, **18**, 1358-1372.
95. Somyajit, K., Subramanya, S. and Nagaraju, G. (2012) Distinct roles of FANCO/RAD51C protein in DNA damage signaling and repair: implications for Fanconi anemia and breast cancer susceptibility. *J. Biol. Chem.*, **287**, 3366-3380.
96. Vaz, F., Hanenberg, H., Schuster, B., Barker, K., Wiek, C., Erven, V., Neveling, K., Endt, D., Kesterton, I., Autore, F. *et al.* (2010) Mutation of the RAD51C gene in a Fanconi anemia-like disorder. *Nat. Genet.*, **42**, 406-409.
97. Shamseldin, H.E., Elfaki, M. and Alkuraya, F.S. (2012) Exome sequencing reveals a novel Fanconi group defined by XRCC2 mutation. *J. Med. Genet.*, **49**, 184-186.
98. Park, D.J., Lesueur, F., Nguyen-Dumont, T., Pertesi, M., Odefrey, F., Hammet, F., Neuhausen, S.L., John, E.M., Andrulis, I.L., Terry, M.B. *et al.* (2012) Rare mutations in XRCC2 increase the risk of breast cancer. *American journal of human genetics*, **90**, 734-739.
99. Huang, M.E., Rio, A.G., Nicolas, A. and Kolodner, R.D. (2003) A genomewide screen in *Saccharomyces cerevisiae* for genes that suppress the accumulation of mutations. *Proc Natl Acad Sci U S A*, **100**, 11529-11534.

100. Shepherd, R., Forbes, S.A., Beare, D., Bamford, S., Cole, C.G., Ward, S., Bindal, N., Gunasekaran, P., Jia, M., Kok, C.Y. *et al.* (2011), *Database : the journal of biological databases and curation*. 2011/05/26 ed, Vol. 2011, pp. bar018.
101. Alvaro, D., Lisby, M. and Rothstein, R. (2007) Genome-Wide Analysis of Rad52 Foci Reveals Diverse Mechanisms Impacting Recombination. *PLoS Genet.*, **3**, e228.
102. Clark, N.L., Alani, E. and Aquadro, C.F. (2012) Evolutionary rate covariation reveals shared functionality and coexpression of genes. *Genome Res*, **22**, 714-720.
103. Clark, N.L., Gasper, J., Sekino, M., Springer, S.A., Aquadro, C.F. and Swanson, W.J. (2009) Coevolution of interacting fertilization proteins. *PLoS Genet.*, **5**, e1000570.
104. Clark, N.L. and Aquadro, C.F. (2010) A novel method to detect proteins evolving at correlated rates: identifying new functional relationships between coevolving proteins. *Mol Biol Evol*, **27**, 1152-1161.
105. Clark, N.L., Alani, E. and Aquadro, C.F. (2013) Evolutionary rate covariation in meiotic proteins results from fluctuating evolutionary pressure in yeasts and mammals. *Genetics*, **193**, 529-538.
106. Findlay, G.D., Sitnik, J.L., Wang, W., Aquadro, C.F., Clark, N.L. and Wolfner, M.F. (2014) Evolutionary Rate Covariation Identifies New Members of a Protein Network Required for *Drosophila melanogaster* Female Post-Mating Responses. *PLoS Genet.*, **10**, e1004108.
107. Bernstein, K.A., Reid, R.J., Sunjevaric, I., Demuth, K., Burgess, R.C. and Rothstein, R. (2011) The Shu complex, which contains Rad51 paralogues, promotes DNA repair through inhibition of the Srs2 anti-recombinase. *Mol Biol Cell*, **22**, 1599-1607.
108. Makarova, K.S., Aravind, L. and Koonin, E.V. (2002) SWIM, a novel Zn-chelating domain present in bacteria, archaea and eukaryotes. *Trends Biochem. Sci.*, **27**, 384-386.
109. Banerjee, R., Dubois, D.Y., Gauthier, J., Lin, S.X., Roy, S. and Lapointe, J. (2004) The zinc-binding site of a class I aminoacyl-tRNA synthetase is a SWIM domain that modulates amino acid binding via the tRNA acceptor arm. *Eur. J. Biochem.*, **271**, 724-733.
110. Liu, J., Gagnon, Y., Gauthier, J., Furenlid, L., L'Heureux, P.J., Auger, M., Nureki, O., Yokoyama, S. and Lapointe, J. (1995) The zinc-binding site of *Escherichia coli* glutamyl-tRNA synthetase is located in the acceptor-binding domain. Studies by extended x-ray absorption fine structure, molecular modeling, and site-directed mutagenesis. *J. Biol. Chem.*, **270**, 15162-15169.
111. Hong, S. and Kim, K.P. (2013) Shu1 promotes homolog bias of meiotic recombination in *Saccharomyces cerevisiae*. *Mol Cells*, **36**, 446-454.
112. St Pierre, S.E., Ponting, L., Stefancsik, R. and McQuilton, P. FlyBase 102--advanced approaches to interrogating FlyBase. *Nucleic Acids Res*, **42**, D780-788.

113. Graveley, B.R., May, G., Brooks, A.N., Carlson, J.W., Cherbas, L., Davis, C.A., Duff, M., Eads, B., Landolin, J., Sandler, J., Wan, K.H., Andrews, J., Brenner, S.E., Cherbas, P., Gingeras, T.R., Hoskins, R., Kaufman, T., Celniker, S.E. . (2011.4.13).
114. Rong, L., Palladino, F., Aguilera, A. and Klein, H.L. (1991) The hyper-gene conversion *hpr5-1* mutation of *Saccharomyces cerevisiae* is an allele of the *SRS2/RADH* gene. *Genetics*, **127**, 75-85.
115. Burgess, R.C., Lisby, M., Altmannova, V., Krejci, L., Sung, P. and Rothstein, R. (2009) Localization of recombination proteins and Srs2 reveals anti-recombinase function in vivo. *J Cell Biol*, **185**, 969-981.
116. Thomas, B.J. and Rothstein, R. (1989) Elevated recombination rates in transcriptionally active DNA. *Cell*, **56**, 619-630.
117. Zhao, X., Muller, E.G. and Rothstein, R. (1998) A suppressor of two essential checkpoint genes identifies a novel protein that negatively affects dNTP pools. *Mol. Cell*, **2**, 329-340.
118. James, P., Halladay, J. and Craig, E.A. (1996) Genomic libraries and a host strain designed for highly efficient two-hybrid selection in yeast. *Genetics*, **144**, 1425-1436.
119. Sherman, F., Fink, G.R. and Hicks, J.B. (1986) *Methods in Yeast Genetics*. Cold Spring Harbor Laboratory Press, Cold Spring Harbor, NY.
120. Guindon, S. and Gascuel, O. (2003) A simple, fast, and accurate algorithm to estimate large phylogenies by maximum likelihood. *Syst Biol*, **52**, 696-704.
121. Edgar, R.C. (2004) MUSCLE: multiple sequence alignment with high accuracy and high throughput. *Nucleic Acids Res.*, **32**, 1792-1797.
122. Sato, T., Yamanishi, Y., Kanehisa, M. and Toh, H. (2005) The inference of protein-protein interactions by co-evolutionary analysis is improved by excluding the information about the phylogenetic relationships. *Bioinformatics*, **21**, 3482-3489.
123. Yang, Z. (2007) PAML 4: phylogenetic analysis by maximum likelihood. *Mol Biol Evol*, **24**, 1586-1591.
124. Balakrishnan, R., Park, J., Karra, K., Hitz, B.C., Binkley, G., Hong, E.L., Sullivan, J., Micklem, G. and Cherry, J.M. (2012) YeastMine--an integrated data warehouse for *Saccharomyces cerevisiae* data as a multipurpose tool-kit. *Database : the journal of biological databases and curation*, **2012**, bar062.
125. Wilson, R.J., Goodman, J.L. and Strelets, V.B. (2008) FlyBase: integration and improvements to query tools. *Nucleic Acids Res.*, **36**, D588-593.
126. Lea, D.E. and Coulson, C.A. (1949) The distribution of the numbers of mutants in bacterial populations. *J. Genetics*, **49**, 264-285.

127. Holthausen, J.T., Wyman, C. and Kanaar, R. (2010) Regulation of DNA strand exchange in homologous recombination. *DNA Repair (Amst)*, **9**, 1264-1272.
128. Sugiyama, T. and Kowalczykowski, S.C. (2002) Rad52 protein associates with replication protein A (RPA)-single-stranded DNA to accelerate Rad51-mediated displacement of RPA and presynaptic complex formation. *J. Biol. Chem.*, **277**, 31663-31672.
129. Sung, P. (1997) Function of yeast Rad52 protein as a mediator between replication protein A and the Rad51 recombinase. *J. Biol. Chem.*, **272**, 28194-28197.
130. Kans, J.A. and Mortimer, R.K. (1991) Nucleotide sequence of the RAD57 gene of *Saccharomyces cerevisiae*. *Gene*, **105**, 139-140.
131. Lovett, S.T. (1994) Sequence of the RAD55 gene of *Saccharomyces cerevisiae*: similarity of RAD55 to prokaryotic RecA and other RecA-like proteins. *Gene*, **142**, 103-106.
132. Fortin, G.S. and Symington, L.S. (2002) Mutations in yeast Rad51 that partially bypass the requirement for Rad55 and Rad57 in DNA repair by increasing the stability of Rad51-DNA complexes. *The EMBO journal*, **21**, 3160-3170.
133. McDonald, J.P. and Rothstein, R. (1994) Unrepaired heteroduplex DNA in *Saccharomyces cerevisiae* is decreased in RAD1 RAD52-independent recombination. *Genetics*, **137**, 393-405.
134. Ivanov, E.L., Sugawara, N., Fishman-Lobell, J. and Haber, J.E. (1996) Genetic requirements for the single-strand annealing pathway of double-strand break repair in *Saccharomyces cerevisiae*. *Genetics*, **142**, 693-704.
135. Stark, J.M., Pierce, A.J., Oh, J., Pastink, A. and Jasin, M. (2004) Genetic steps of mammalian homologous repair with distinct mutagenic consequences. *Mol. Cell. Biol.*, **24**, 9305-9316.
136. Lovett, S.T. and Mortimer, R.K. (1987) Characterization of null mutants of the RAD55 gene of *Saccharomyces cerevisiae*: effects of temperature, osmotic strength and mating type. *Genetics*, **116**, 547-553.
137. Symington, L.S. (2002) Role of RAD52 epistasis group genes in homologous recombination and double-strand break repair. *Microbiol Mol Biol Rev*, **66**, 630-670, table of contents.
138. Hays, S.L., Firmenich, A.A. and Berg, P. (1995) Complex formation in yeast double-strand break repair: participation of Rad51, Rad52, Rad55, and Rad57 proteins. *Proc. Natl. Acad. Sci. U S A*, **92**, 6925-6929.
139. Johnson, R.D. and Symington, L.S. (1995) Functional differences and interactions among the putative RecA homologs Rad51, Rad55, and Rad57. *Mol. Cell. Biol.*, **15**, 4843-4850.

140. Benson, F.E., Baumann, P. and West, S.C. (1998) Synergistic actions of Rad51 and Rad52 in recombination and DNA repair. *Nature*, **391**, 401-404.
141. Gasior, S.L., Wong, A.K., Kora, Y., Shinohara, A. and Bishop, D.K. (1998) Rad52 associates with RPA and functions with rad55 and rad57 to assemble meiotic recombination complexes. *Genes Dev.*, **12**, 2208-2221.
142. New, J.H., Sugiyama, T., Zaitseva, E. and Kowalczykowski, S.C. (1998) Rad52 protein stimulates DNA strand exchange by Rad51 and replication protein A. *Nature*, **391**, 407-410.
143. Fung, C.W., Fortin, G.S., Peterson, S.E. and Symington, L.S. (2006) The rad51-K191R ATPase-defective mutant is impaired for presynaptic filament formation. *Mol. Cell. Biol.*, **26**, 9544-9554.
144. Sugawara, N., Wang, X. and Haber, J.E. (2003) In vivo roles of Rad52, Rad54, and Rad55 proteins in Rad51-mediated recombination. *Mol Cell*, **12**, 209-219.
145. Modesti, M., Ristic, D., van der Heijden, T., Dekker, C., van Mameren, J., Peterman, E.J., Wuite, G.J., Kanaar, R. and Wyman, C. (2007) Fluorescent human RAD51 reveals multiple nucleation sites and filament segments tightly associated along a single DNA molecule. *Structure*, **15**, 599-609.
146. Hilario, J., Amitani, I., Baskin, R.J. and Kowalczykowski, S.C. (2009) Direct imaging of human Rad51 nucleoprotein dynamics on individual DNA molecules. *Proc. Natl. Acad. Sci. U S A*, **106**, 361-368.
147. Antony, E., Tomko, E.J., Xiao, Q., Krejci, L., Lohman, T.M. and Ellenberger, T. (2009) Srs2 disassembles Rad51 filaments by a protein-protein interaction triggering ATP turnover and dissociation of Rad51 from DNA. *Mol. Cell*, **35**, 105-115.
148. Seong, C., Colavito, S., Kwon, Y., Sung, P. and Krejci, L. (2009) Regulation of Rad51 recombinase presynaptic filament assembly via interactions with the Rad52 mediator and the Srs2 anti-recombinase. *J. Biol. Chem.*, **284**, 24363-24371.
149. Colavito, S., Macris-Kiss, M., Seong, C., Gleeson, O., Greene, E.C., Klein, H.L., Krejci, L. and Sung, P. (2009) Functional significance of the Rad51-Srs2 complex in Rad51 presynaptic filament disruption. *Nucleic Acids Res*, **37**, 6754-6764.
150. Karpenshif, Y. and Bernstein, K.A. (2012) From yeast to mammals: recent advances in genetic control of homologous recombination. *DNA Repair*, **11**, 781-788.
151. Hu, Y., Raynard, S., Sehorn, M.G., Lu, X., Bussen, W., Zheng, L., Stark, J.M., Barnes, E.L., Chi, P., Janscak, P. *et al.* (2007) RECQL5/Recql5 helicase regulates homologous recombination and suppresses tumor formation via disruption of Rad51 presynaptic filaments. *Genes Dev.*, **21**, 3073-3084.

152. Moldovan, G.L., Dejsuphong, D., Petalcorin, M.I., Hofmann, K., Takeda, S., Boulton, S.J. and D'Andrea, A.D. (2012) Inhibition of homologous recombination by the PCNA-interacting protein PARI. *Mol. Cell*, **45**, 75-86.
153. Barber, L.J., Youds, J.L., Ward, J.D., McIlwraith, M.J., O'Neil, N.J., Petalcorin, M.I.R., Martin, J.S., Collis, S.J., Cantor, S.B., Auclair, M. *et al.* (2008) RTEL1 Maintains Genomic Stability by Suppressing Homologous Recombination. *Cell*, **135**, 261-271.
154. Hey, T., Lipps, G. and Krauss, G. (2001) Binding of XPA and RPA to damaged DNA investigated by fluorescence anisotropy. *Biochemistry (Mosc)*. **40**, 2901-2910.
155. Lisby, M., Rothstein, R. and Mortensen, U.H. (2001) Rad52 forms DNA repair and recombination centers during S phase. *Proc. Natl. Acad. Sci. U S A*, **98**, 8276-8282.
156. Heyer, W.D. (2007) Biochemistry of eukaryotic homologous recombination. *Top. Curr. Genet.*, **17**, 95-133.
157. Symington, L.S., Rothstein, R. and Lisby, M. (2014) Mechanisms and Regulation of Mitotic Recombination in *Saccharomyces cerevisiae*. *Genetics*, **198**, 795-835.
158. Godin, S.K., Meslin, C., Kabbinavar, F., Bratton-Palmer, D.S., Hornack, C., Mihalevic, M.J., Yoshida, K., Sullivan, M., Clark, N.L. and Bernstein, K.A. (2015) Evolutionary and functional analysis of the invariant SWIM domain in the conserved Shu2/SWS1 protein family from *Saccharomyces cerevisiae* to *Homo sapiens*. *Genetics*, **199**, 1023-1033.
159. Davis, A.P. and Symington, L.S. (2001) The yeast recombinational repair protein Rad59 interacts with Rad52 and stimulates single-strand annealing. *Genetics*, **159**, 515-525.
160. Esta, A., Ma, E., Dupaigne, P., Maloisel, L., Guerois, R., Le Cam, E., Veaute, X. and Coic, E. (2013) Rad52 sumoylation prevents the toxicity of unproductive Rad51 filaments independently of the anti-recombinase Srs2. *PLoS Genet.*, **9**, e1003833.
161. St Onge, R.P., Mani, R., Oh, J., Proctor, M., Fung, E., Davis, R.W., Nislow, C., Roth, F.P. and Giaever, G. (2007) Systematic pathway analysis using high-resolution fitness profiling of combinatorial gene deletions. *Nat. Genet.*, **39**, 199-206.
162. Petukhova, G., Van Komen, S., Vergano, S., Klein, H. and Sung, P. (1999) Yeast Rad54 promotes Rad51-dependent homologous DNA pairing via ATP hydrolysis-driven change in DNA double helix conformation. *J. Biol. Chem.*, **274**, 29453-29462.
163. Mehio, W., Kemp, G.J., Taylor, P. and Walkinshaw, M.D. (2010) Identification of protein binding surfaces using surface triplet propensities. *Bioinformatics*, **26**, 2549-2555.
164. Smith, J. and Rothstein, R. (1999) An allele of *RFA1* suppresses *RAD52*-dependent double-strand break repair in *Saccharomyces cerevisiae*. *Genetics*, **151**, 447-458.

165. Shah, P.P., Zheng, X., Epshtein, A., Carey, J.N., Bishop, D.K. and Klein, H.L. (2010) Swi2/Snf2-related translocases prevent accumulation of toxic Rad51 complexes during mitotic growth. *Mol. Cell*, **39**, 862-872.
166. Wright, W.D. and Heyer, W.D. (2014) Rad54 functions as a heteroduplex DNA pump modulated by its DNA substrates and Rad51 during D loop formation. *Mol. Cell*, **53**, 420-432.
167. Jensen, R.B., Ozes, A., Kim, T., Estep, A. and Kowalczykowski, S.C. (2013) BRCA2 is epistatic to the RAD51 paralogs in response to DNA damage. *DNA Repair (Amst)*, **12**, 306-311.
168. Van Komen, S., Macris, M., Sehorn, M.G. and Sung, P. (2006) Purification and assays of *Saccharomyces cerevisiae* homologous recombination proteins. *Methods Enzymol.*, **408**, 445-463.
169. Raschle, M., Van Komen, S., Chi, P., Ellenberger, T. and Sung, P. (2004) Multiple interactions with the Rad51 recombinase govern the homologous recombination function of Rad54. *J. Biol. Chem.*, **279**, 51973-51980.
170. Song, B. and Sung, P. (2000) Functional interactions among yeast Rad51 recombinase, Rad52 mediator, and replication protein A in DNA strand exchange. *J. Biol. Chem.*, **275**, 15895-15904.
171. Lindsley, J.E. and Wang, J.C. (1993) On the coupling between ATP usage and DNA transport by yeast DNA topoisomerase II. *J Biol Chem*, **268**, 8096-8104.
172. San Filippo, J., Chi, P., Sehorn, M.G., Etchin, J., Krejci, L. and Sung, P. (2006) Recombination mediator and Rad51 targeting activities of a human BRCA2 polypeptide. *J. Biol. Chem.*, **281**, 11649-11657.
173. Taylor, M.R., Spirek, M., Chaurasiya, K.R., Ward, J.D., Carzaniga, R., Yu, X., Egelman, E.H., Collinson, L.M., Rueda, D., Krejci, L. *et al.* (2015) Rad51 Paralogs Remodel Pre-synaptic Rad51 Filaments to Stimulate Homologous Recombination. *Cell*, **162**, 271-286.
174. Cloud, V., Chan, Y.L., Grubb, J., Budke, B. and Bishop, D.K. (2012) Rad51 is an accessory factor for Dmcl-mediated joint molecule formation during meiosis. *Science*, **337**, 1222-1225.
175. Hong, S. and Kim, K.P. (2013) Shu1 promotes homolog bias of meiotic recombination in *Saccharomyces cerevisiae*. *Mol Cells*, **36**, 446-454.
176. Busygina, V., Sehorn, M.G., Shi, I.Y., Tsubouchi, H., Roeder, G.S. and Sung, P. (2008) Hed1 regulates Rad51-mediated recombination via a novel mechanism. *Genes & development*, **22**, 786-795.

177. Tsubouchi, H. and Roeder, G.S. (2006) Budding yeast Hed1 down-regulates the mitotic recombination machinery when meiotic recombination is impaired. *Genes & development*, **20**, 1766-1775.
178. Say, A.F., Ledford, L.L., Sharma, D., Singh, A.K., Leung, W.K., Sehorn, H.A., Tsubouchi, H., Sung, P. and Sehorn, M.G. (2011) The budding yeast Mei5-Sae3 complex interacts with Rad51 and preferentially binds a DNA fork structure. *DNA Repair*, **10**, 586-594.